Angular Momentum in Fission through Isomeric Ratio measurements with the Lohengrin spectrometer

Anna Skouloudaki[1,2], A. Chebboubi[1], G. Kessedjian[1], M. Diakaki[2], O. Serot[1], D. Bernard[1], U. Koester[3], J.M. Daugas[3], P. Mutti[3], O. Meplan[4], C. Sage[4]

[1] CEA, DES, IRESNE, DER, SPRC, Cadarache, Physics Studies Laboratory, 13108 Saint-Paul-lès-Durance, France
[2] National Technical University of Athens, Iroon polytechniou 9, Zografou Campus 15780, Athens, Greece
[3] Institut Laue-Langevin, 38042 Grenoble Cedex 9, France
[4] LPSC, Université Grenoble-Alpes, CNRS/IN2P3, 38026 Grenoble Cedex, France

Contents

1. Motivation
2. **Isomeric Ratios of Fission Products** as observables of Angular Momentum through **^{241}Am(2n$_{th}$,f)**
3. Analysis Process
4. Preliminary results of **^{100}Nb** and perspectives

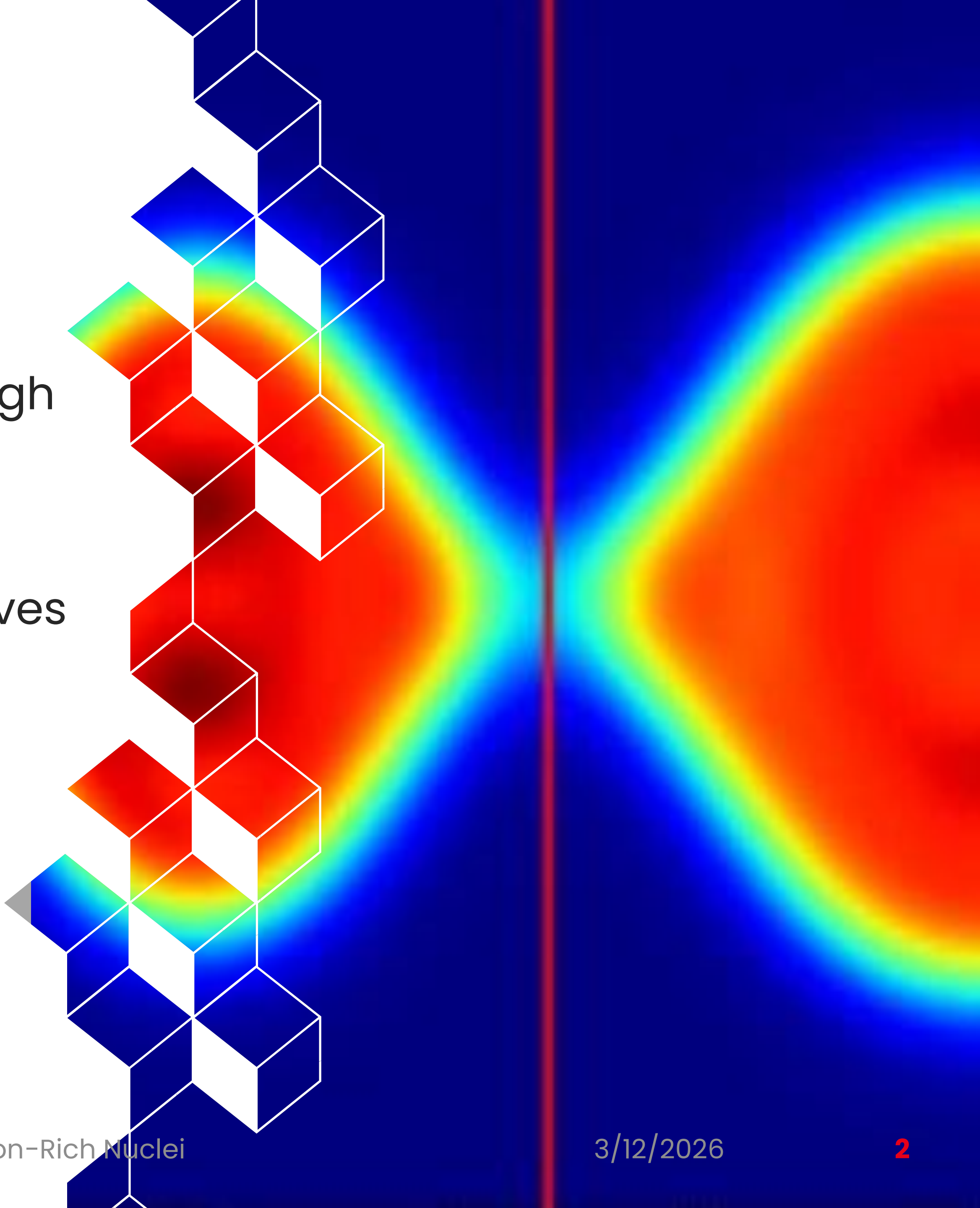

Number of Particles in Fission Fragments, 2019, M. Verriere, T. Kawano, N. Schunck

Motivation: Angular momentum generation mechanism of Fission Fragments

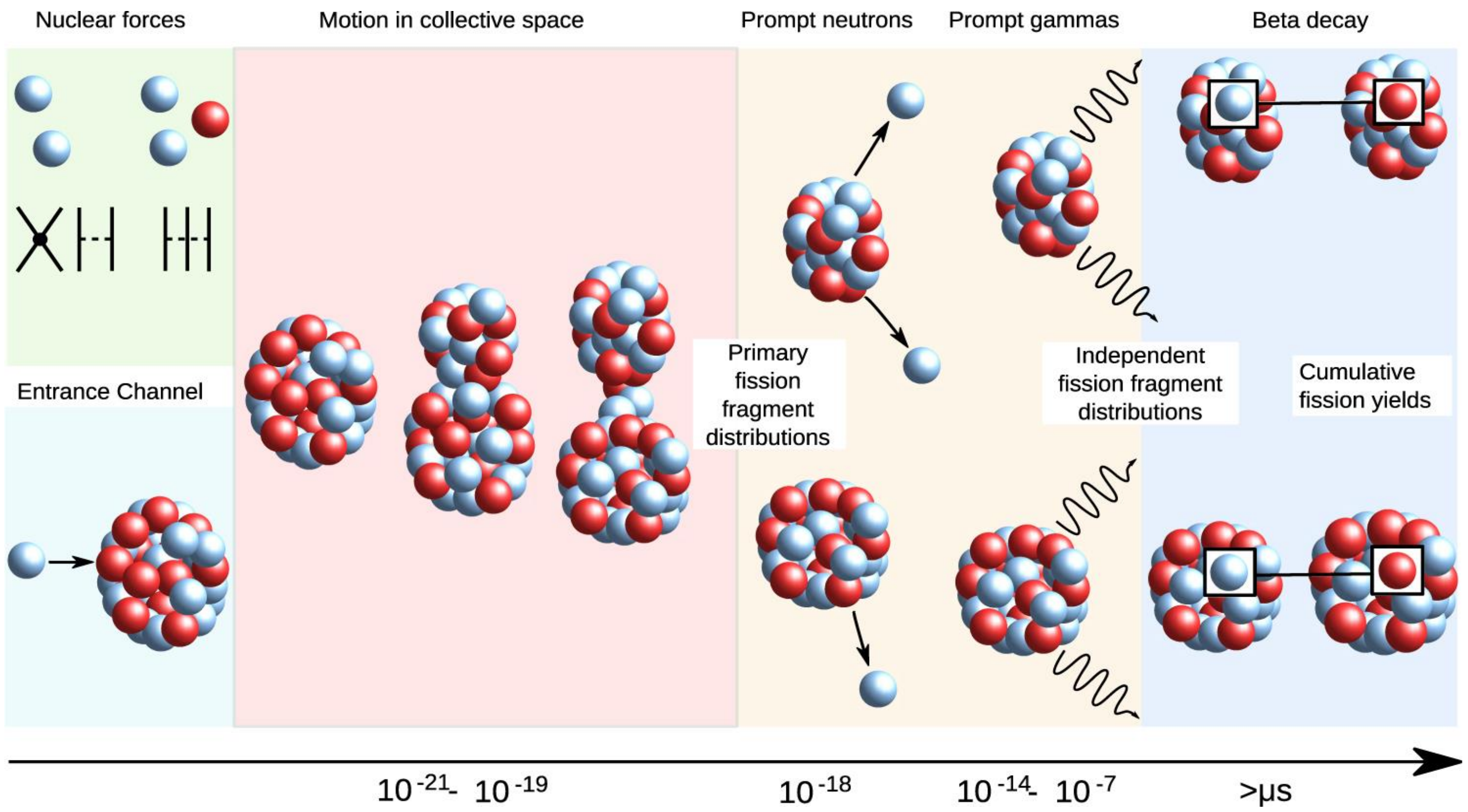

M. Bender *et al.*, *Future of nuclear fission theory*, J. Phys. G: Nucl. Part. Phys. 47 113002 (2020)

Motivation: Angular momentum generation mechanism of Fission Fragments

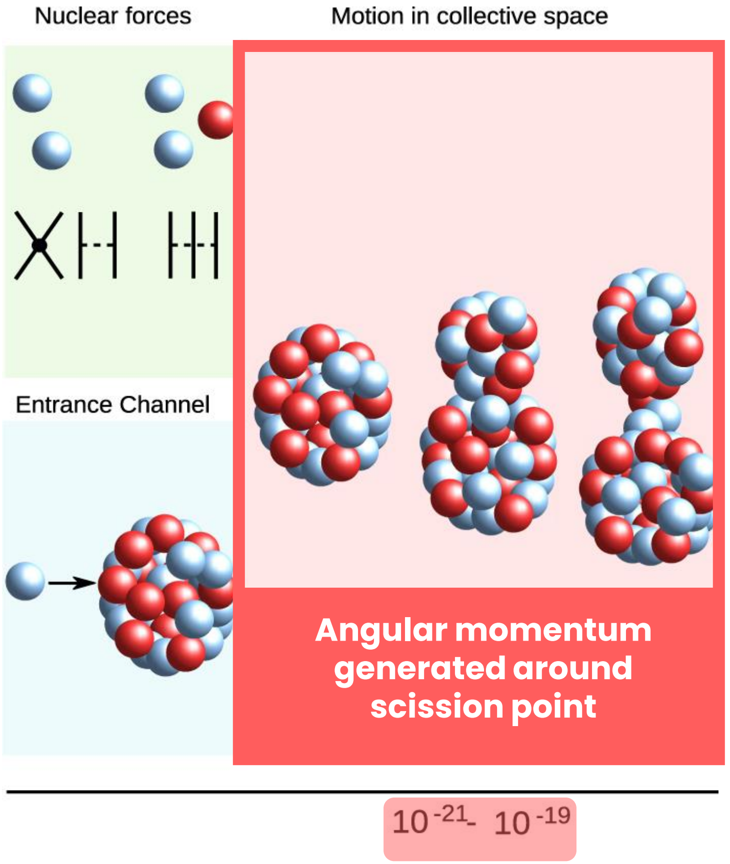

Applications:

Angular Momentum → **PFNS** / **PFGS** → **Nuclear Reactor modeling**

criticality calculations

Radioprotection, shielding

Open questions:

- ❑ the general properties of the Angular Momenta (AM)
- ❑ the mechanism(s) behind their generation and correlation of the angular momentum of the two fission fragments

M. Bender *et al.*, *Future of nuclear fission theory*, J. Phys. G: Nucl. Part. Phys. 47 113002 (2020)

Motivation: Angular momentum generation mechanism of Fission Fragments

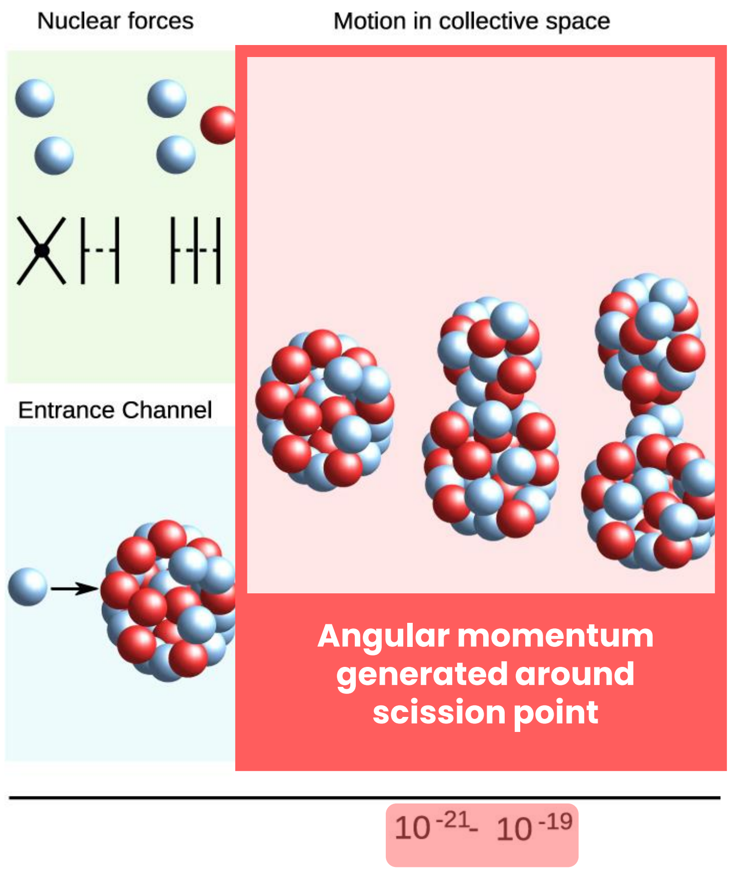

Competing theories

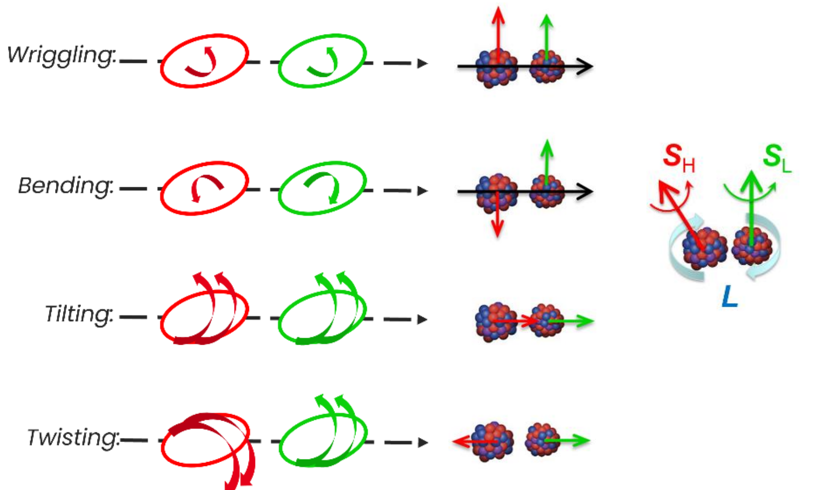

J. Randrup et al., Generation of Fragment Angular Momentum in Nuclear Fission, EPJ WoC, 284,04004 (2023)

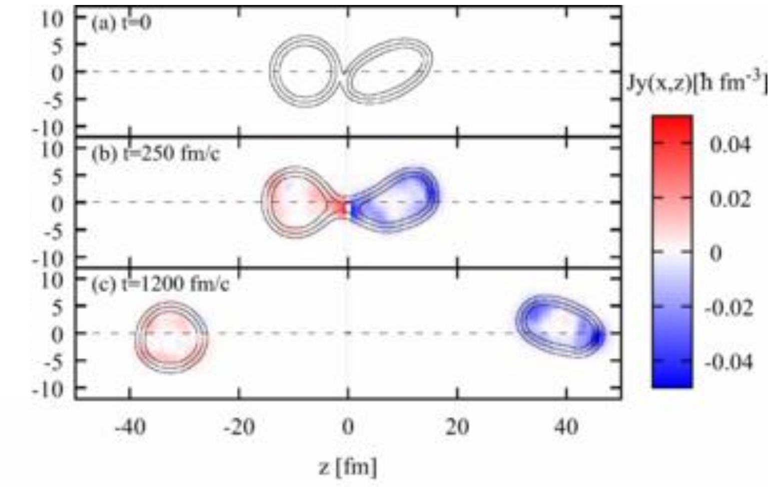

G. Scamps, Microscopic description of the torque acting on fission fragments, Phys. Rev. C 106, 054614 (2022)

M. Bender *et al.*, *Future of nuclear fission theory*, J. Phys. G: Nucl. Part. Phys. 47 113002 (2020)

Motivation: Angular momentum generation mechanism of Fission Fragments

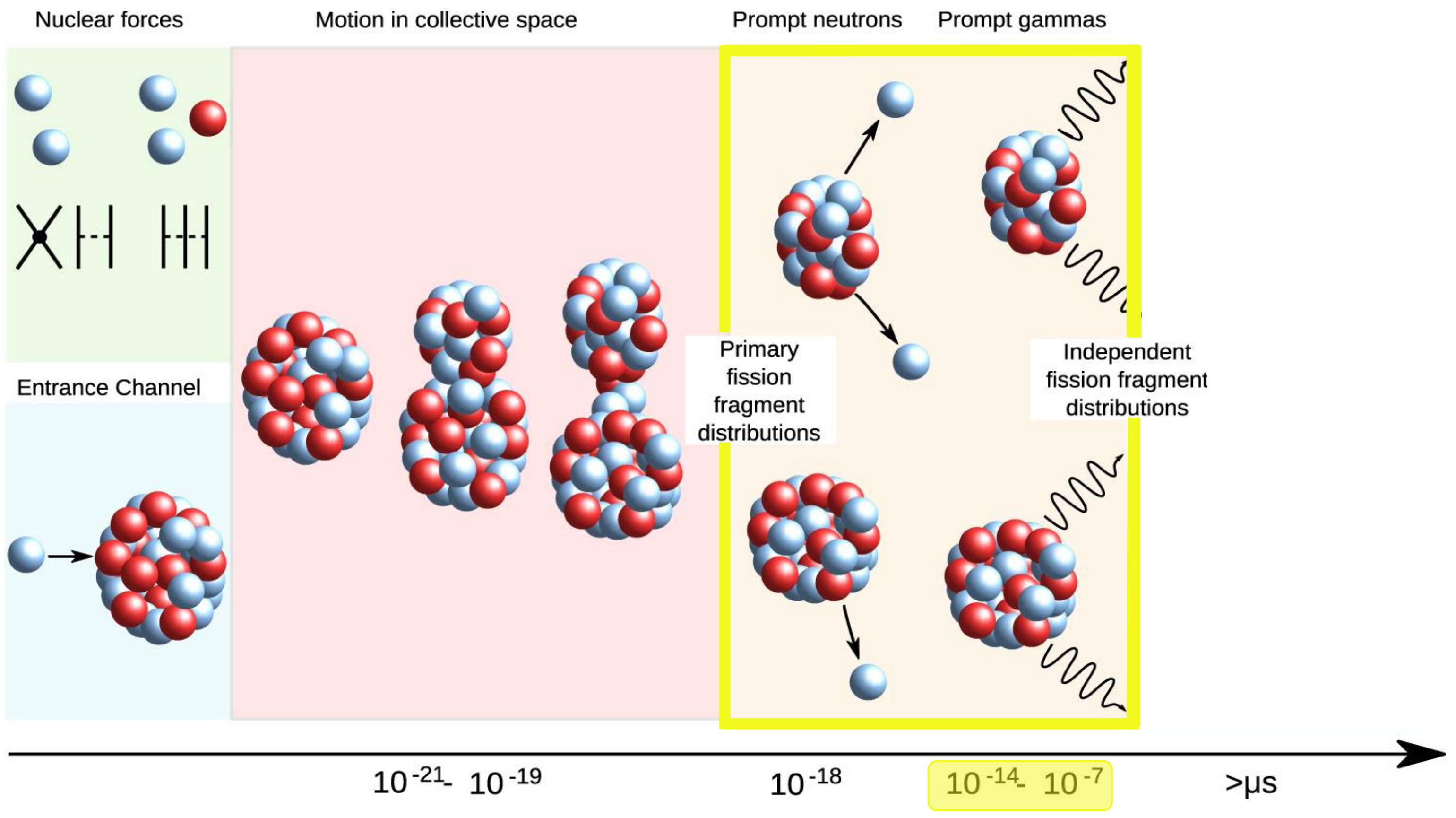

µs Isomers

M. Bender *et al.*, *Future of nuclear fission theory*, J. Phys. G: Nucl. Part. Phys. 47 113002 (2020)

Motivation: Angular momentum generation mechanism of Fission Fragments

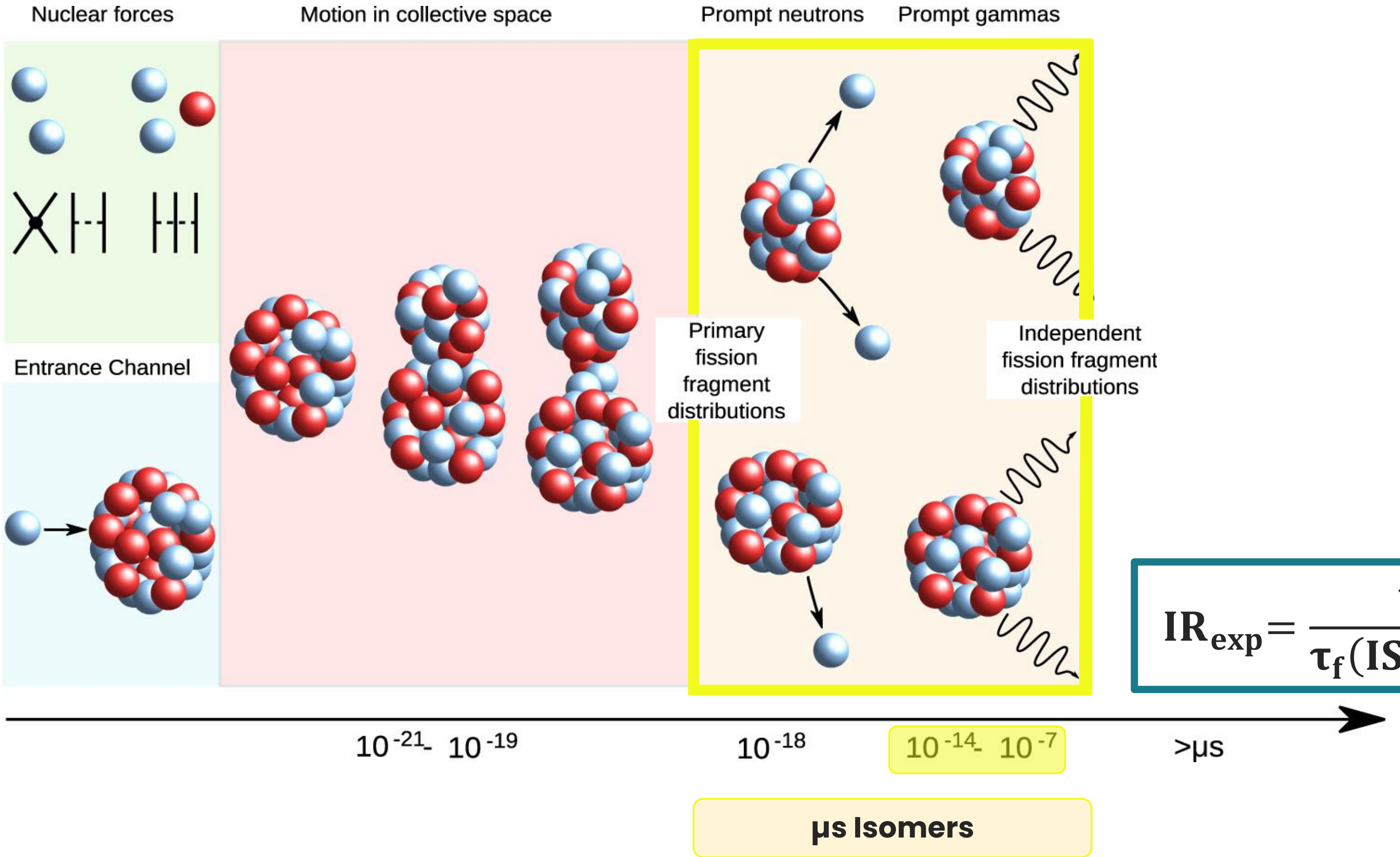

$$IR_{exp} = \frac{\tau_f(IS)}{\tau_f(IS) + \tau_f(GS)}$$

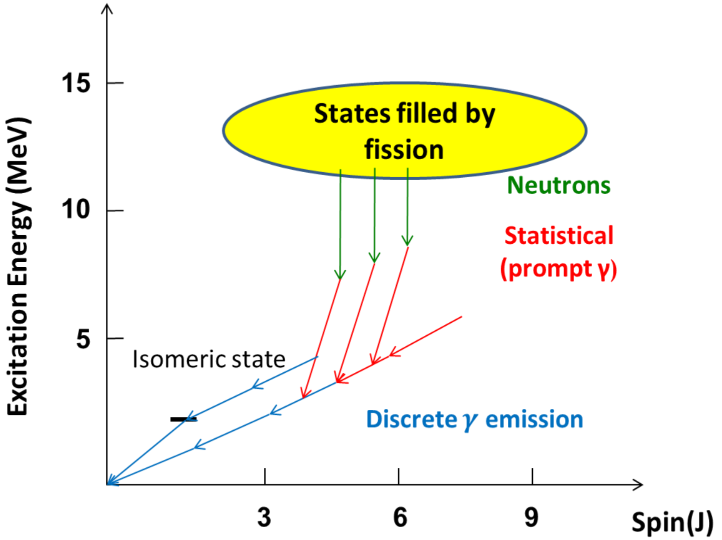

J. Randrup et al., Generation of Fragment Angular Momentum in Nuclear Fission, EPJ WoC, 284,04004 (2023)

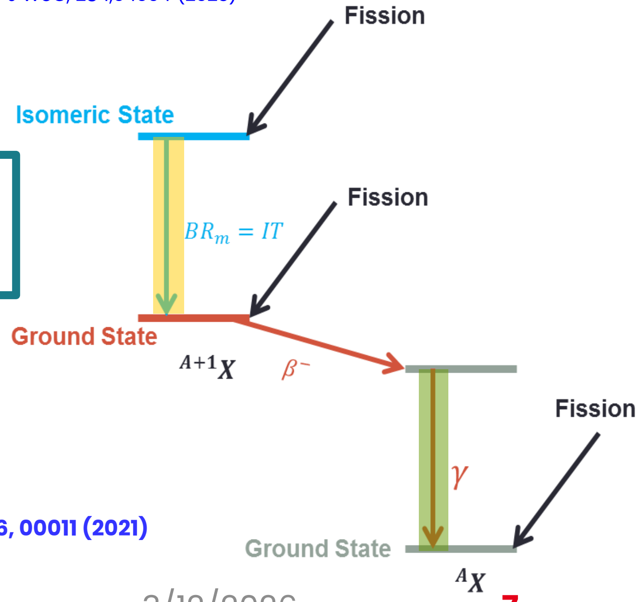

Investigation of fission product isomeric ratios and angular momenta of 132Sn populated in the 241Pu(nth,f) reaction, A. Chebbouibi, EPJ Web of Conferences 256, 00011 (2021)

M. Bender *et al.*, *Future of nuclear fission theory*, J. Phys. G: Nucl. Part. Phys. 47 113002 (2020)

Goals

Through experimental campaigns and interpretation, coupled with theoretical models, we aim to:

- constrain the different models of generation of the angular momentum of fission fragments

- find a possible correlation with excitation energy, through Isomeric Ratio (IR) measurements.

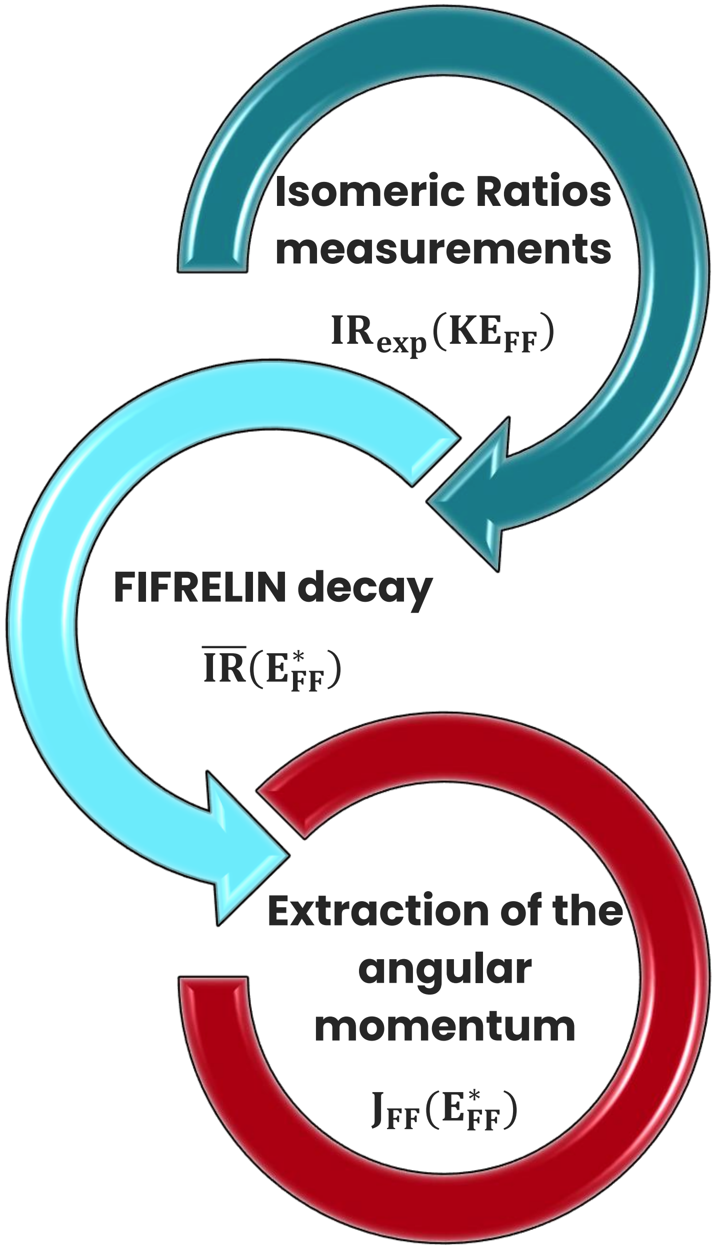

Fission modelling with FIFRELIN, O. Litaize, O. Serot, L. Berge, The European Physical Journal A 51, 177 (2015)

Experimental setup of LOHENGRIN spectrometer in ILL

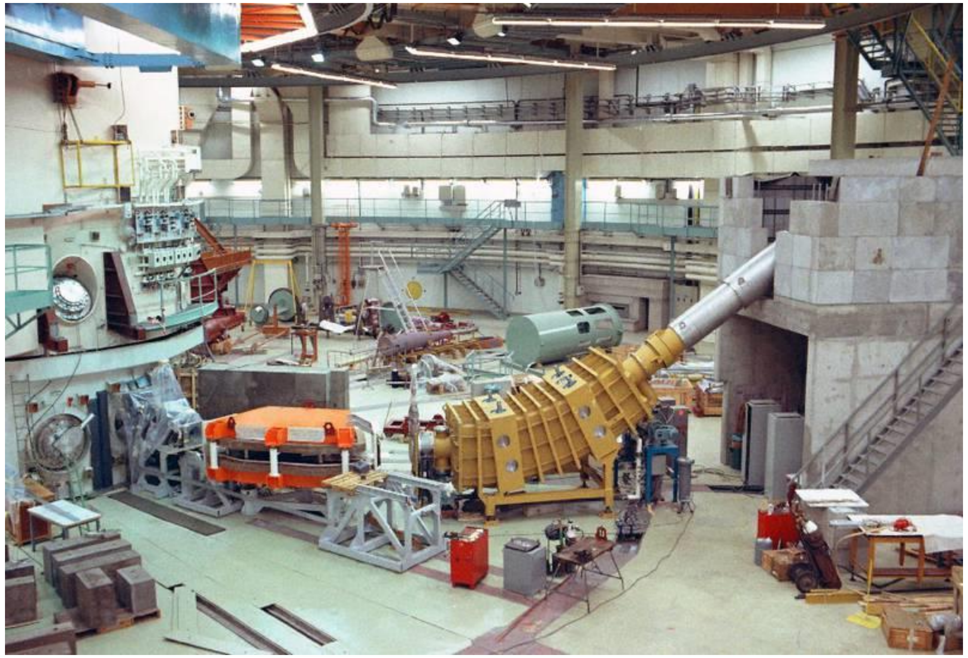

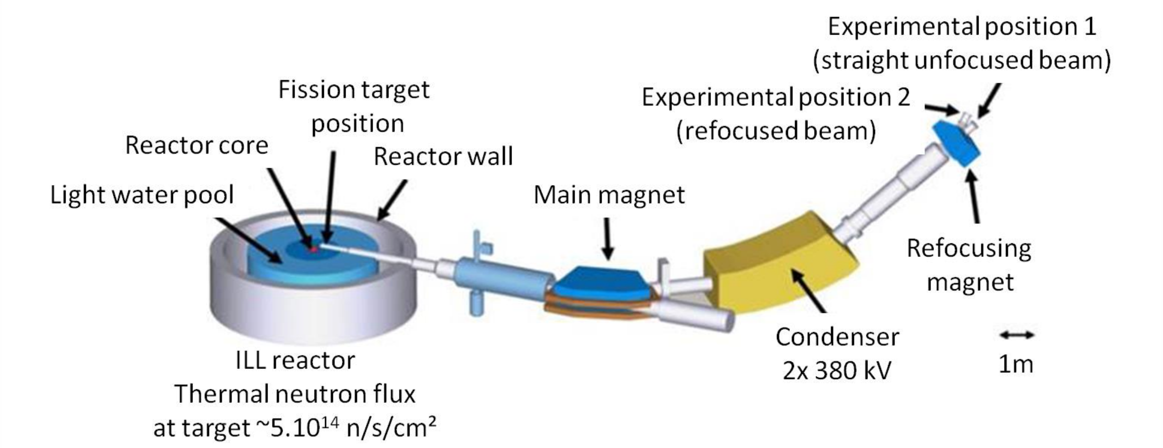

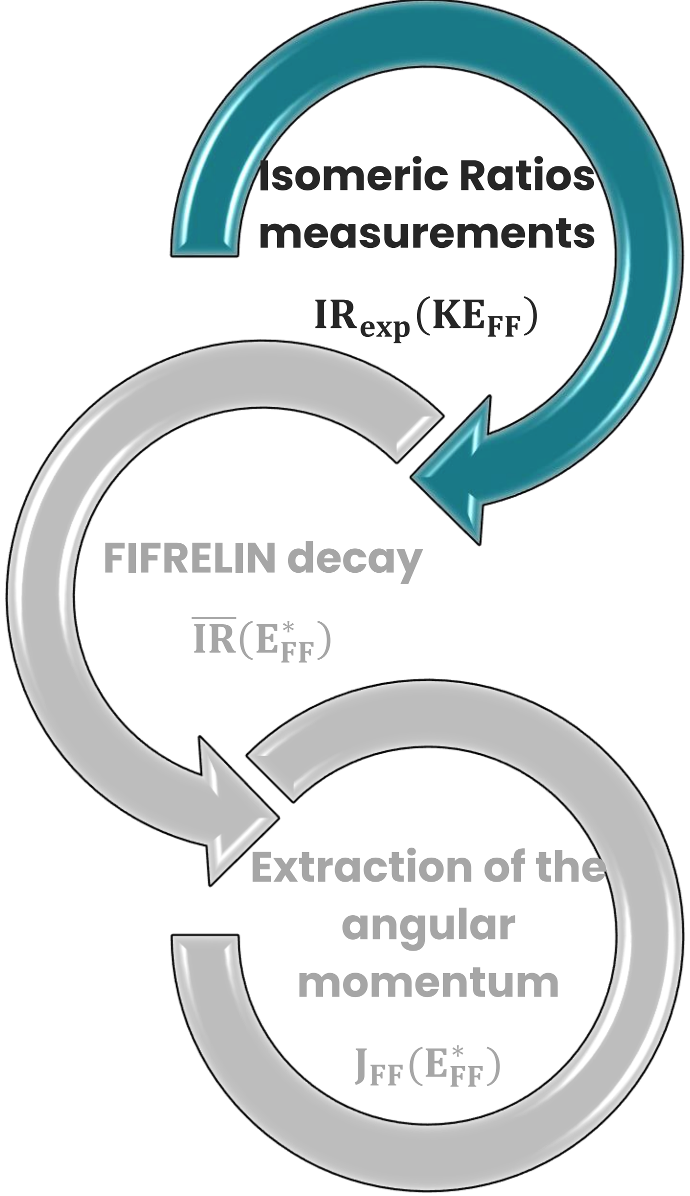

Experimental setup of LOHENGRIN spectrometer in ILL

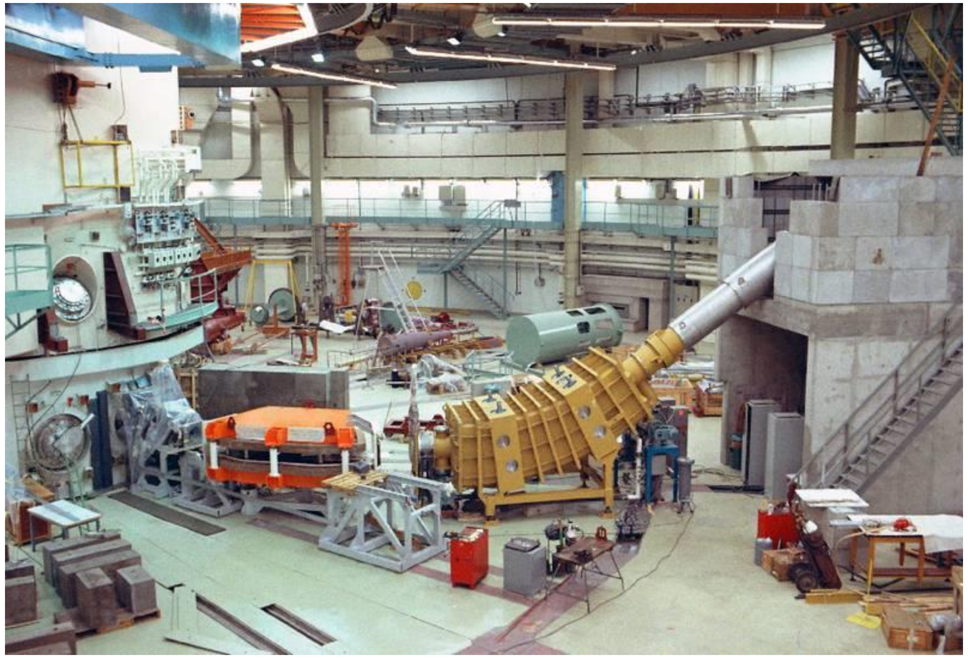

Choice of $\vec{B}$ and $\vec{E}$ → Selection of A/q and E_K/q → Only isotopes of chosen A/q are deflected into the exit slit

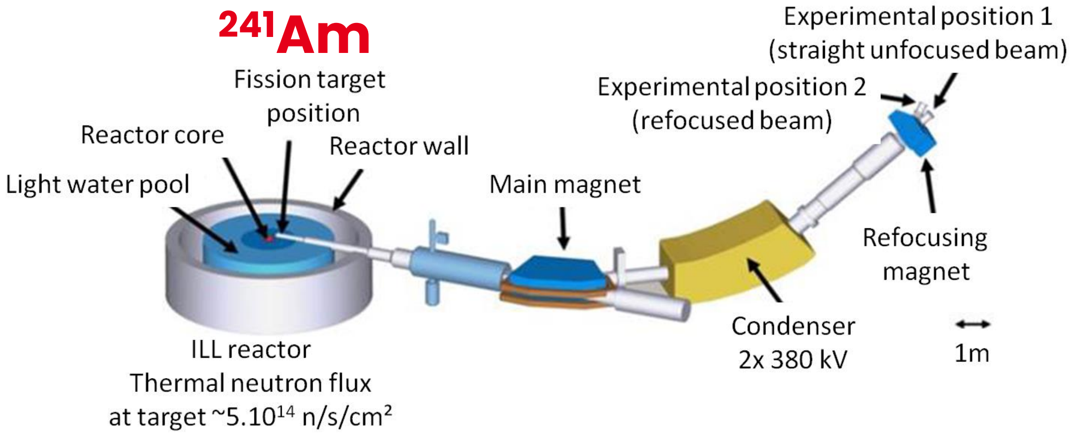

Experimental setup of LOHENGRIN spectrometer in ILL

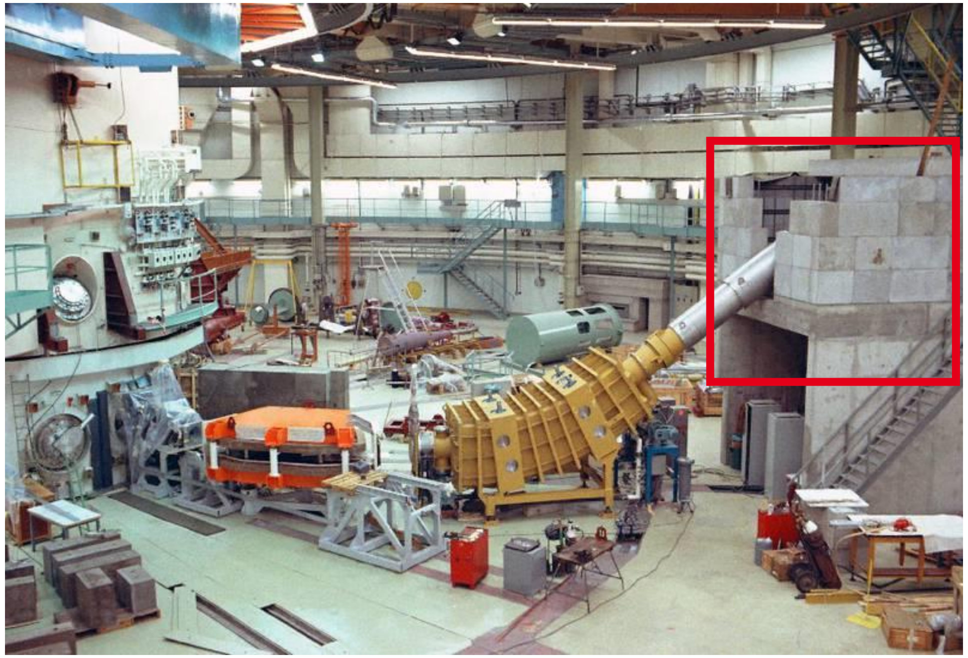

Choice of $\vec{B}$ and $\vec{E}$

Selection of ${}^{A}/_{q}$ and ${}^{E_K}/_{q}$

Only isotopes of chosen ${}^{A}/_{q}$ are deflected into the exit slit

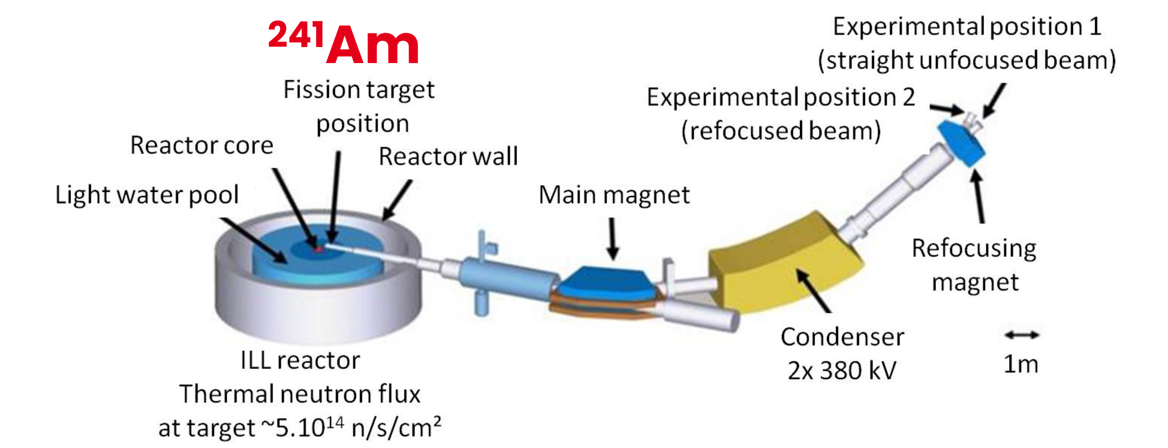

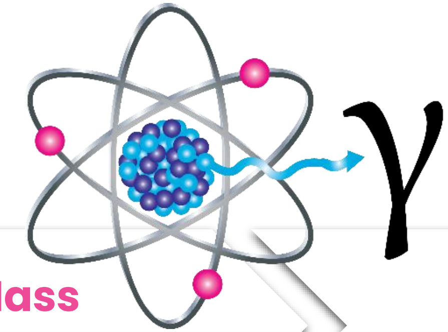

Mass spectrometry

Gamma spectroscopy

Experimental setup of LOHENGRIN spectrometer in ILL

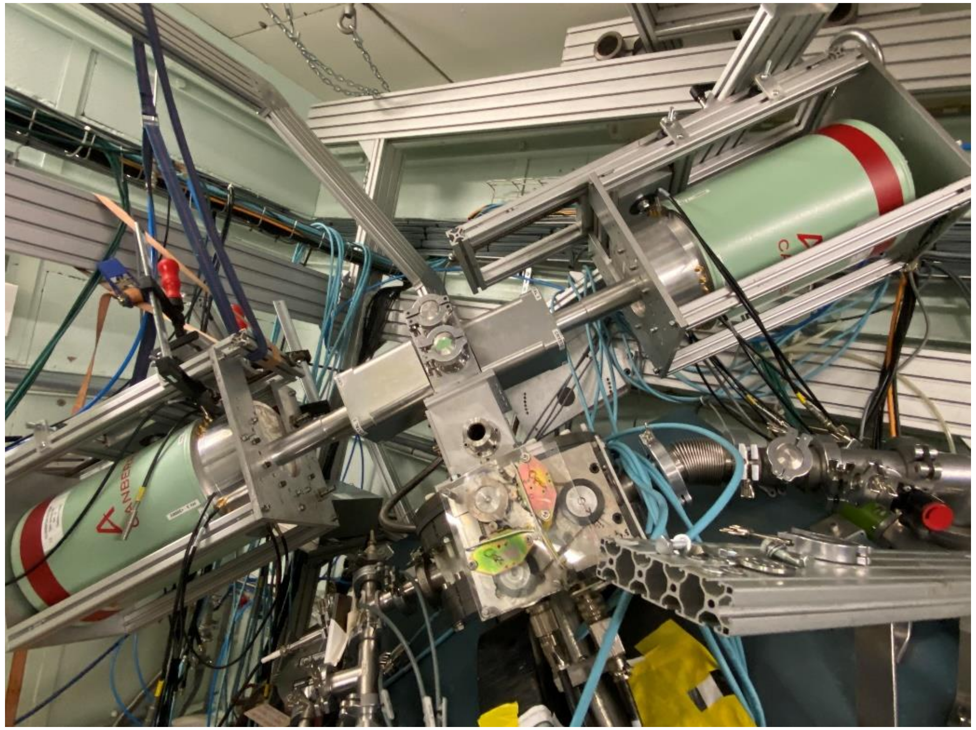

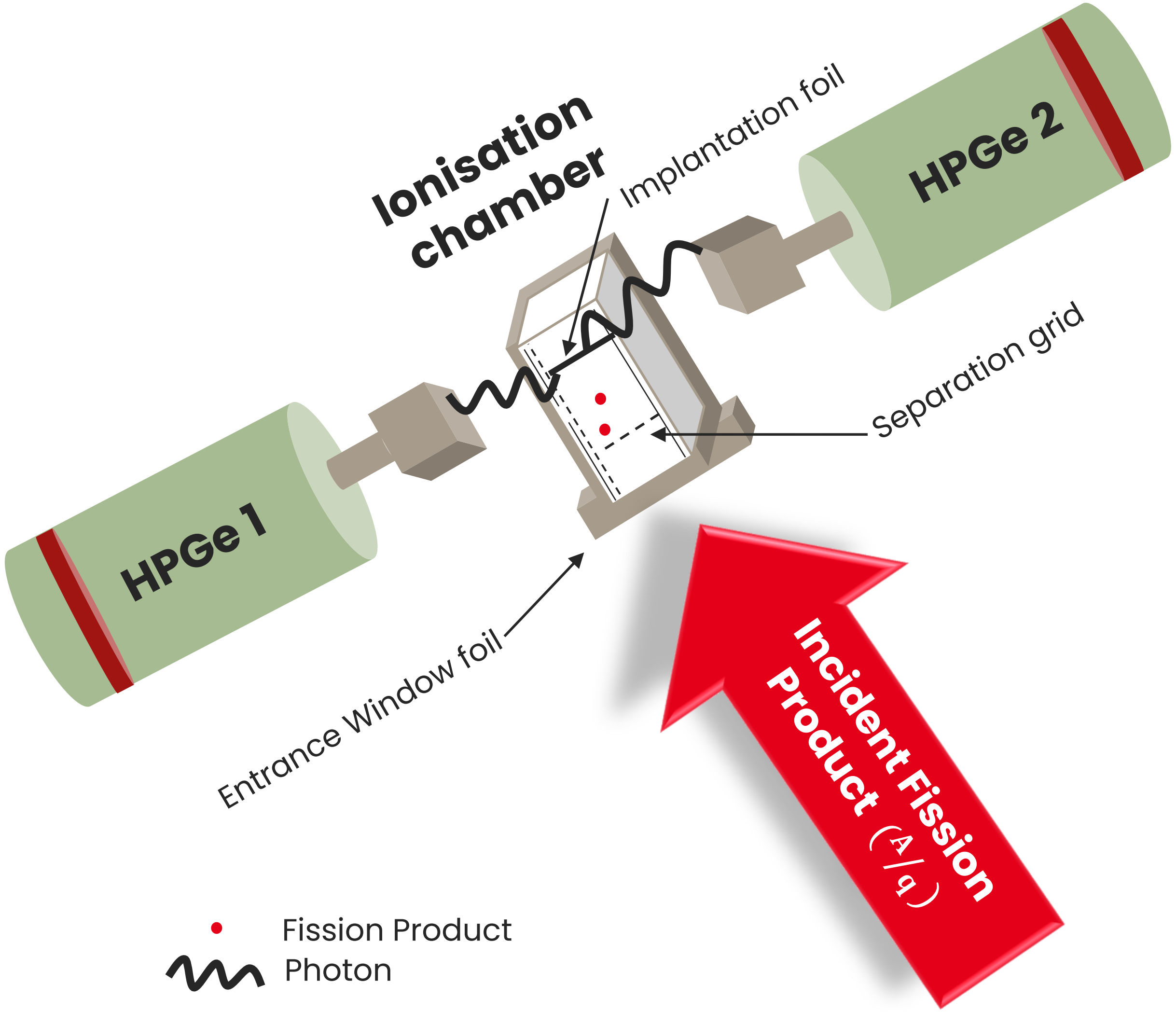

Analysis – ^{100}Nb from ^{241}Am($2n_{th}$,f)

Delayed γ-Spectrum without selection

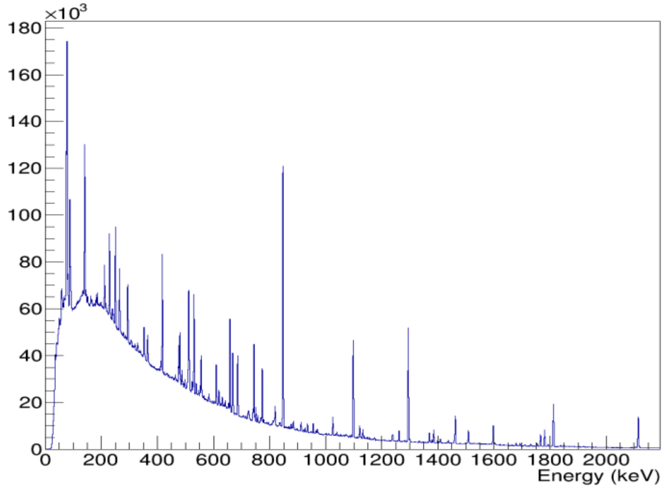

Analysis – ^{100}Nb from ^{241}Am($2n_{th}$,f)

Delayed γ-Spectrum without selection

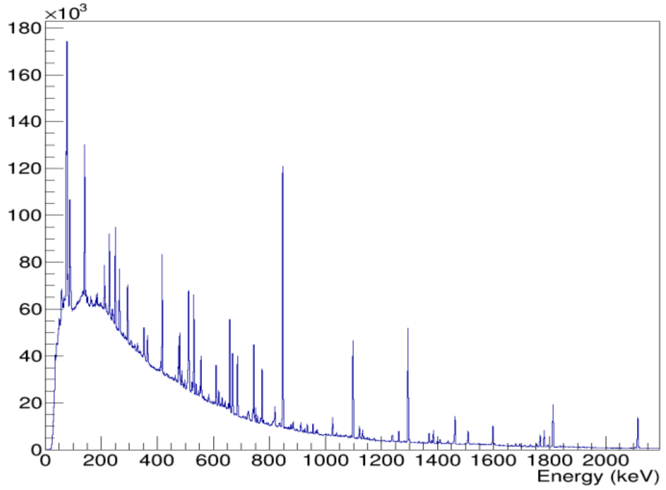

Mass, KE Filter

LOHENGRIN: mass separator

Ungated Spectrum

→ β-decay states measurement → $\mathbf{N_\gamma}$, $\mathbf{N_\gamma}$

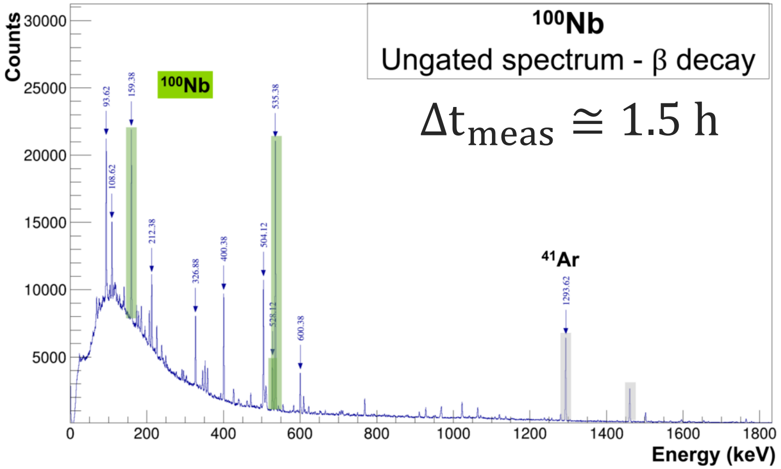

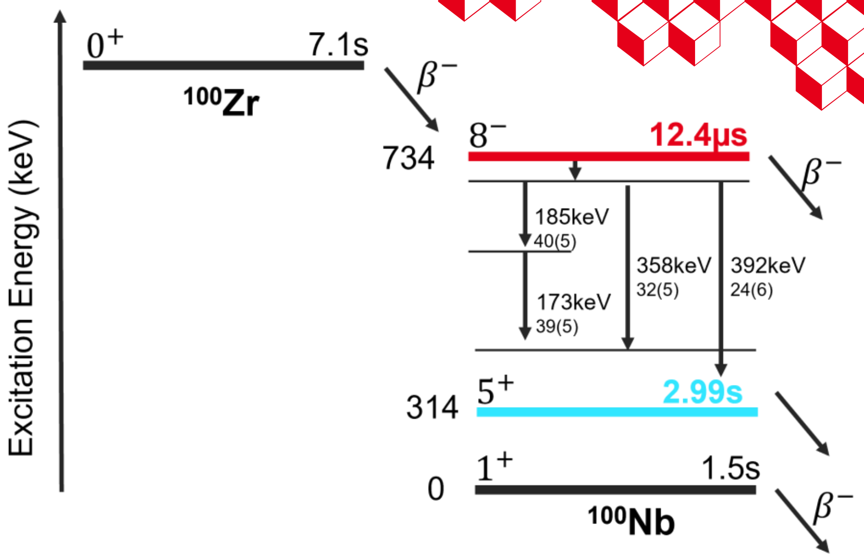

Analysis – ^{100}Nb from ^{241}Am($2n_{th}$,f)

Delayed γ-Spectrum without selection

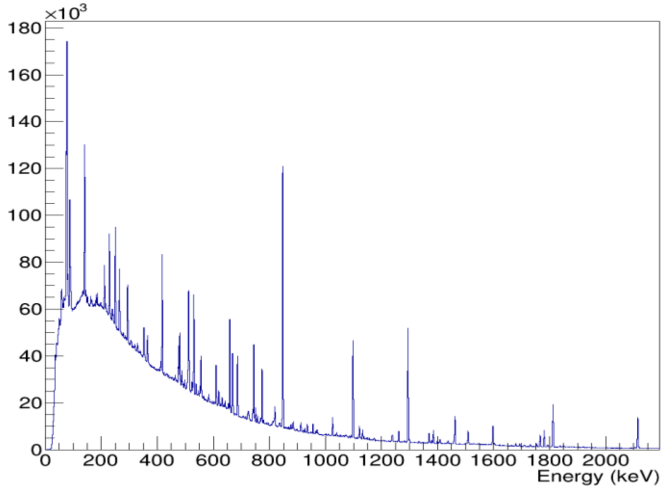

Mass, KE Filter

LOHENGRIN: mass separator

Ungated Spectrum

→ β-decay states measurement → $\mathbf{N_\gamma}$, $\mathbf{N_\gamma}$

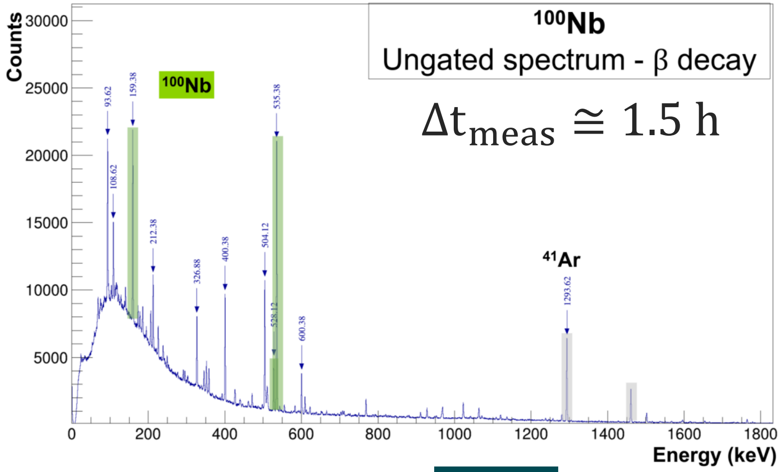

Time Coincidence Filter

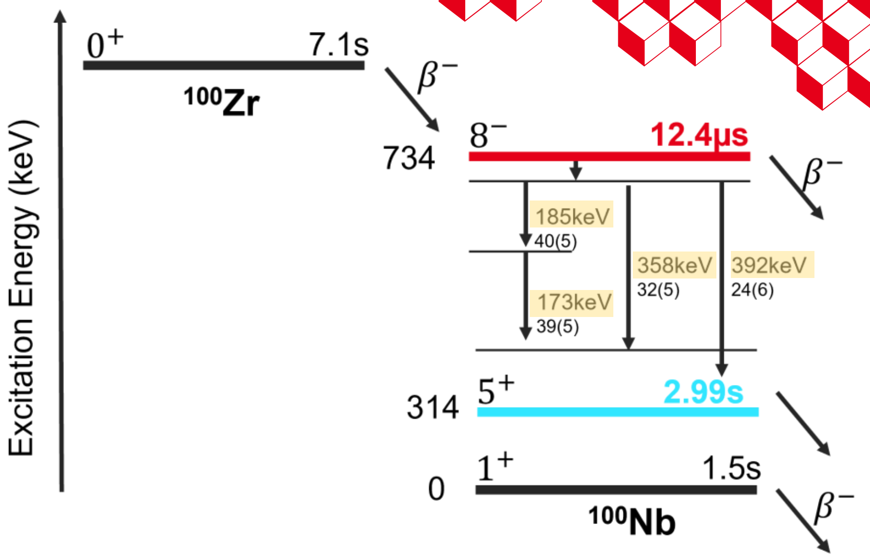

Gated Spectrum

Time coincidence between ionization chamber and HPGe detectors
→ µs Isomeric state measurement → $\mathbf{N_\gamma}$

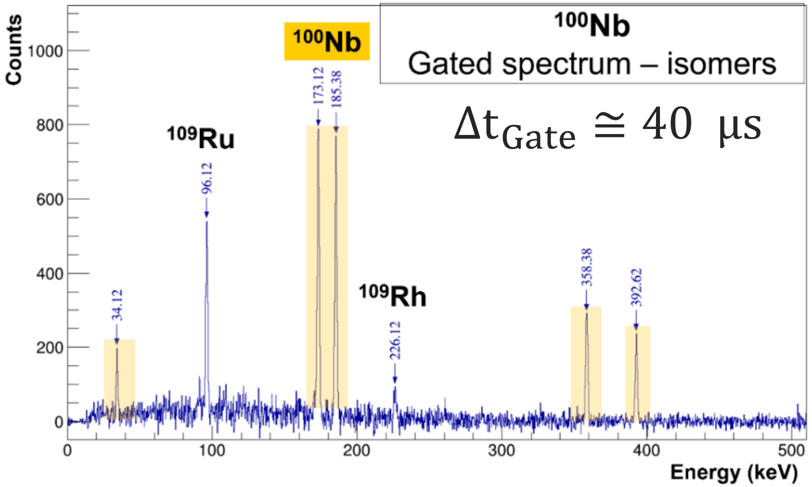

Analysis – Δt_{Gate} – ^{100}Nb

For which Δt_{Gate} is the $t_{1/2}$ of the isomeric level re-produced ?

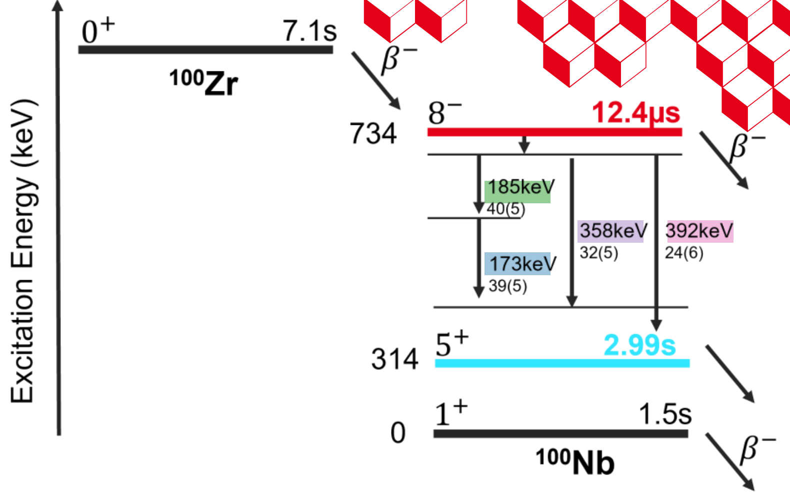

$\Delta t_{Gate} \cong 60$ μs $\cong 5^* t_{1/2,ms}$

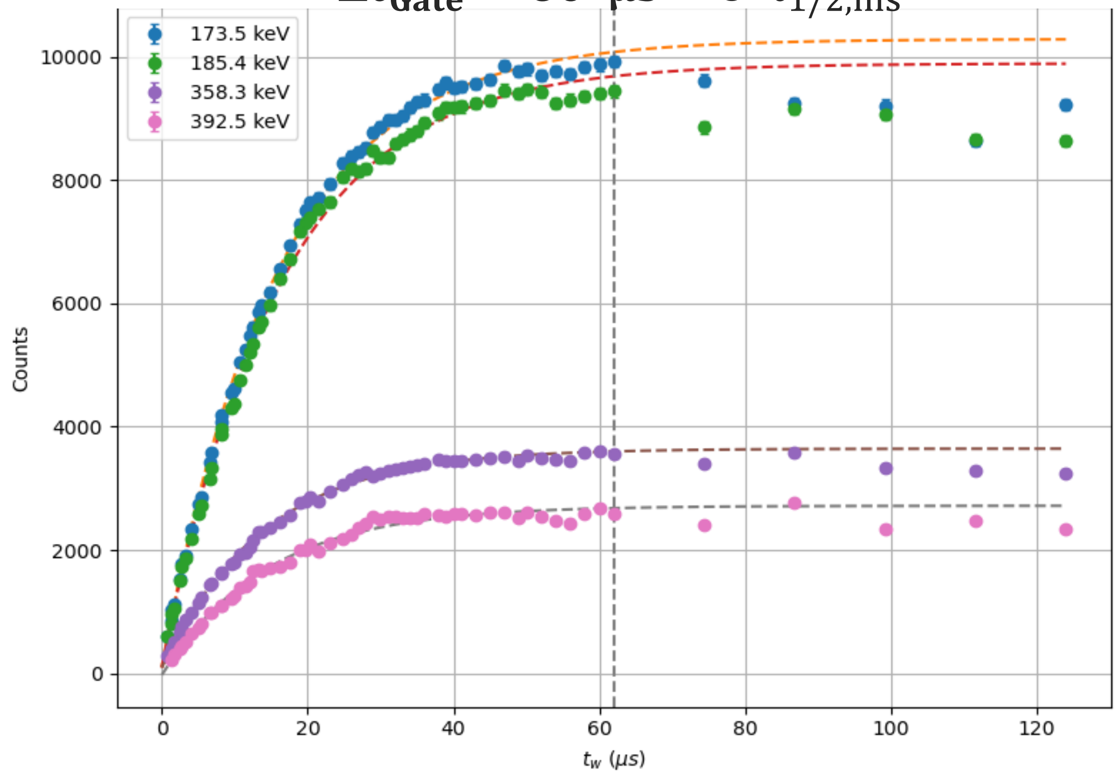

Analysis – Δt_{Gate} – ^{100}Nb

For which Δt_{Gate} is the $t_{1/2}$ of the isomeric level re-produced ?

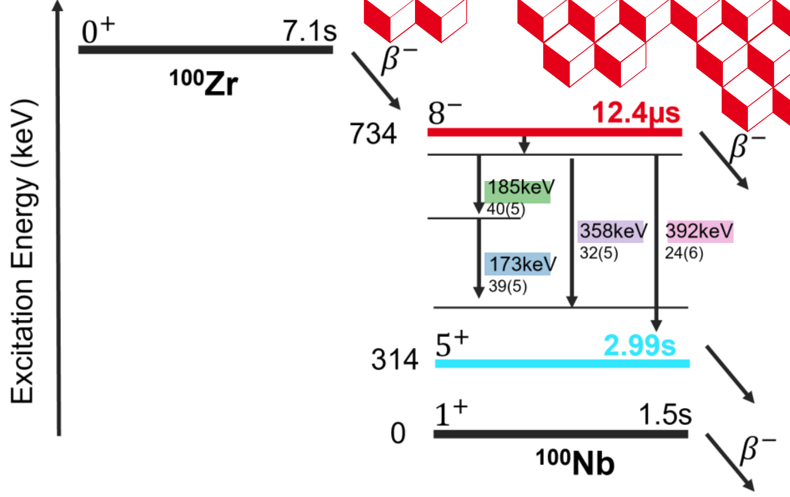

$\Delta t_{Gate} \cong 60\ \mu s \cong 5{*}t_{1/2,ms}$

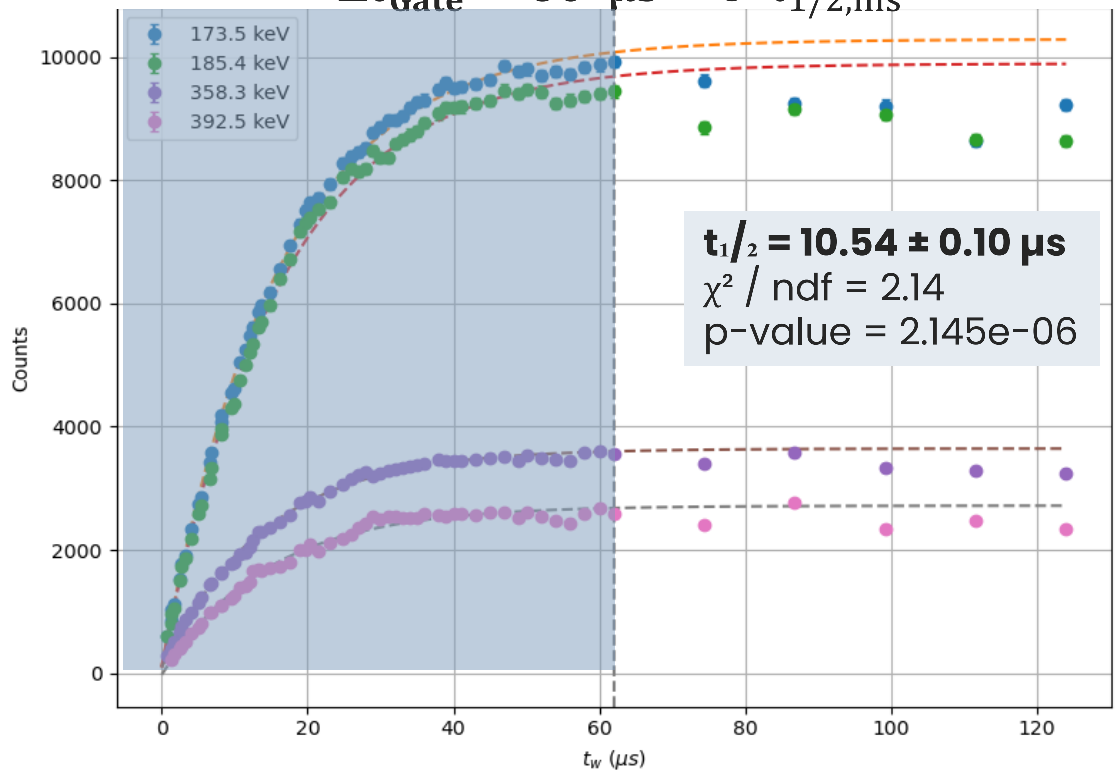

Analysis – Δt_{Gate} – ^{100}Nb

For which Δt_{Gate} is the $t_{1/2}$ of the isomeric level re-produced ?

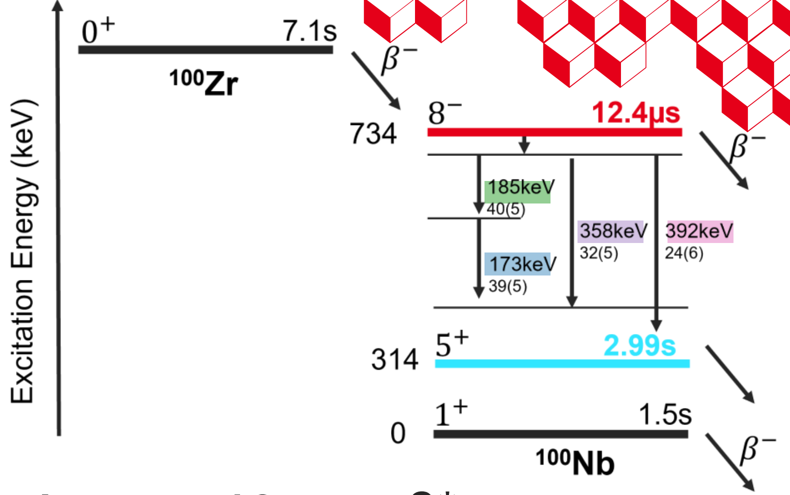

$\Delta t_{Gate} \cong 60$ µs $\cong 5^{*}t_{1/2,ms}$

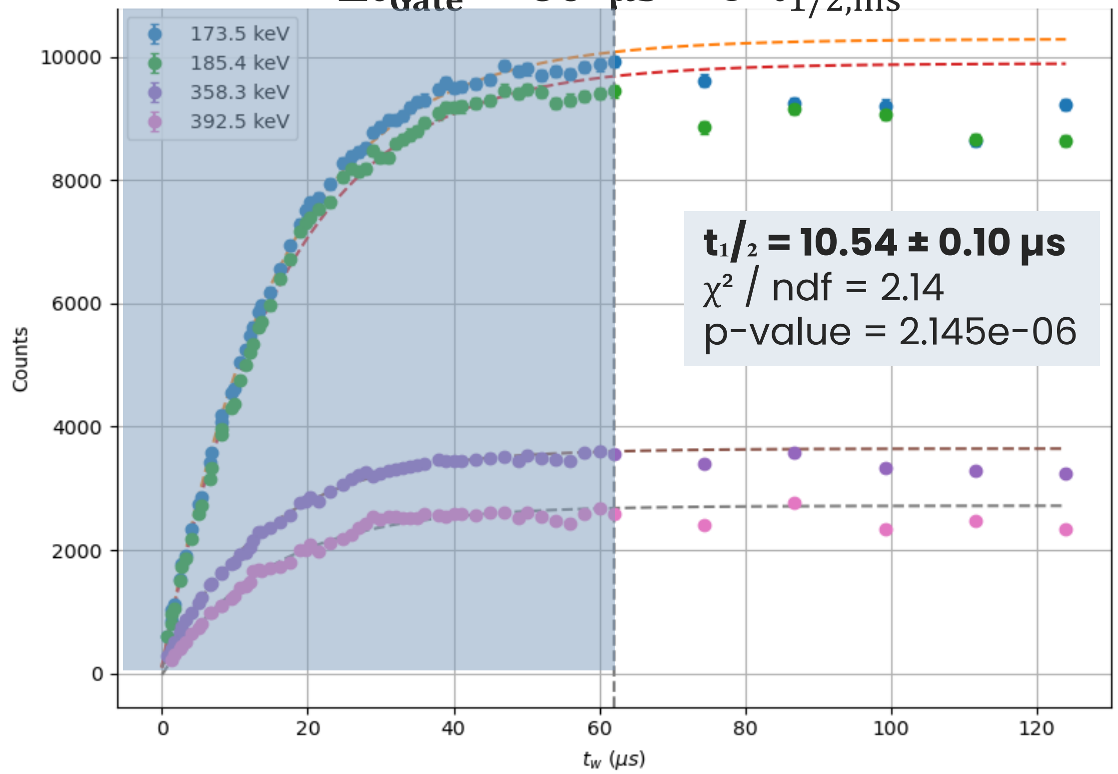

$\Delta t_{Gate} \cong 40$ µs $\cong 3^{*}t_{1/2,ms}$

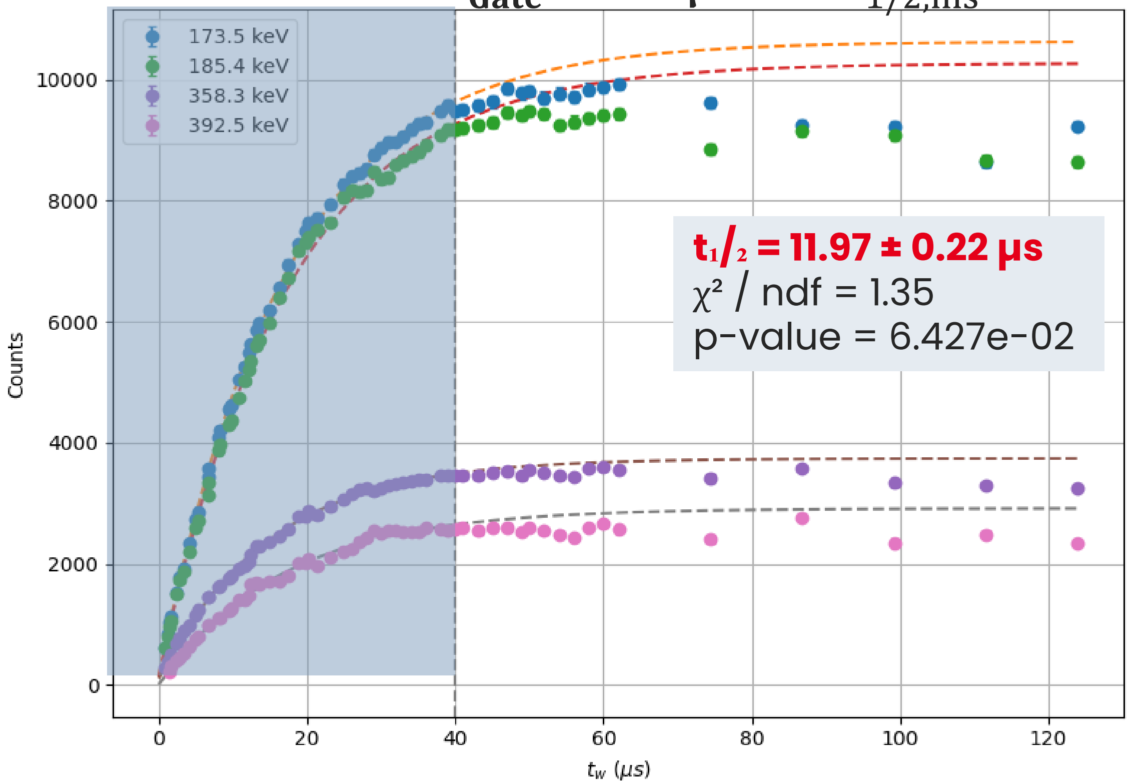

Analysis – Δt_{Gate}

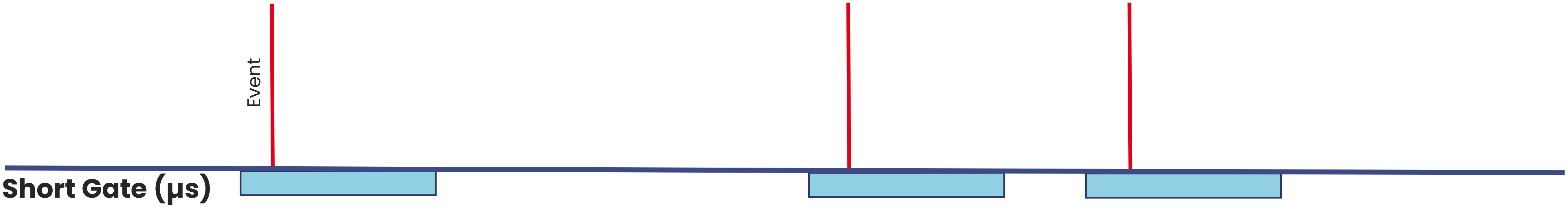

Analysis – Δt_{Gate}

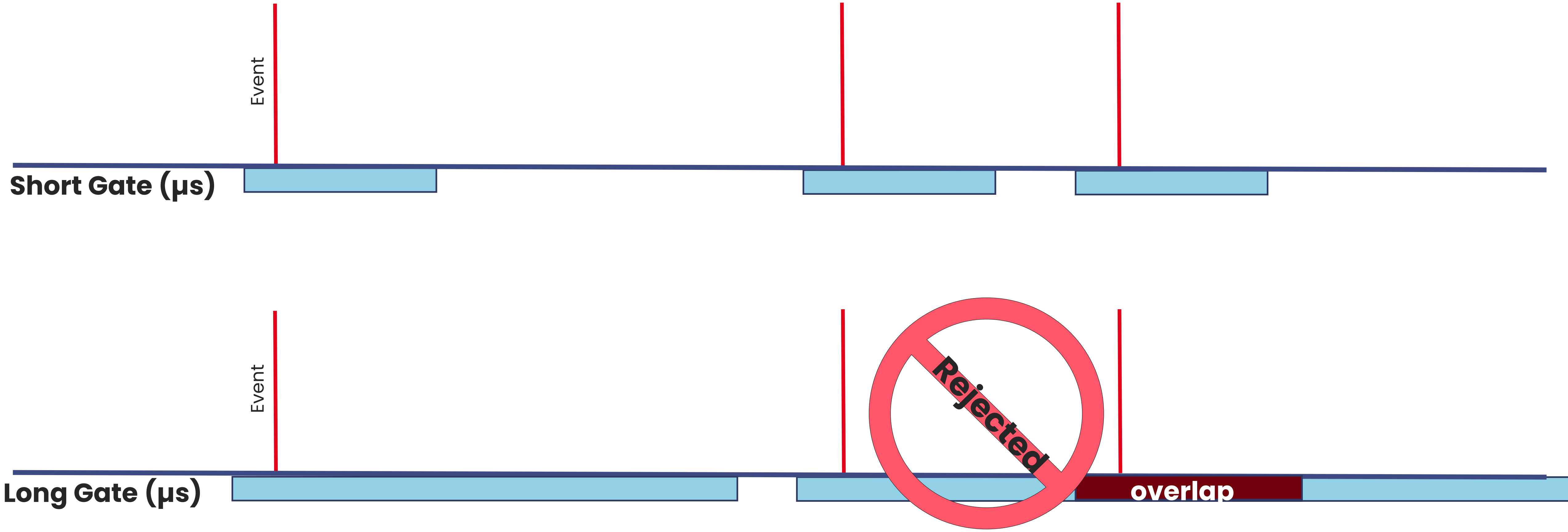

Importance of data sorting

Analysis – ^{100}Nb from ^{241}Am($2n_{th}$,f)

$$N_\gamma \rightarrow N_d = \frac{N_\gamma}{\varepsilon_\gamma \times I_\gamma \times f_\gamma} \xrightarrow{\text{Average}} \overline{N_d} \xrightarrow{\text{Bateman Equation Resolution}} \tau_f \rightarrow \boxed{IR_{exp} = \frac{\tau_f(IS)}{\tau_f(IS) + \tau_f(GS)}}$$

IR: Isomeric Ratio, IS: Isomeric State, GS: Ground State

ε_γ: Detector Efficiency,

f_γ: Correction factor for Sum-Effect,

will be derived from **TrueCoinc**[1] and Monte Carlo Simulation **MCNP6**[2] (in progress).

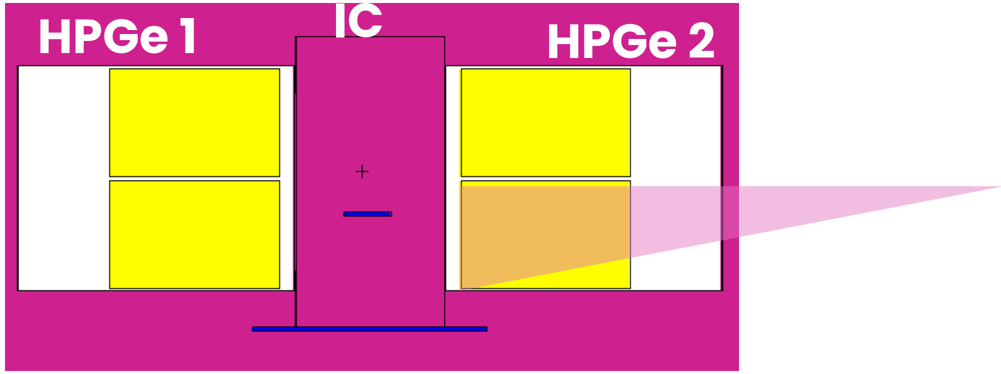

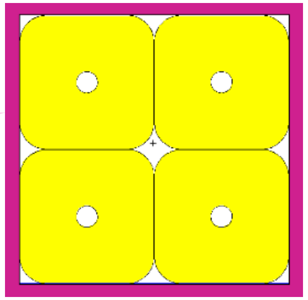

1. Sudar, S. (2002). 'TrueCoinc' software utility for calculation of the true coincidence correction (IAEA-TECDOC--1275). International Atomic Energy Agency (IAEA)
2. D.B. Pelowitz *et al.*, Tech. Rep. LA-CP-13-00634, LosAlamos National Laboratory, Los Alamos, NM, USA, 2013

^{241}Am(2n$_{th}$,f) mechanism

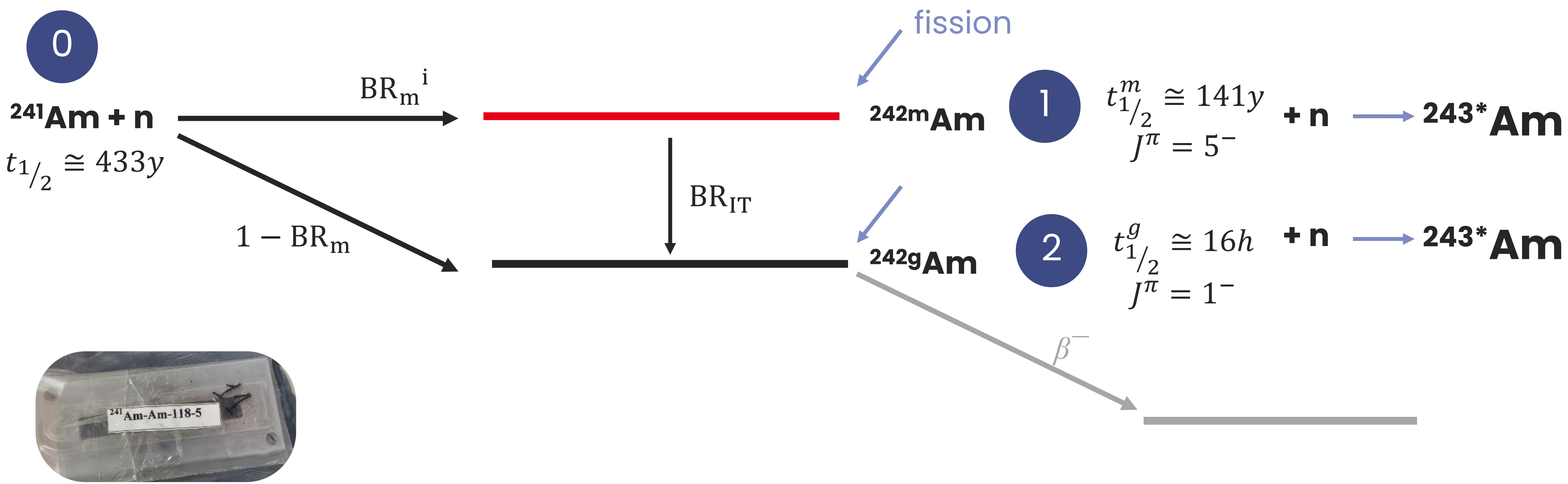

The branching ratio of **^{241}Am** is spectrum dependent

$i : BR_m = \mathbf{0.093}$

Am-241 thermal neutron capture cross section and neutron capture resonance integral from reactor activation and oscillation measurements, G. Žerovnik, G. Noguère et al., EPJ Web of Conferences 284, 01042 (2023), ND2022

Preliminary Results – ^{100}Nb from ^{241}Am(2n$_{th}$,f)

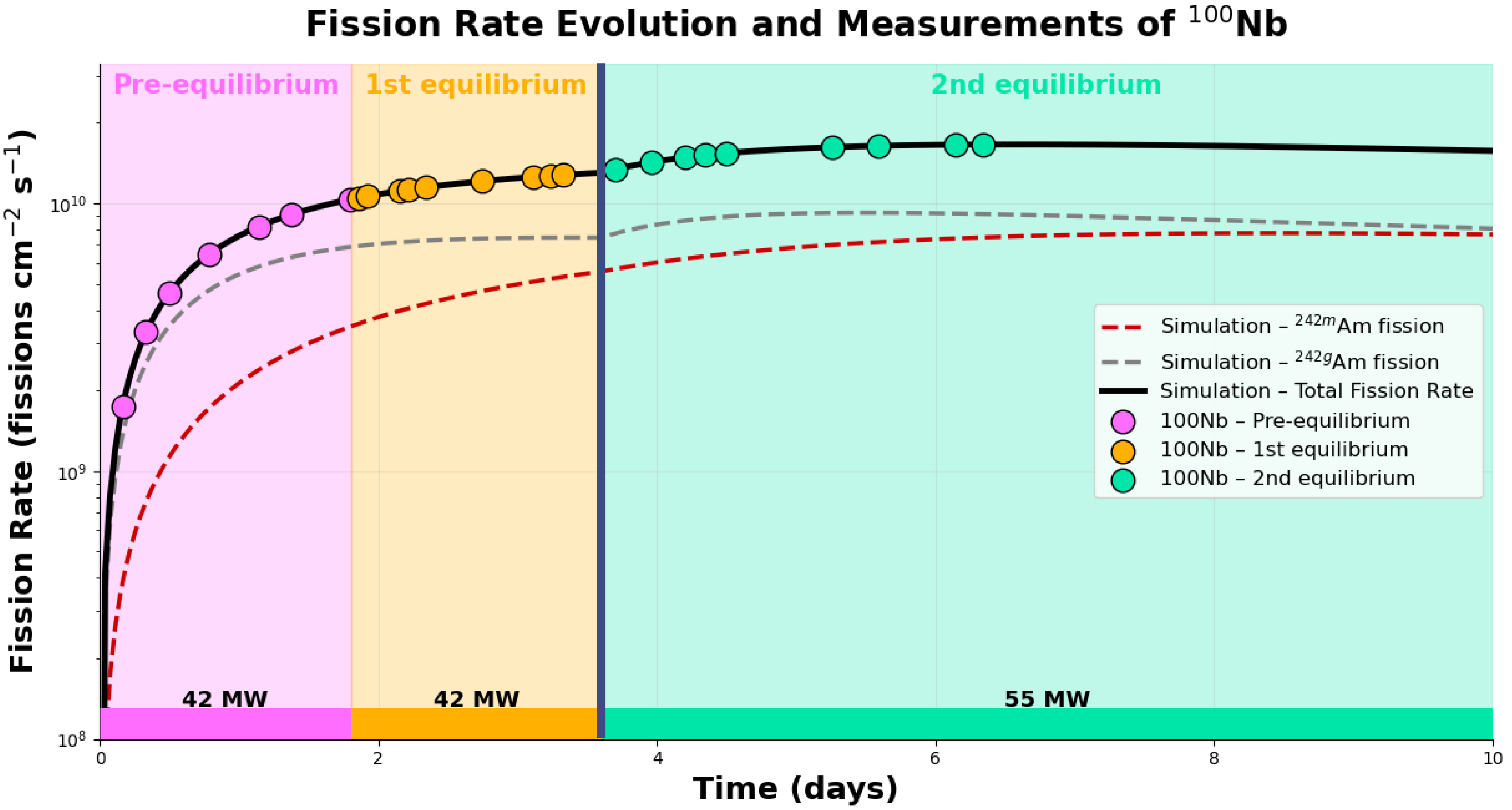

Preliminary Results – ^{100}Nb from ^{241}Am$(2n_{th},f)$ IR(t)

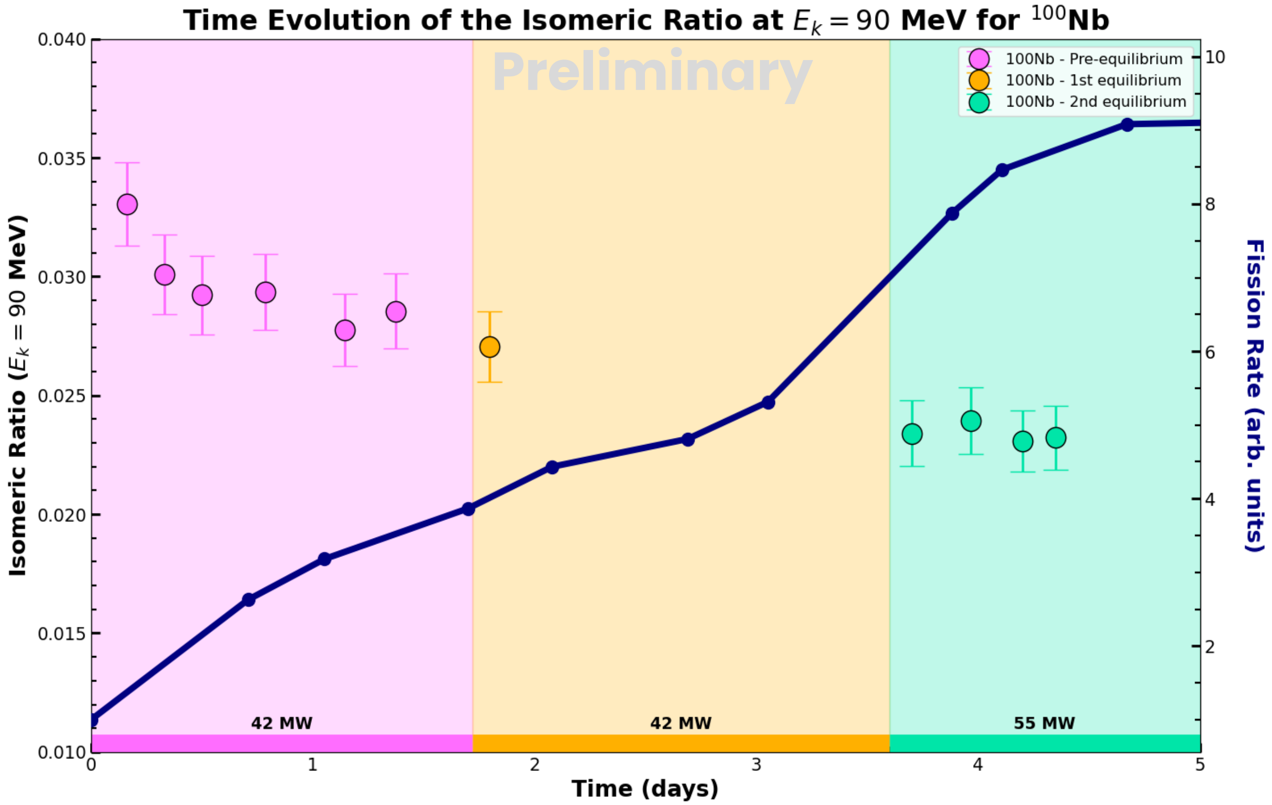

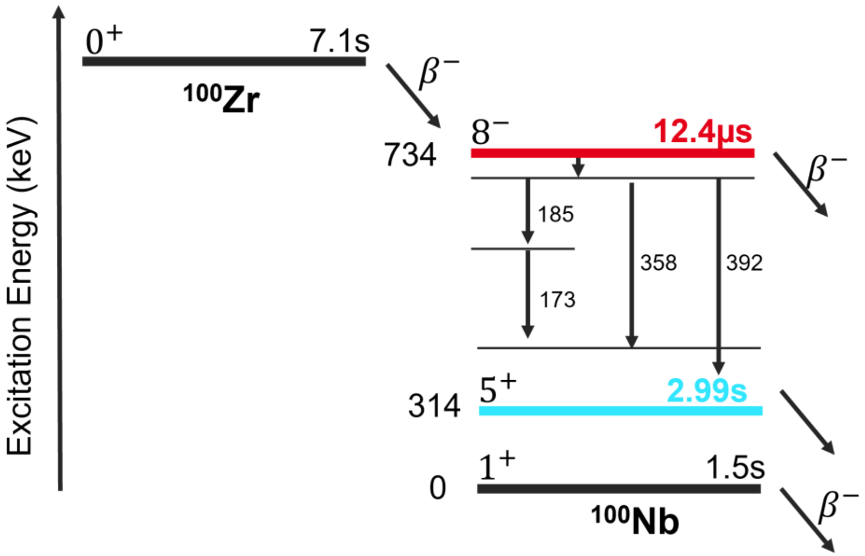

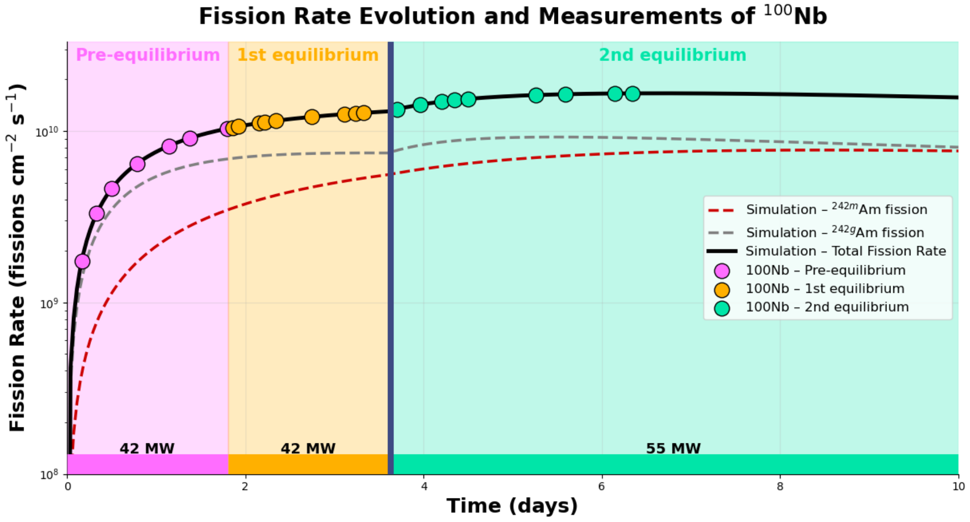

$J^{\pi} = 8^-$

$t^{m}_{1/2} \cong 12\ \mu s$

Preliminary Results – ^{100}Nb from ^{241}Am(2n$_{th}$,f)

IR(t)

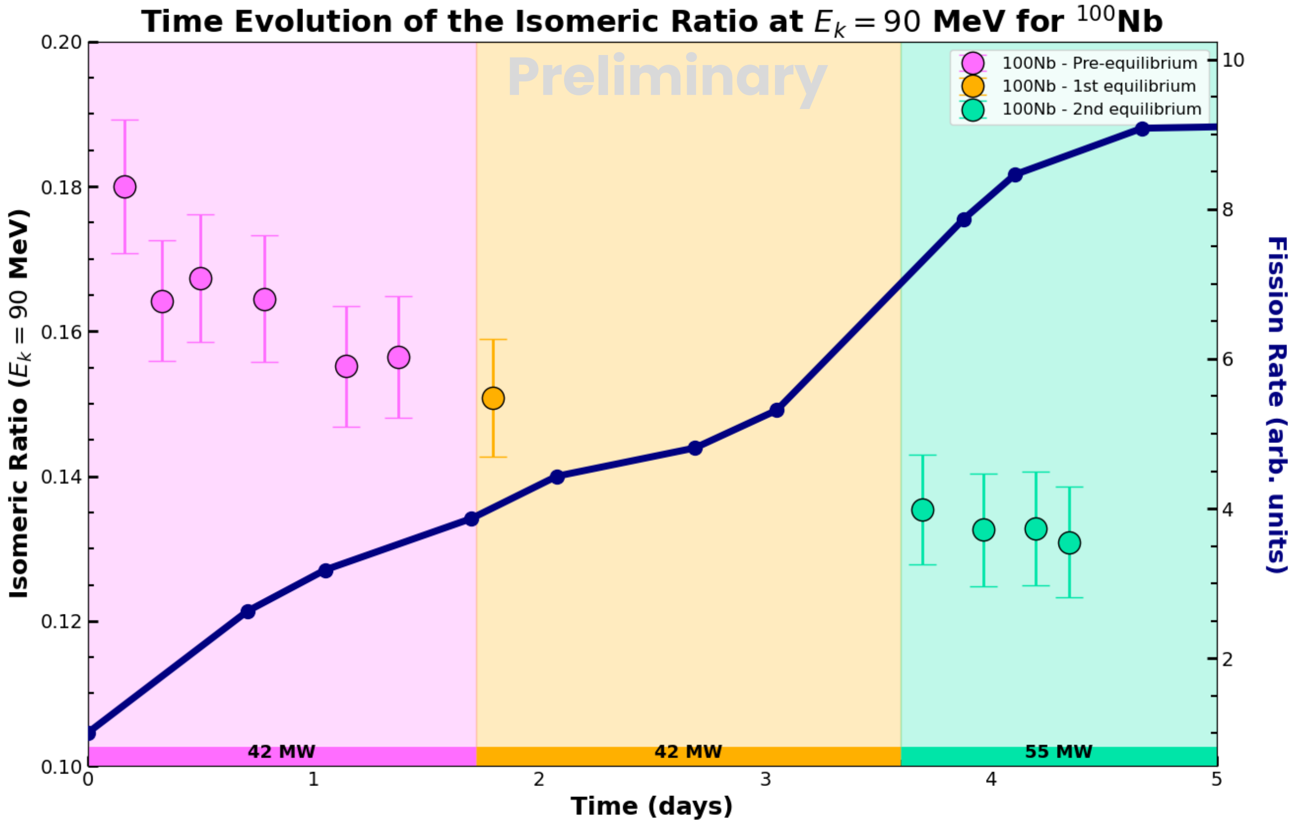

$J^{\pi} = 5^{+}$

$t^{m}_{1/2} \cong 3$ s

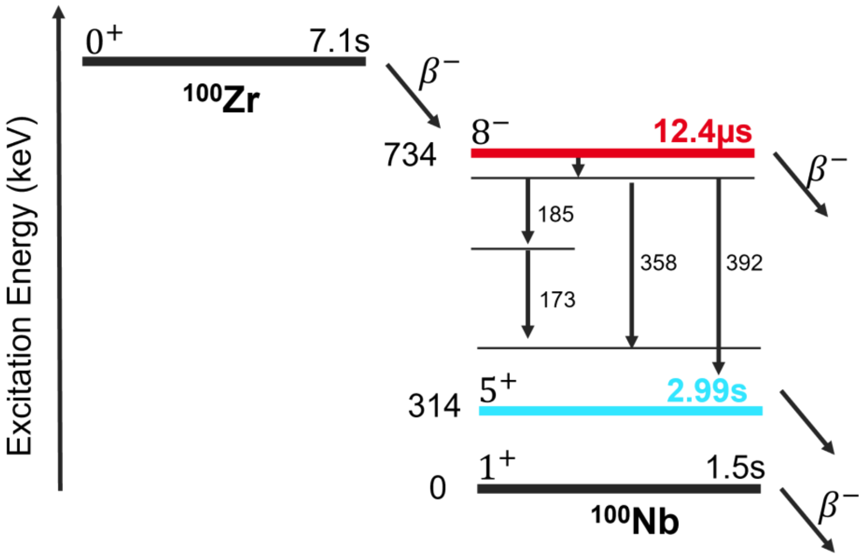

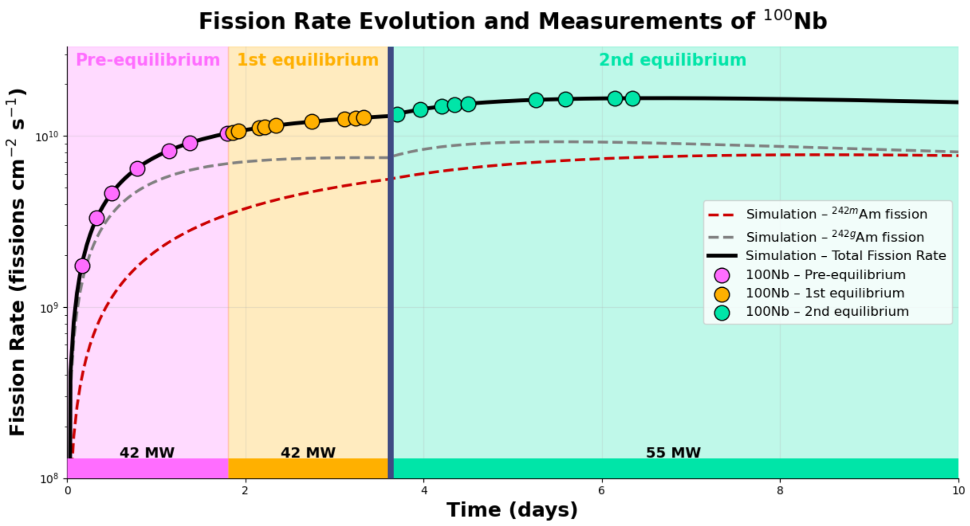

Preliminary Results – ^{100}Nb from ^{241}Am($2n_{th}$,f) IR(KE)

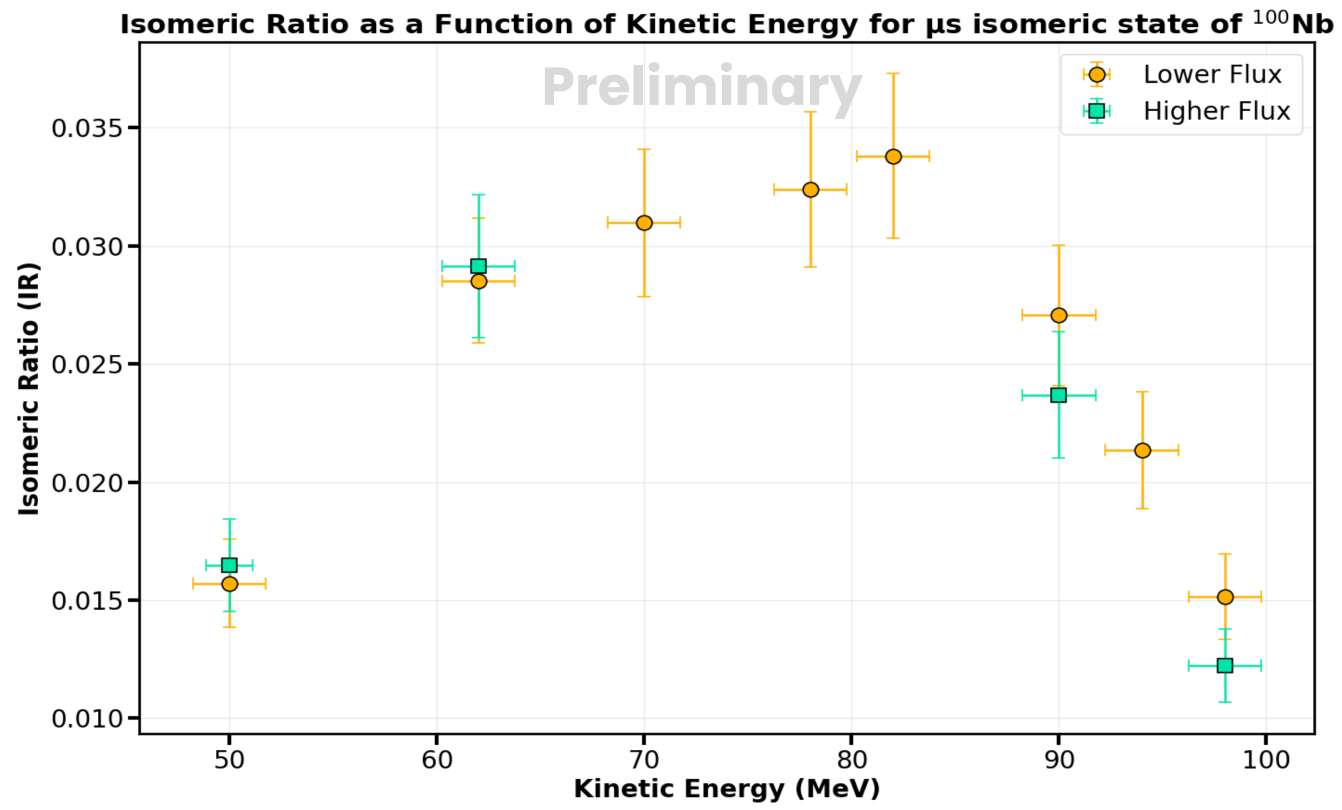

$J^{\pi} = 8^{-}$
$t^{m}_{1/2} \cong 12\ \mu s$

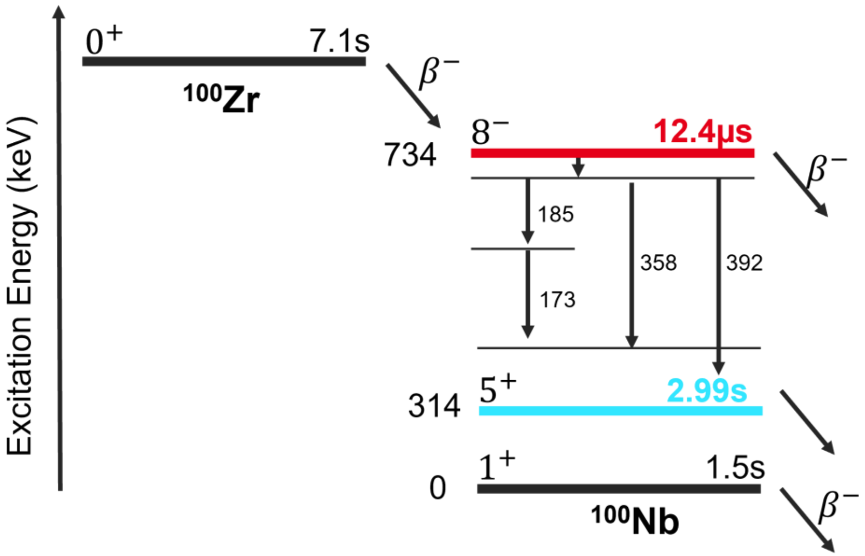

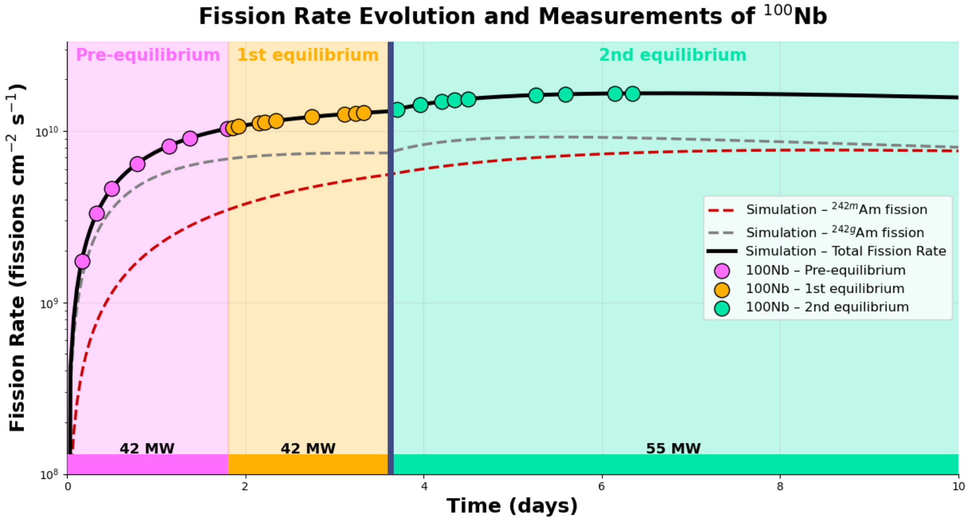

Preliminary Results – ^{100}Nb from ^{241}Am(2n$_{th}$,f)

IR(KE)

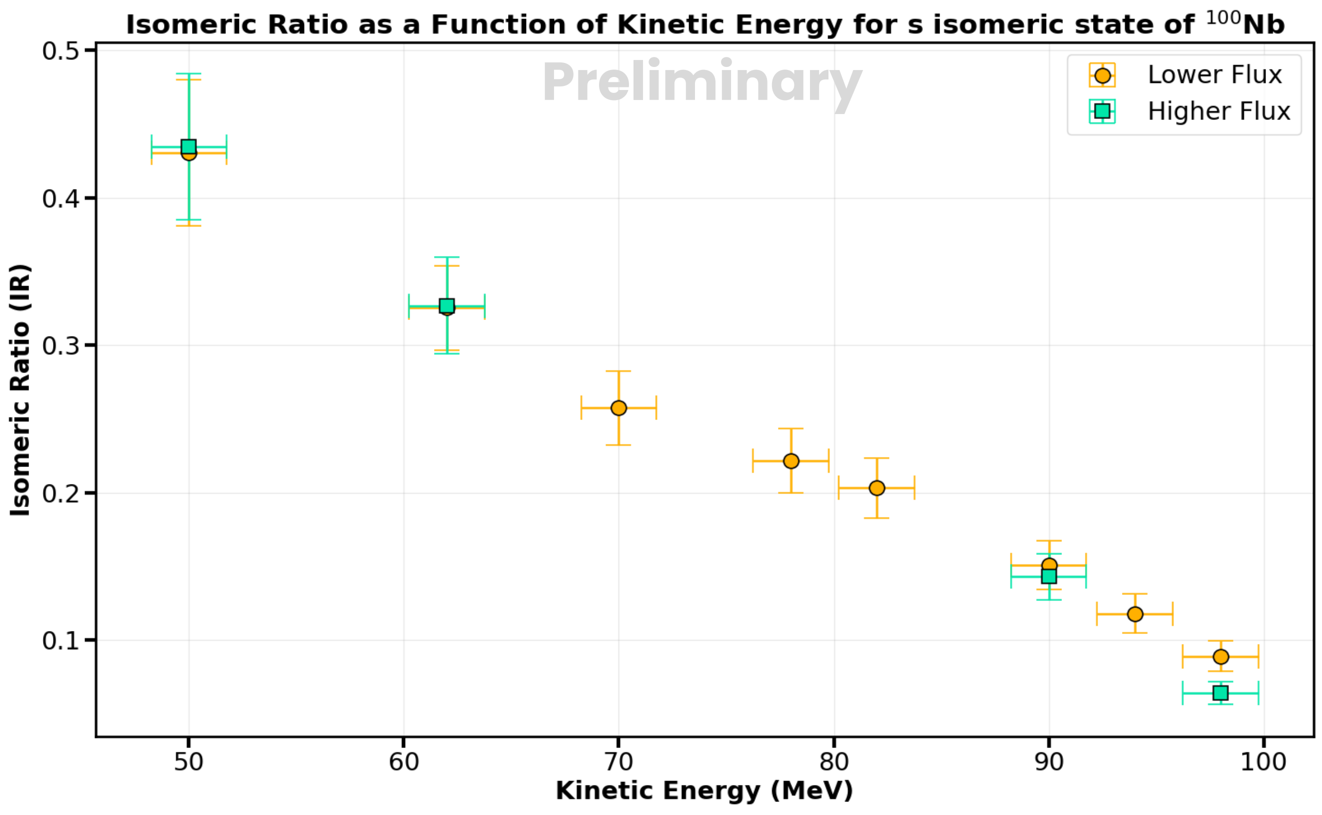

$J^{\pi} = 5^{+}$

$t^{m}_{1/2} \cong 3\ s$

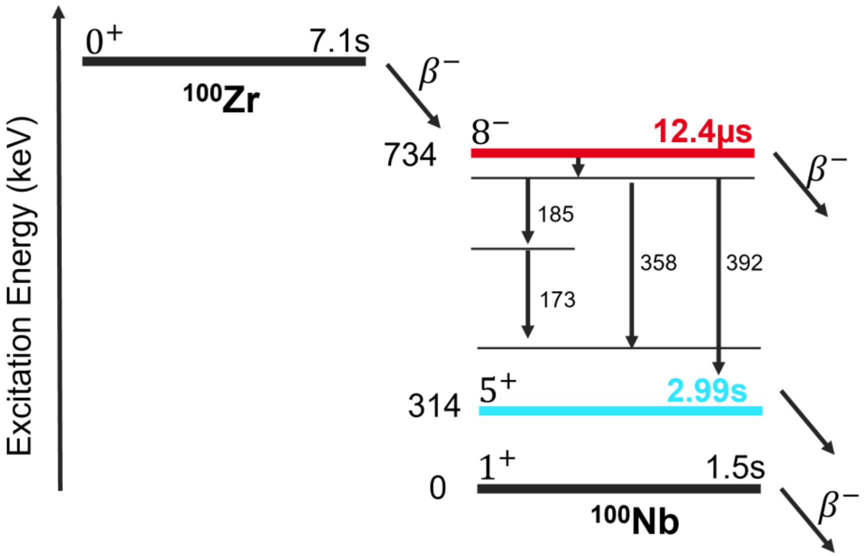

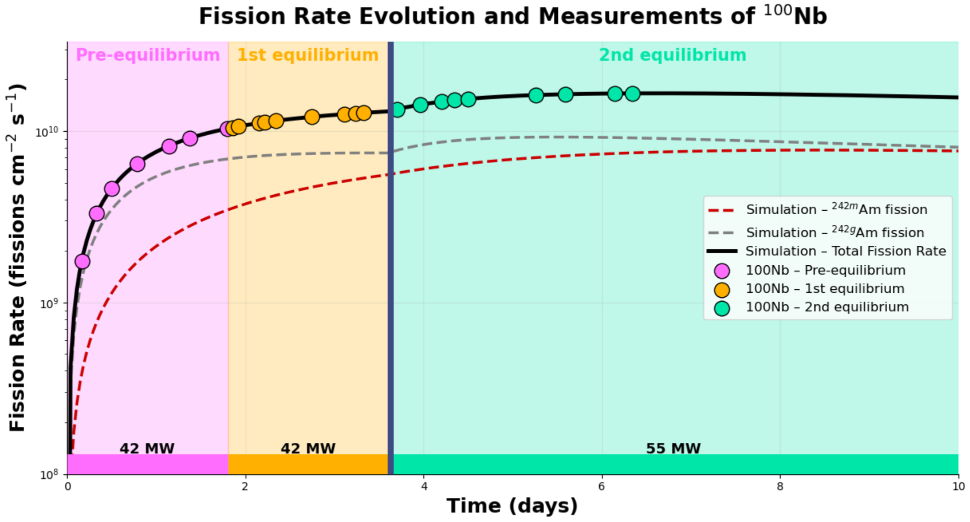

Future prospects

Absolute efficiency & correction factors → Consistent analysis of the $^{241}Am(2n_{th},f)$ experiment → $IR(KE)$ → Comparison with the FIFRELIN code →

Finalise the MCNP6 simulation and compute the correction factors

Consistent analysis for the 13 masses in total measured during this experiment

Future prospects

Absolute efficiency & correction factors → Consistent analysis of the $^{241}Am(2n_{th},f)$ experiment → **IR(KE)** → Comparison with the FIFRELIN code →

Finalise the MCNP6 simulation and compute the correction factors

Consistent analysis for the 13 masses in total measured during this experiment

Upcoming experiment ^{237}**Np**$(2n_{th},f)$ **&**
Analysis of existing data for ^{239,241}**Pu**(n_{th},f)

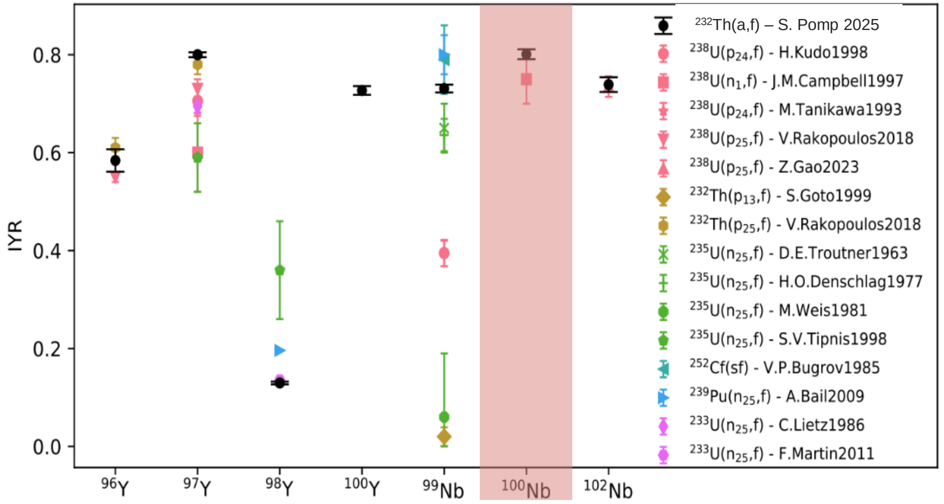

Isomeric yield ratios and mass spectrometry of Y and Nb isotopes in the neutron-rich N=60 region: The unusual case of 98Y, Physics Letters B, Cannarozzo, Pomp *et al.*

" Thank you for your attention !

Back-up

Isotopes measured at Lohengrin experiment – Oct. 2025

Isotope	$t_{1/2}$ (µs) level (NNDS)
88Br	5.3
94Y	1.35
98Y	0.78
	0.45
	6.9
	0.69
99Y	8
100Nb	12.4
109Ru	0.68
126In	26
128Sn	2.91
129Sn	2.22
	3.40
130Sn	1.61
131Sb	1.1
	4.3
	91
132Te	3.7
	28.1

Correlation Matrix IR(KE)

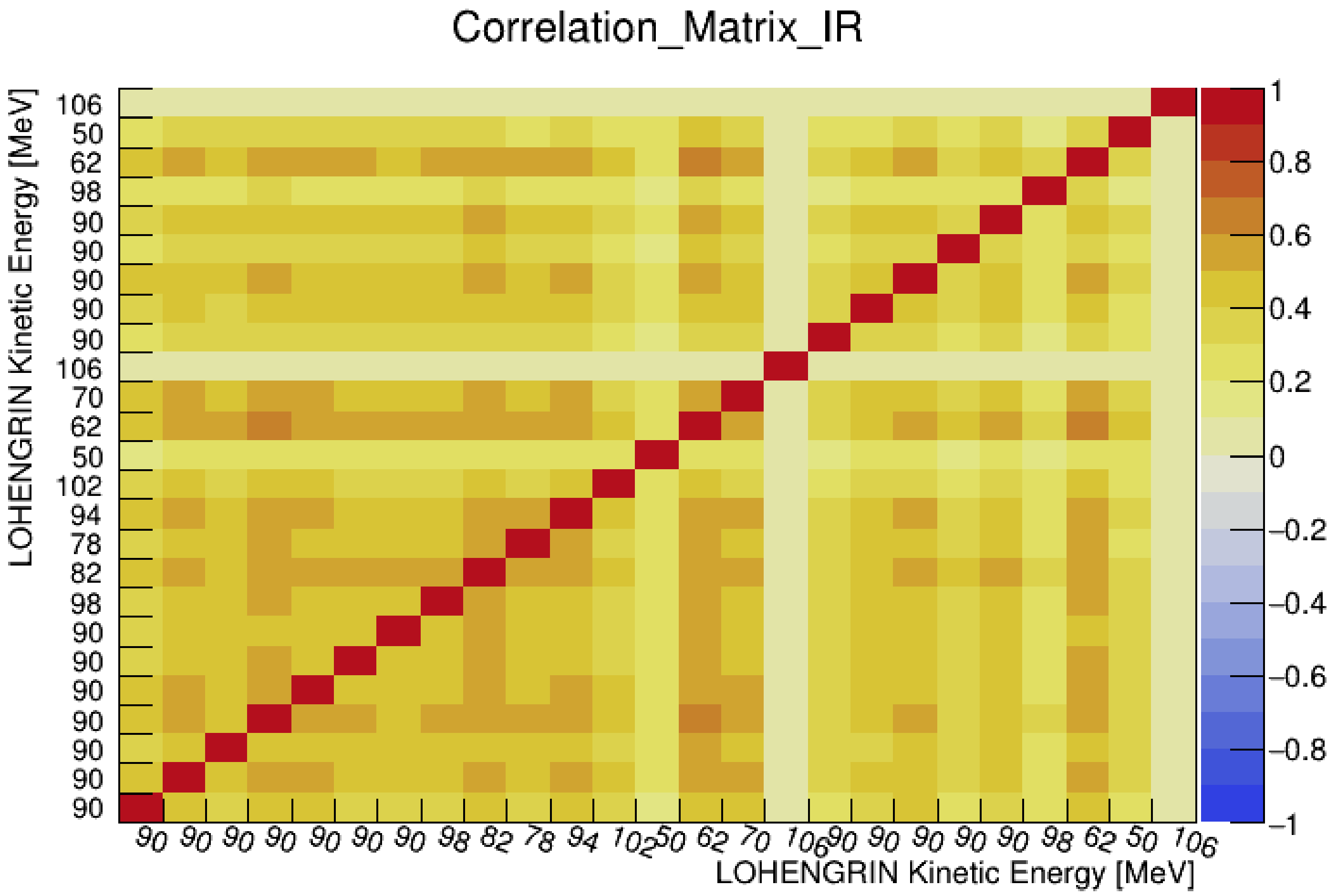

Analysis

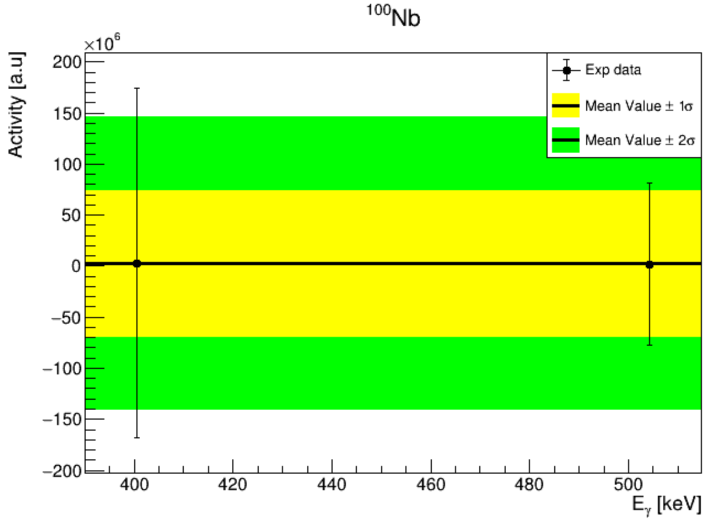

100Nb
×10^6
Activity [a.u]
Exp data
Mean Value ± 1σ
Mean Value ± 2σ
200
150
100
50
0
−50
−100
−150
−200
400
420
440
460
480
500
Eγ [keV]

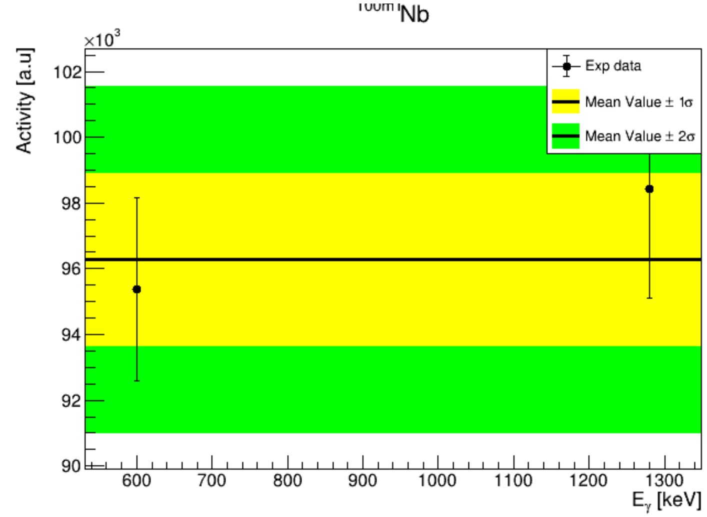

100m1Nb
×10^3
Activity [a.u]
Exp data
Mean Value ± 1σ
Mean Value ± 2σ
102
100
98
96
94
92
90
600
700
800
900
1000
1100
1200
1300
Eγ [keV]

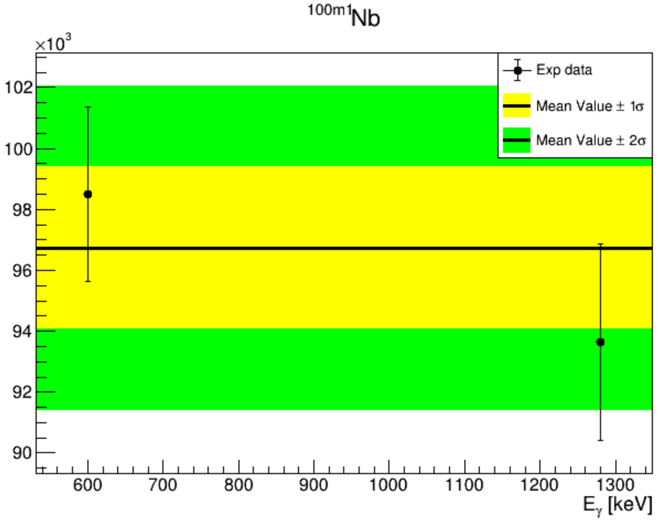

100m1Nb
×10^3
Exp data
Mean Value ± 1σ
Mean Value ± 2σ
102
100
98
96
94
92
90
600
700
800
900
1000
1100
1200
1300
Eγ [keV]

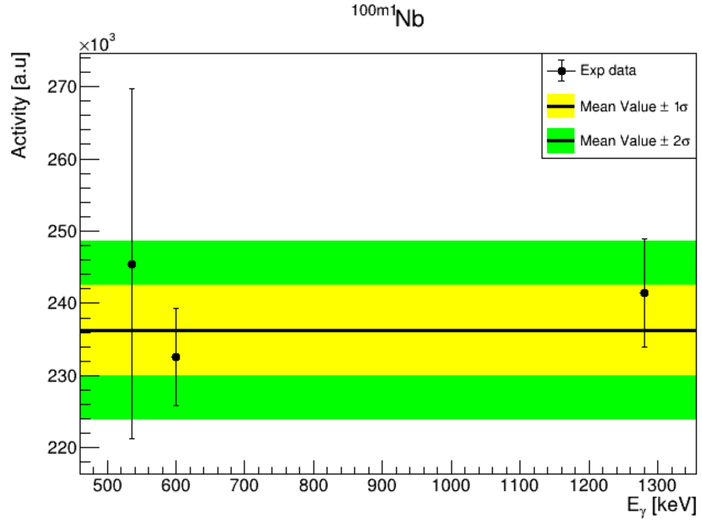

100m1Nb
×10^3
Activity [a.u]
Exp data
Mean Value ± 1σ
Mean Value ± 2σ
270
260
250
240
230
220
500
600
700
800
900
1000
1100
1200
1300
Eγ [keV]

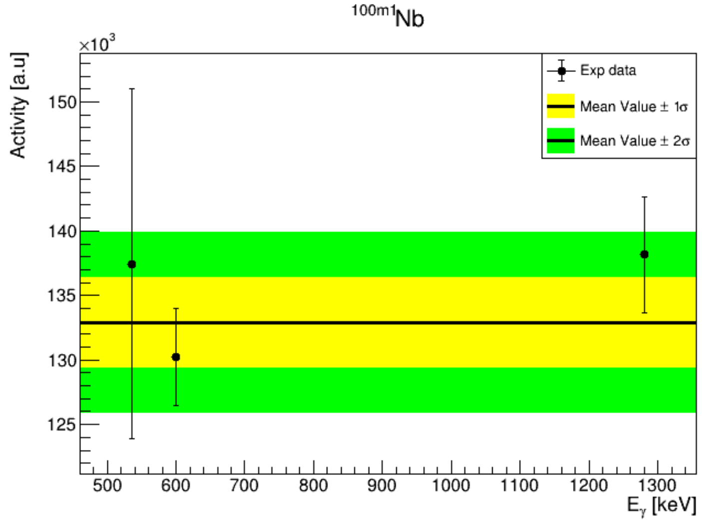

100m1Nb
×10^3
Activity [a.u]
Exp data
Mean Value ± 1σ
Mean Value ± 2σ
150
145
140
135
130
125
500
600
700
800
900
1000
1100
1200
1300
Eγ [keV]

Comparison with theoretical model (Bateman Eq.)

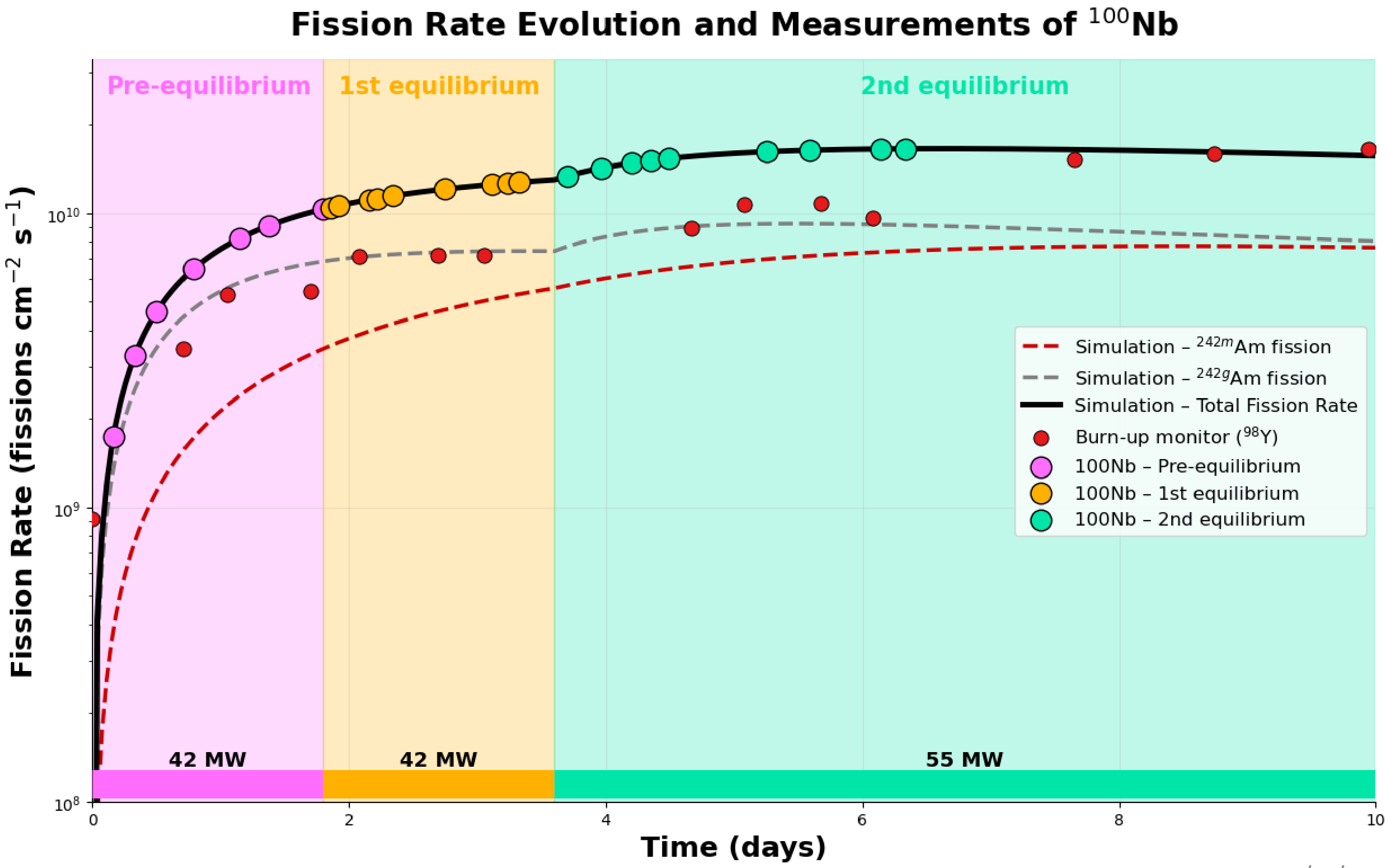

The Bateman Equation

$$\frac{dN_0}{dt} = -a_0 \times N_0$$

$$\frac{dN_1}{dt} = -a_1 \times N_1 + BR_m \times CS_{c,0} \times F \times N_0$$

$$\frac{dN_2}{dt} = -a_2 \times N_2 + (1 - BR_m) \times CS_{c,0} \times F \times N_0 + \underbrace{BR_{IT} \times \lambda_1 \times N_1}_{\text{negligible}}$$

Where

$$a_i = \lambda_i + (CS_{f,i} \times F) + (CS_{c,i} \times F)$$

$$\lambda_i : due\ to\ the\ decay$$

$$F : Flux$$

$$CS_{f,i} : Cross\ Section\ due\ to\ fission$$

$$CS_{c,i} : Cross\ Section\ due\ to\ capture$$

Analysis – Δt_{Gate} – ^{100}Nb

For which Δt_{Gate} is the $t_{1/2}$ of the isomeric level re-produced ?

$\Delta t_{Gate} \cong 40\ \mu s \cong 3^* t_{1/2,ms}$

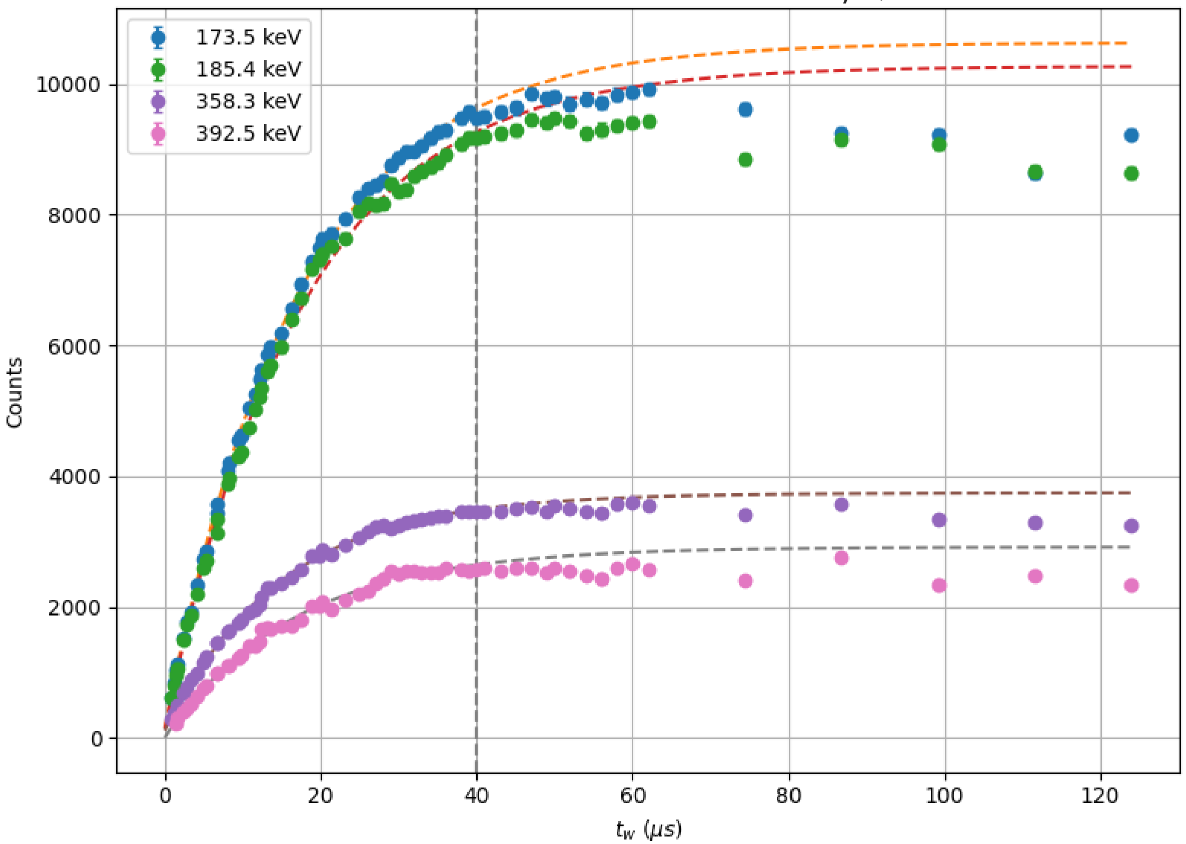

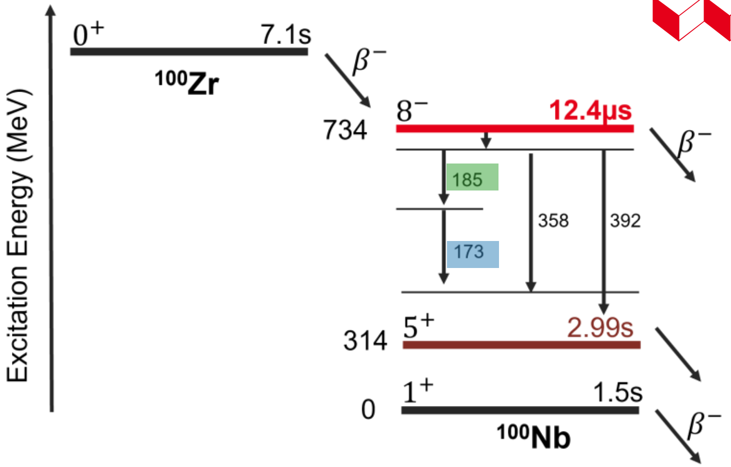

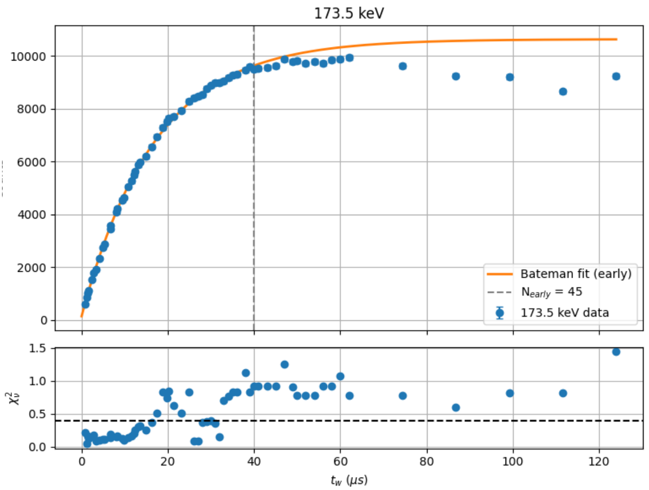

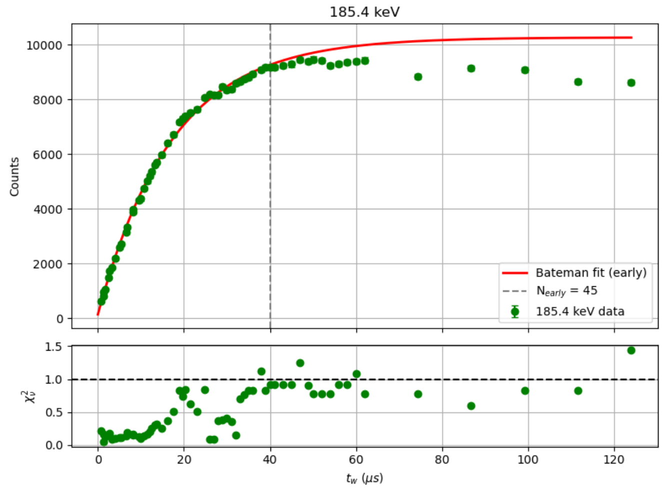

$t_{1/2}$ = 11.97 ± 0.22 µs
χ^2 / ndf = 1.35
p-value = 6.427e-02

$t_{1/2}$ = 12.27 ± 0.21 µs
χ^2 / ndf = 3.06
p-value = 9.947e-11

Importance of data shorting

Analysis – Δt_{Gate}

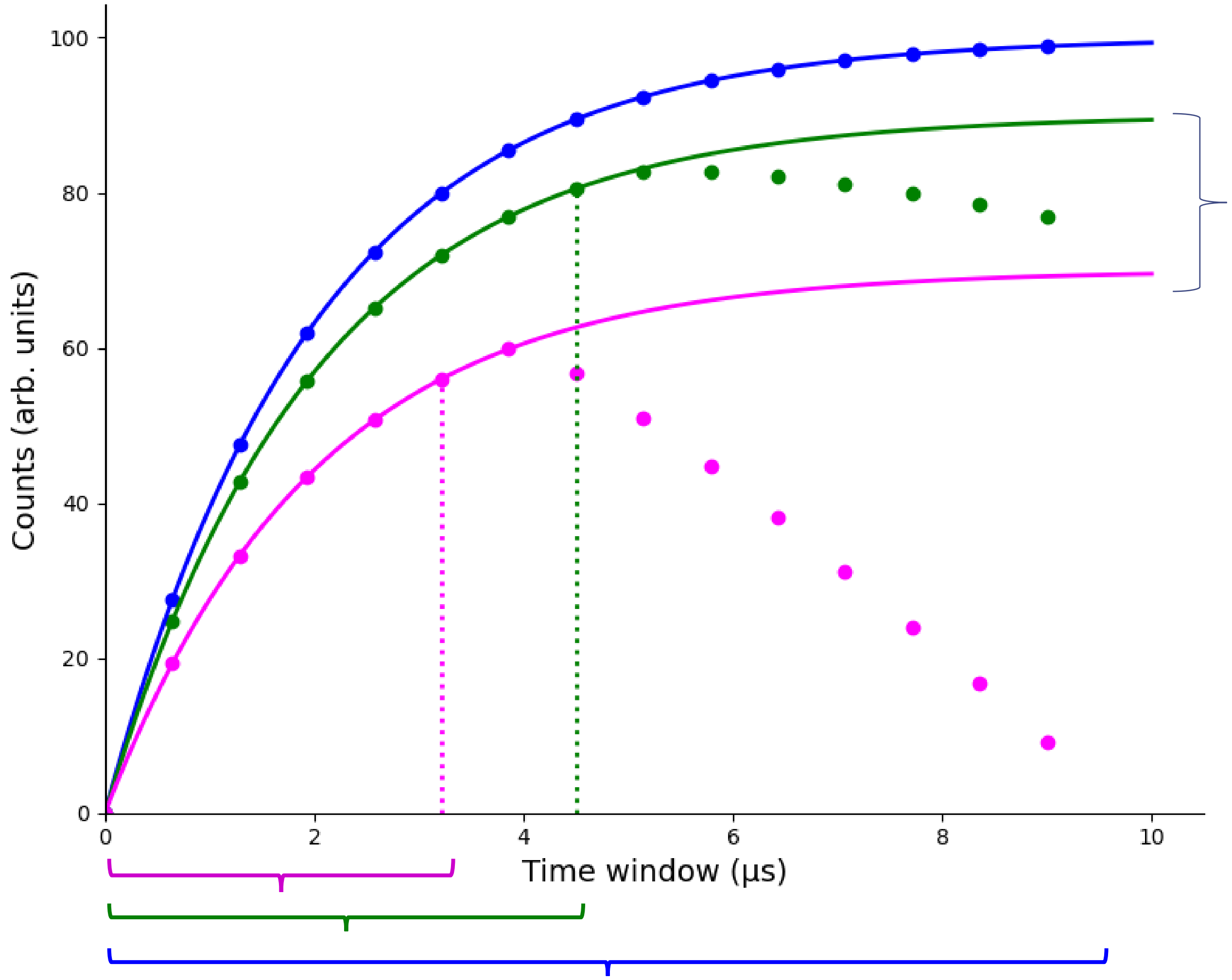

Different cases:

Short half-life of isomeric level $(< 10\mu s)$ → no correction needed

Longer half-life of isomeric level $(> 10\mu s)$ → correction needed → $\mathbf{f_{gate}}$

Fully controled analysis

^{100}Nb

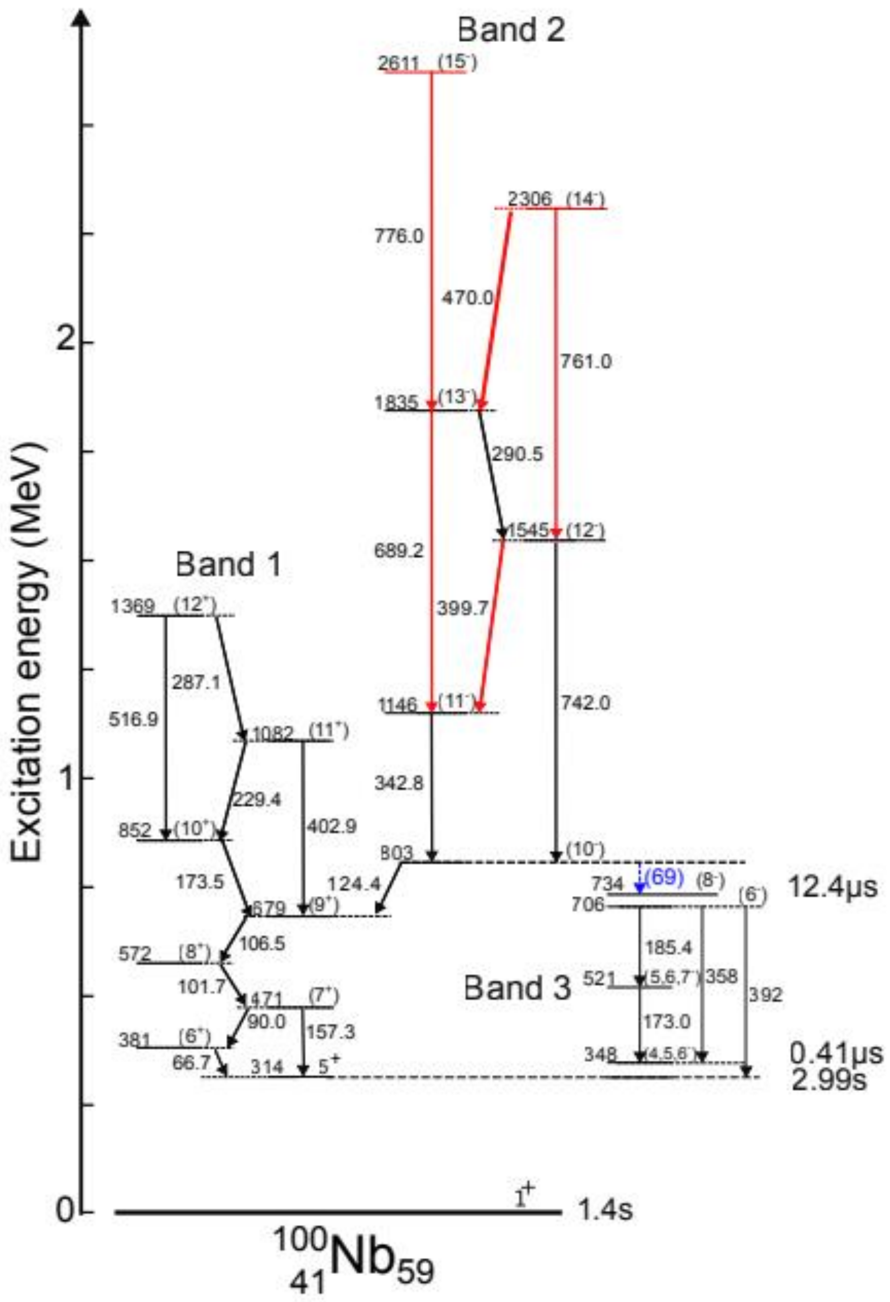
Band 2
Band 1
Band 3
Excitation energy (MeV)
2611 (15⁻)
2306 (14⁻)
776.0
470.0
761.0
1835 (13⁻)
290.5
1545 (12⁻)
689.2
399.7
1146 (11⁻)
742.0
342.8
803
(10⁻)
1369 (12⁺)
287.1
516.9
1082 (11⁺)
229.4
402.9
852 (10⁺)
173.5
124.4
679 (9⁺)
106.5
572 (8⁺)
101.7
471 (7⁺)
90.0
157.3
381 (6⁺)
66.7
314 5⁺
734 (69) (8⁻)
706
(6⁻)
12.4μs
185.4
521 (5,6,7⁻) 358
392
173.0
348 (4,5,6⁻)
0.41μs
2.99s
1⁺
1.4s
$^{100}_{41}$Nb$_{59}$

Theory…

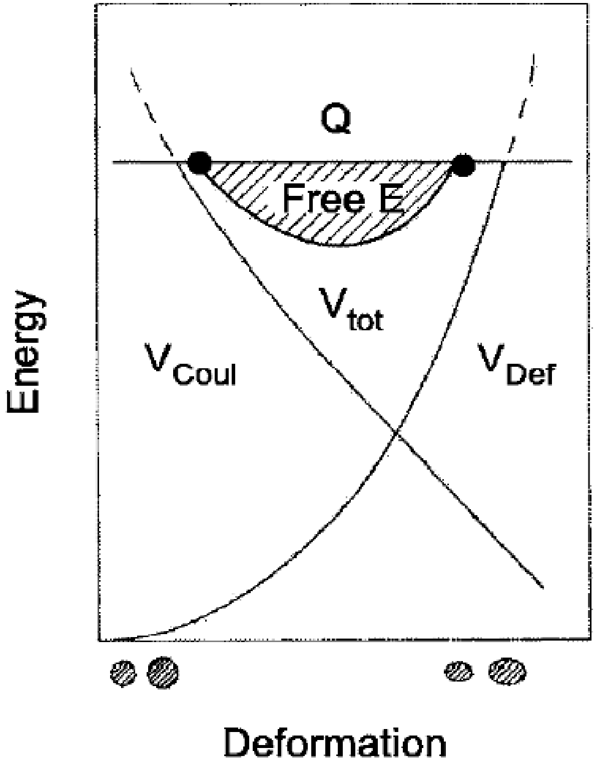

$$Q = E_{int} + V_{Coul} + V_{Def}$$

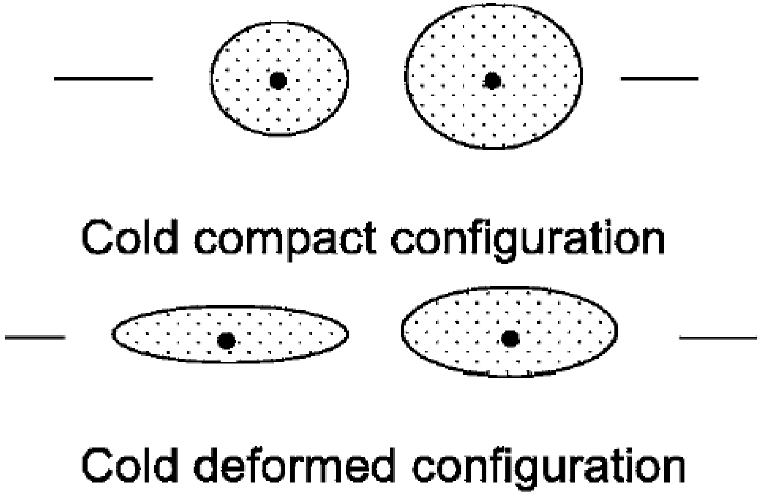

F. Gonnenwein et al., Angular Momenta of near-spherical fission fragments, Int. J Mod. Phys. E, 16,2,410-424 (2007)

Theory…

being maximal or minimal, respectively. This is because the large Coulomb repulsion in compact fission leads to high kinetic energies of the fragments while in deformed fission the smaller Coulomb repulsion entails low kinetic energies. In dedicated experiments a pronounced enhancement of odd-even effect in the charge yields both at the highest and the lowest kinetic energies of fragments was observed.[17] Since large odd-even effects reveal low intrinsic excitation energies the label "cold" given is justified.

$$Q = E_{int} + V_{Coul} + V_{Def}$$

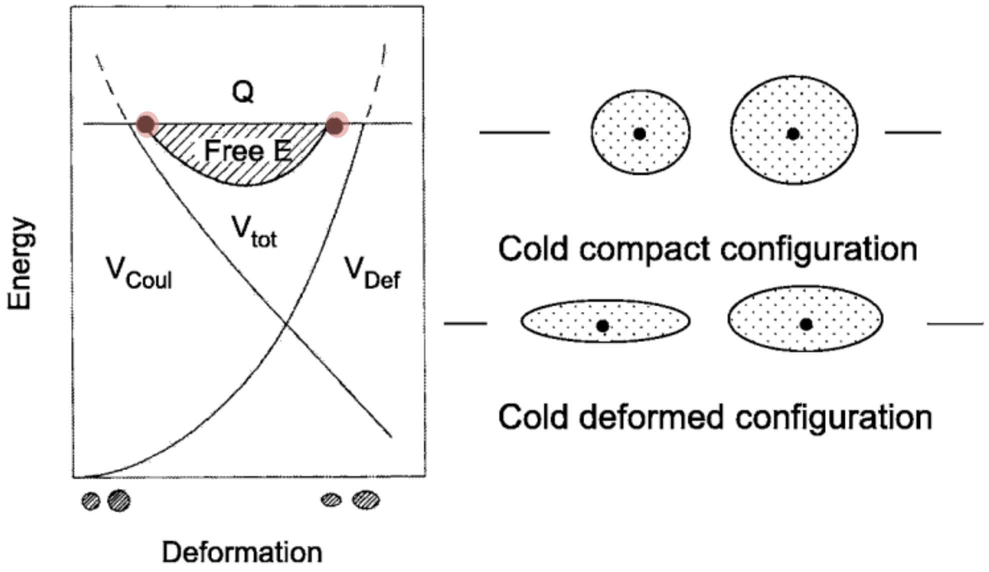

Fig. 4. Scheme of scission point model for fixed tip distance between fragments. The tip distance mimics the neck at rupture. The total potential energy V_{tot} is the sum of the Coulomb energy VCoul and the deformation energy V_{Def}. The difference (Q - V_{tot}) is called the free energy; it is available for intrinsic excitation of fragments at scission. No free energy is left at the two intersections of Q and V_{tot} as a function of fragment deformation, i.e. the fragments are cold.

F. Gonnenwein et al., Angular Momenta of near-spherical fission fragments, Int. J Mod. Phys. E, 16,2,410-424 (2007)

Investigation of fission product isomeric ratios and angular momenta of 132Sn populated in the 241Pu(nth,f) reaction

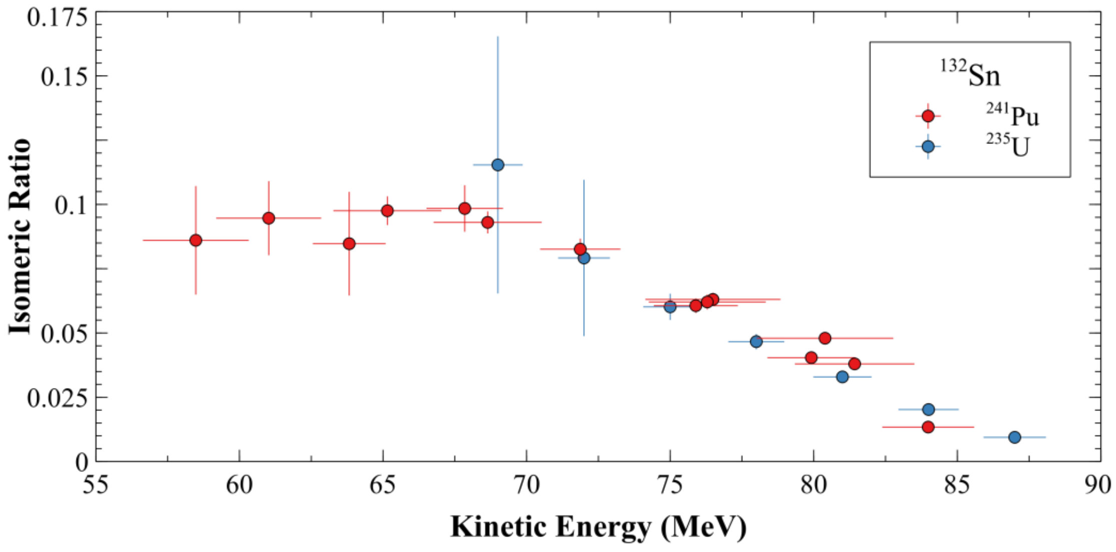

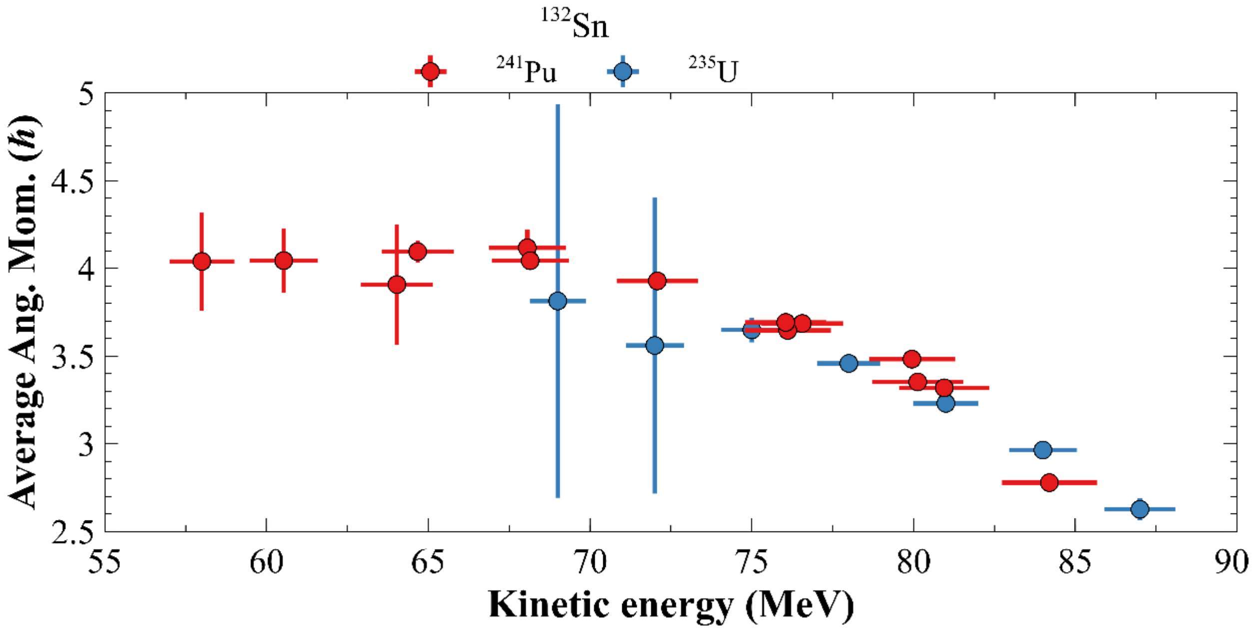

FIFRELIN: connecting experiment with theory

FIFRELIN (FIssion FRagments Evaporation modeLINg), used only as de-excitation code

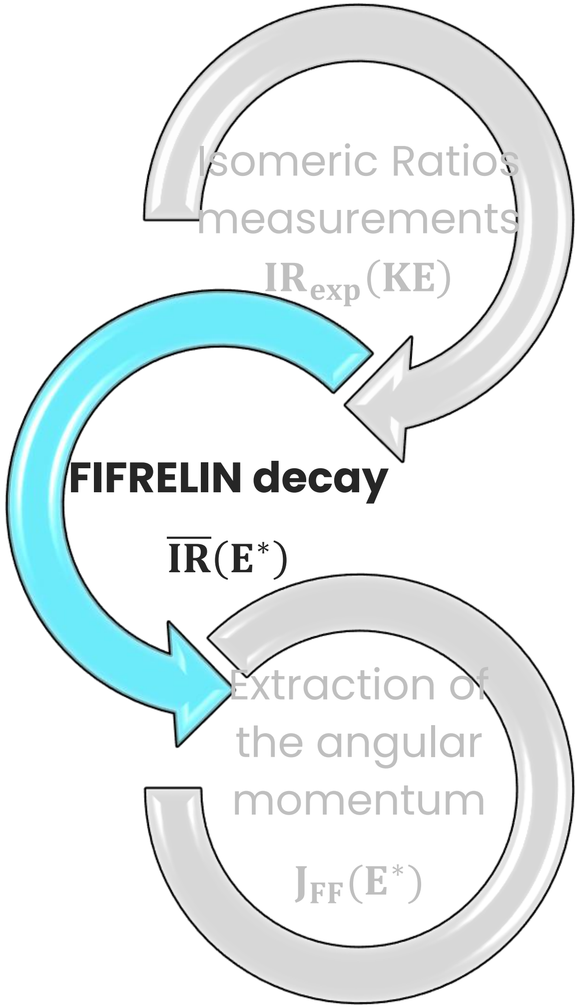

Input parameters: $\mathbf{A, Z, E^*, J^\pi}$
For particular $(\mathbf{E^*, J^\pi})$ combination: Models and experimental level schemes are used to create the nuclear schemes of the fission fragments
→ calculate the $\mathbf{IR_{FIF}(E^*, J^\pi)}$

For comparison with experimental results, they are averaged by:

$$\mathrm{IR_{FIF}(E^*, J_{cutoff})} = \sum_J \sum_\pi \mathrm{P(\pi)P(J)IR_{FIF}(E^*, J^\pi)}\text{, with:}$$

- $\mathrm{P(J)} \propto (2J+1)\exp\left(-\frac{\left(J+\frac{1}{2}\right)^2}{J_{cutoff}^2}\right)$, spin cut-off
  $\mathbf{J_{cutoff}}$ is a free parameter
- $\mathrm{P(\pi)} = \frac{1}{2}$

GOAL: extract the $\mathbf{J_{cutoff}(KE)}$ to reproduce experimental data

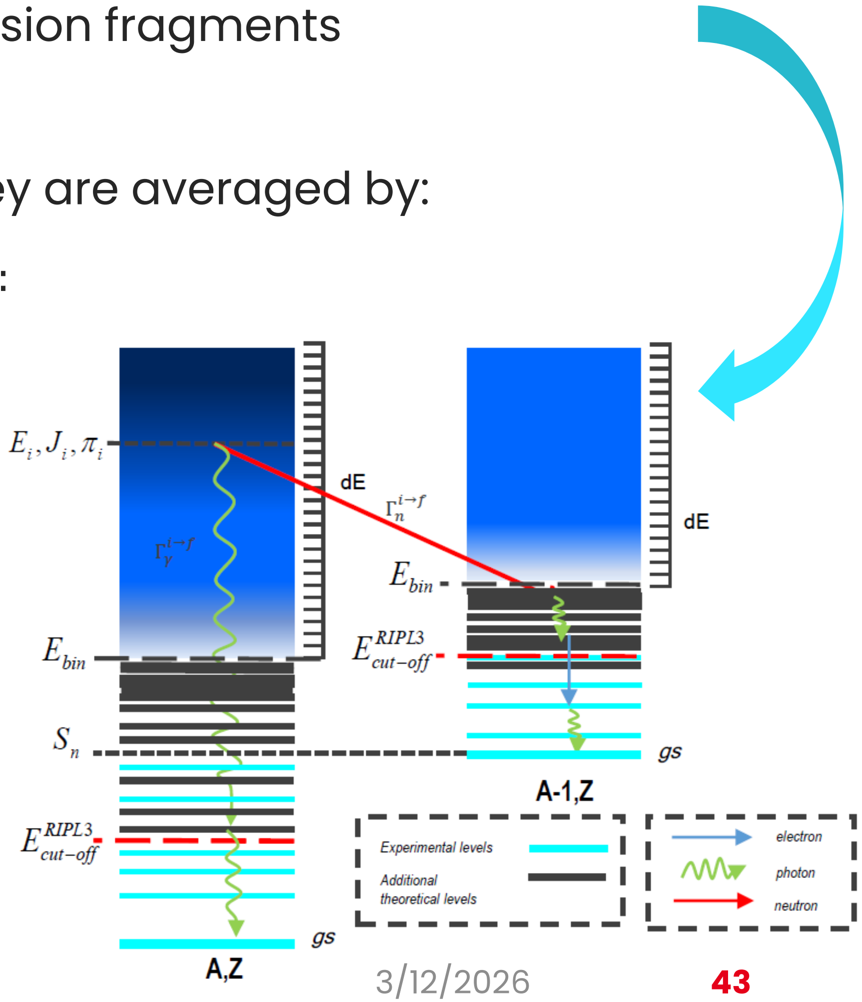

O. Litaize, O. Serot, L. Berge, The European Physical Journal A 51, 177 (2015)

Analysis

$$N_\gamma \rightarrow N_d = \frac{N_\gamma}{\varepsilon_\gamma \times I_\gamma \times f_\gamma} \xrightarrow{\text{Average}} \overline{N_d} \xrightarrow[f_{gate} \pm \sigma_{f_{gate}}]{\text{Bateman Equation Resolution}} \tau_f \xrightarrow{\text{ToF}} \boxed{IR_{exp} = \frac{\tau_f(IS)}{\tau_f(IS) + \tau_f(GS)}}$$

IR: Isomeric Ratio, IS: Isomeric State, GS: Ground State

ε_γ: Detector Efficiency,
f_γ: Correction factor for Sum-Effect,
f_{gate}: Correction factor for coincidence time gate,
will be derived from **TrueCoinc**[1] and Monte Carlo Simulation **MCNP6**[2] (in progress):

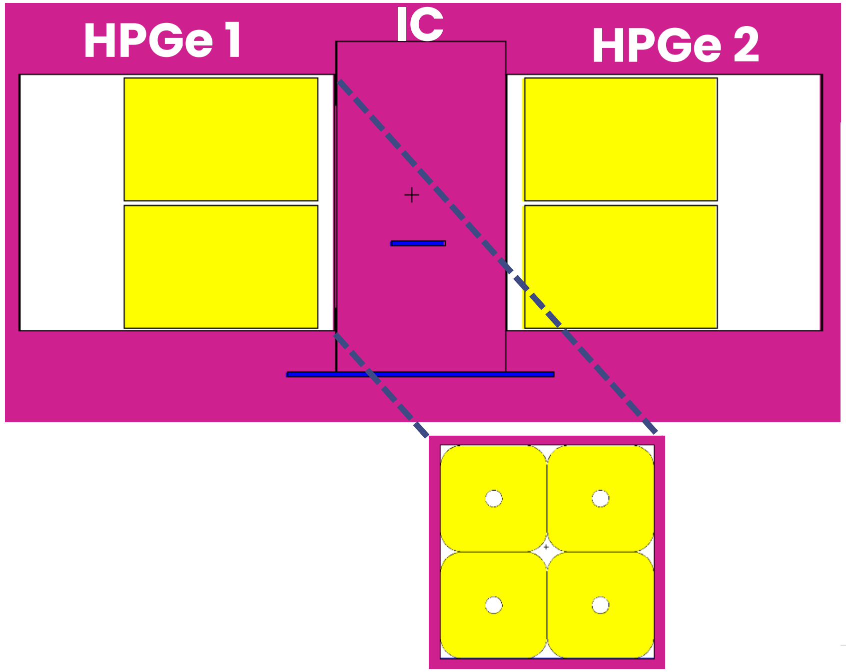

^{60}Co+^{137}Cs efficiency run

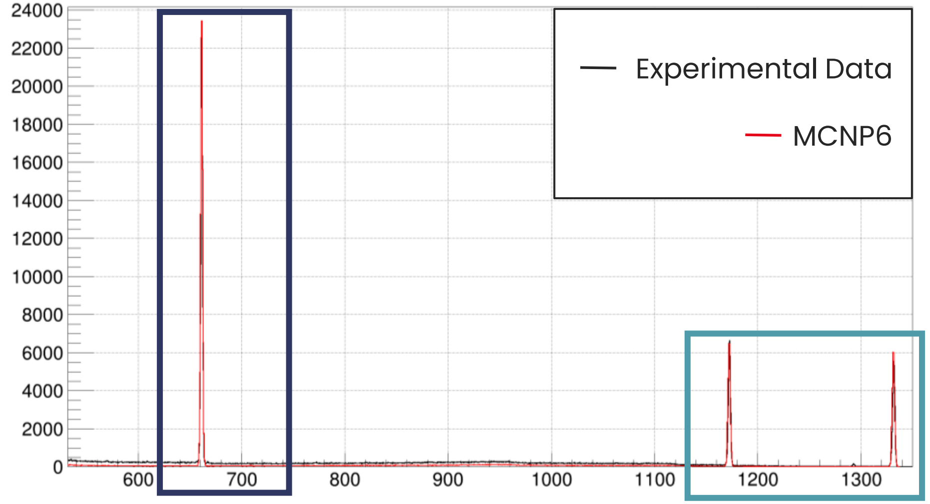

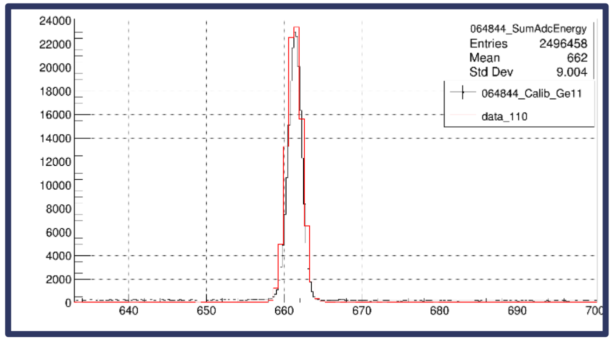

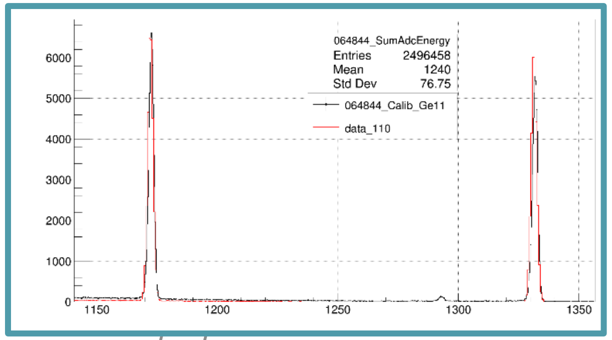

1. Sudar, S. (2002). 'TrueCoinc' software utility for calculation of the true coincidence correction (IAEA-TECDOC--1275). International Atomic Energy Agency (IAEA)
2. D.B. Pelowitz *et al.*, Tech. Rep. LA-CP-13-00634, LosAlamos National Laboratory, Los Alamos, NM, USA, 2013

Analysis: Sum-effect – TrueCoinc

Expected output:

HPGe: Co-60

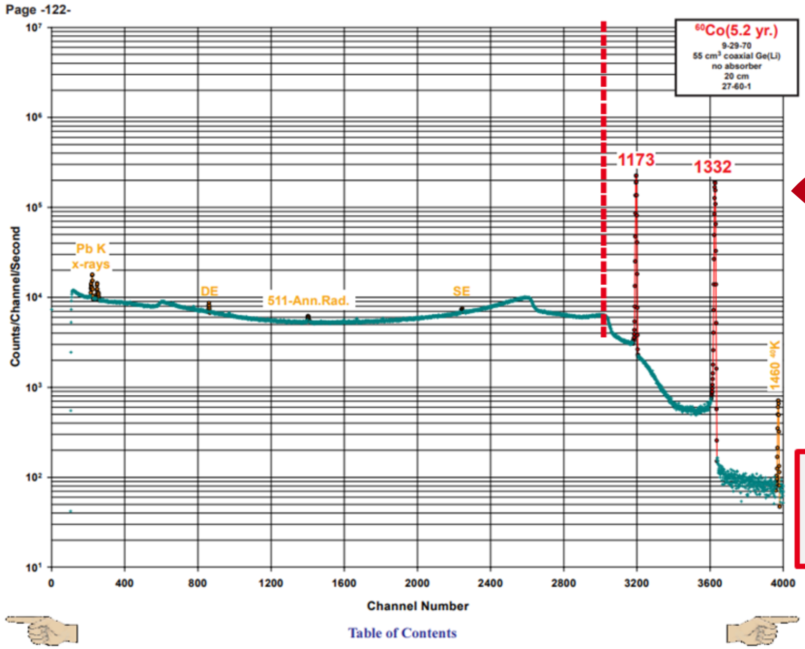

$$\varepsilon_\gamma^{ph} = \frac{N_\gamma^{ph}}{N_\gamma^{emit}}, \; \varepsilon_\gamma^{tot} = \frac{N_\gamma^{tot}}{N_\gamma^{emit}}$$

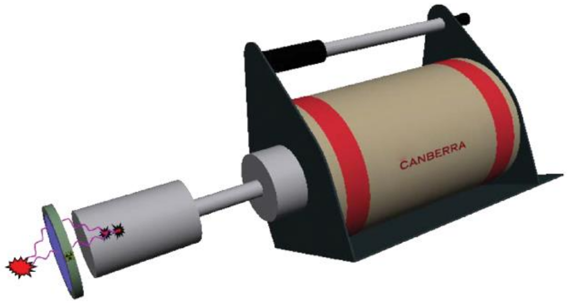

https://www.mirion.com/discover/knowledge-hub/articles/education/true-coincidence-summing

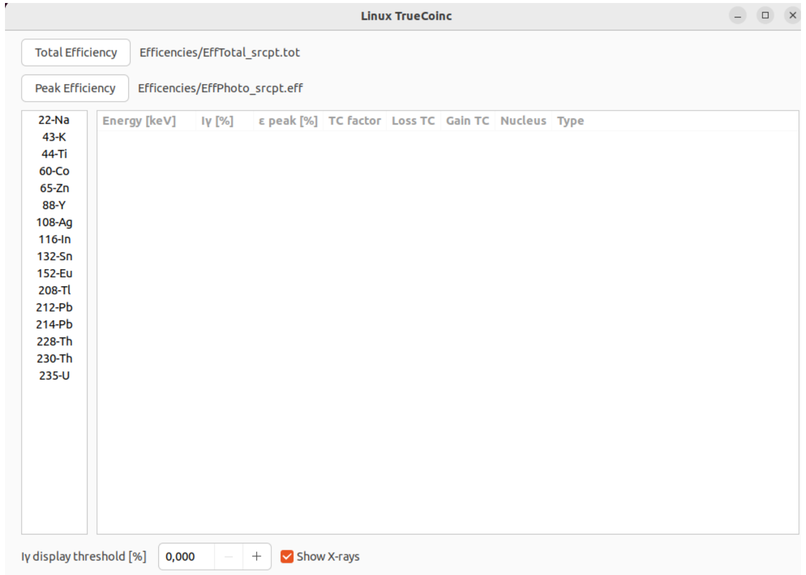

Compute the Sum-effect correction factors using **TrueCoinc**
Input: ENSDF files for decay

Olivier Meplan, LPSC, Université Grenoble-Alpes, CNRS/IN2P3, 38026 Grenoble Cedex, France

MCNP6 – ^{60}Co+^{137}Cs run

NPS 1e7

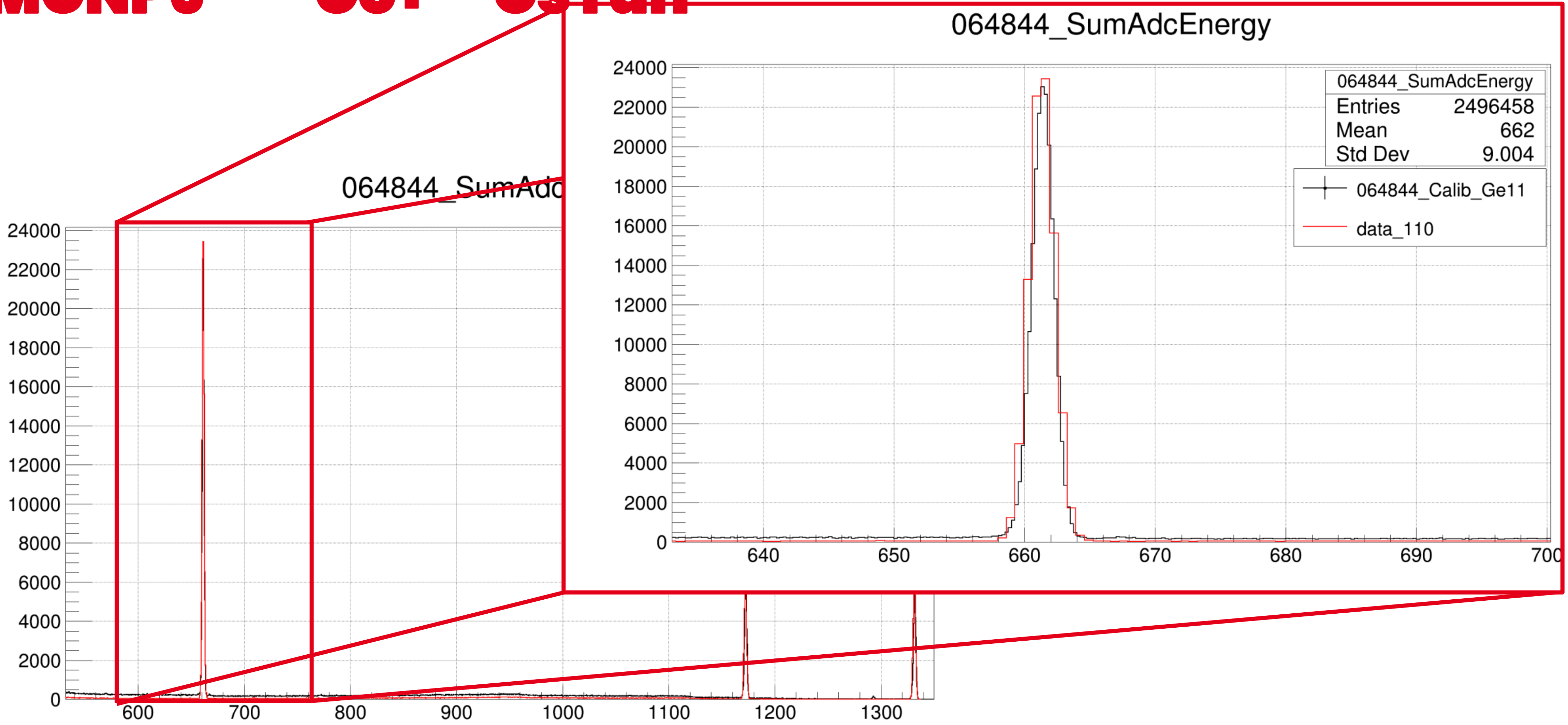

points→bins: Gaussian Energy Broadening (GEB) + same binning with experimental

GEB parameters based on specific crystal response

GEB a b c which defines **FWHM:** $FWHM(E) = a + b\sqrt{E + cE^2}$, ^{134}Te + ^{96}Y runs used

MCNP6 – $^{60}Co + ^{137}Cs$ run

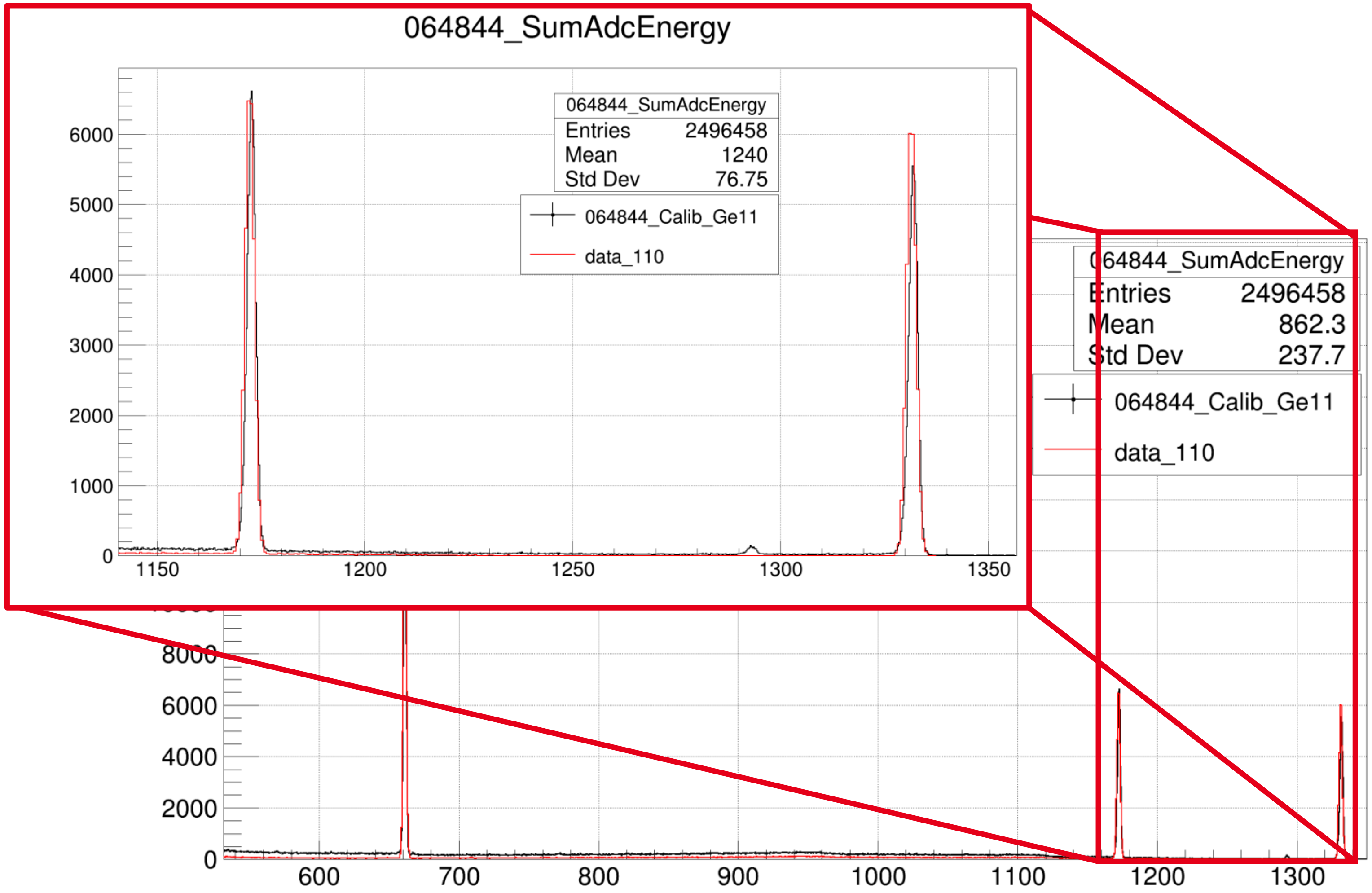

MCNP6 – ^{60}Co+^{207}Bi run

NPS 1e8

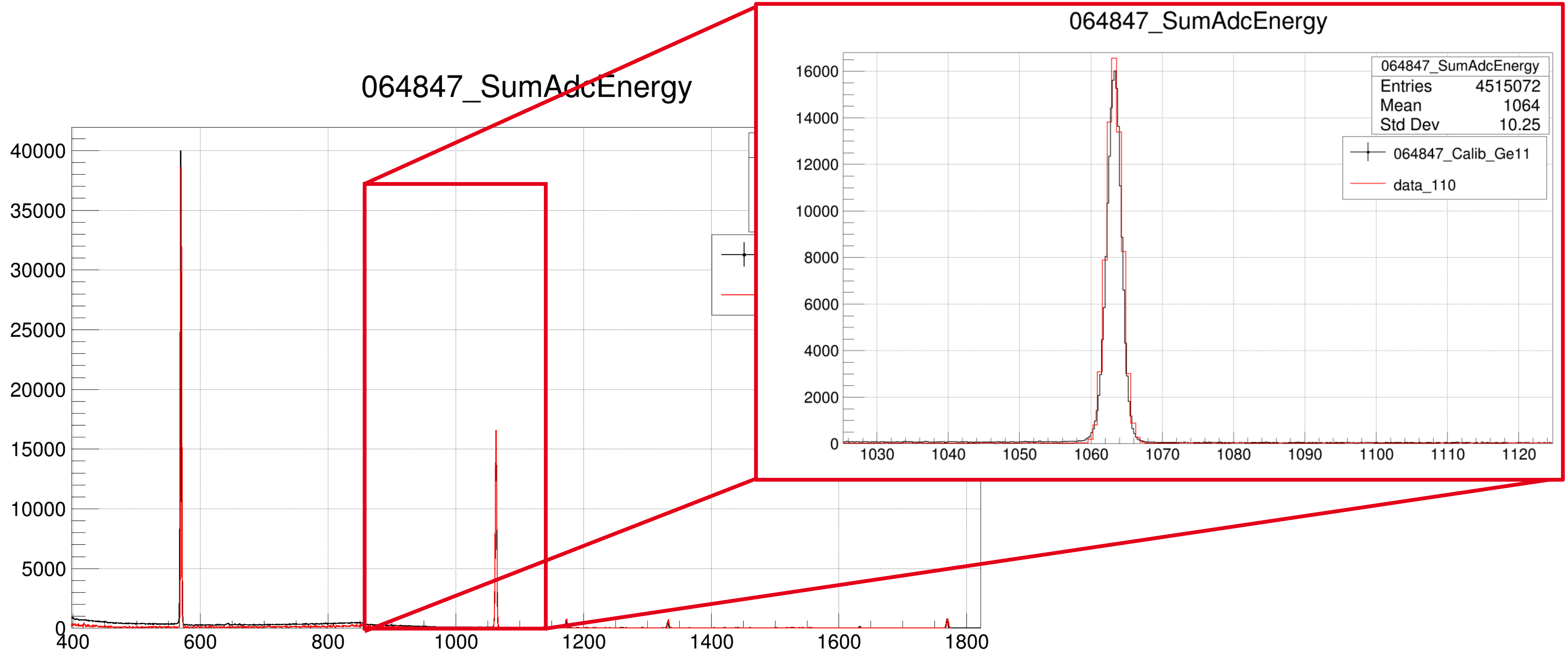

MCNP6 – ^{60}Co+^{207}Bi run

NPS 1e8

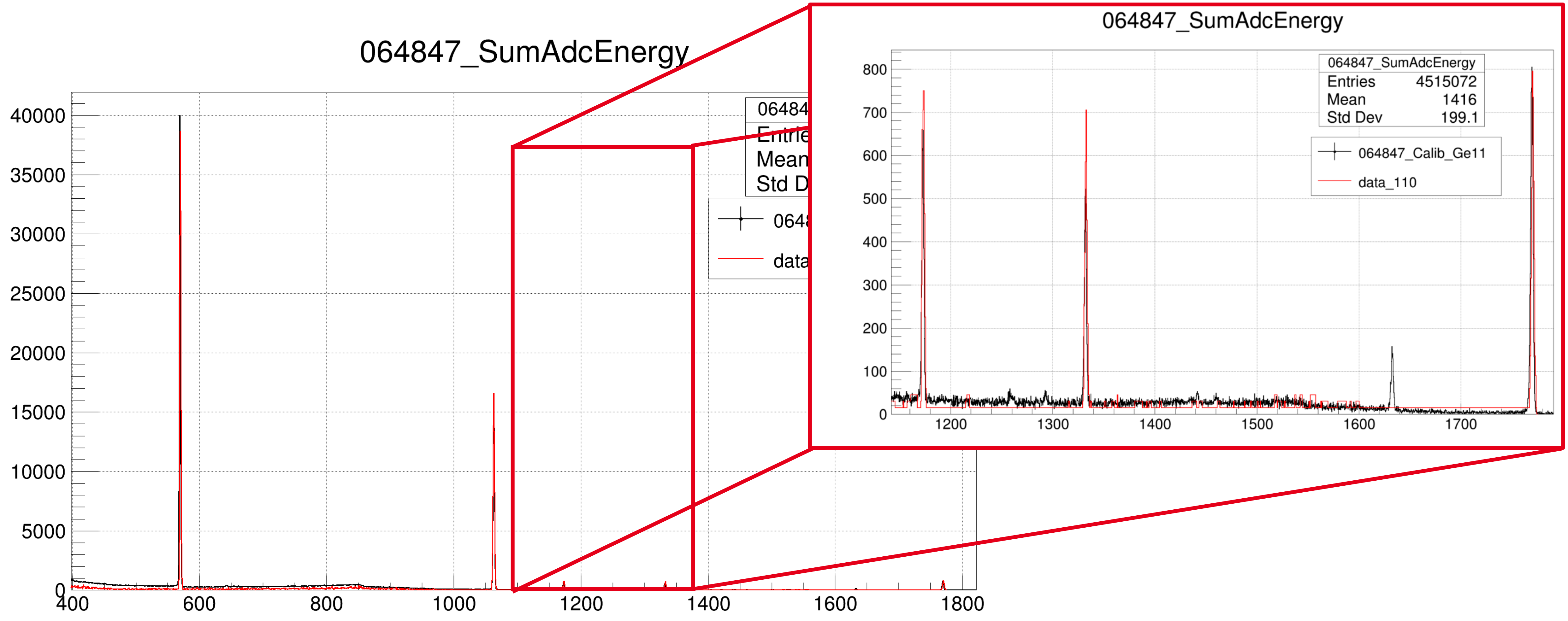

Upcoming

Nuclide	Energy [keV]	J^{π}	$T_{1/2}$ or Width Abund. [mole fract.]
$^{241}_{95}\mathrm{Am}_{146}$	0.0	5/2-	432.6 y *6*
$^{241m1}_{95}\mathrm{Am}_{146}$	2200		1.2 μs *3*

Nuclide	Energy [keV]	J^{π}	$T_{1/2}$ or Width Abund. [mole fract.]
$^{237}_{93}\mathrm{Np}_{144}$	0.0	5/2+	2.144×10^{6} y *7*
$^{237}_{93}\mathrm{Np}_{144}$	945.20 *10*	11/2,13/2	0.71 μs *4*

Nuclide	Energy [keV]	J^{π}	$T_{1/2}$ or Width Abund. [mole fract.]
$^{239}_{94}\mathrm{Pu}_{145}$	0	1/2+	24110 y *30*
$^{239}_{94}\mathrm{Pu}_{145}$	391.584 *3*	7/2-	193 ns *4*
$^{239m1}_{94}\mathrm{Pu}_{145}$	$31. \times 10^{2}$ *2*	(5/2+)	7.5 μs *10*

Nuclide	Energy [keV]	J^{π}	$T_{1/2}$ or Width Abund. [mole fract.]
$^{241}_{94}\mathrm{Pu}_{147}$	0.0	5/2+	14.329 y *29*
$^{241}_{94}\mathrm{Pu}_{147}$	161.6853 *9*	1/2+	0.88 μs *5*
$^{241m1}_{94}\mathrm{Pu}_{147}$	2200		20.5 μs *22*

New output:

t_Gate (µs)	Coincidence Entries-Ge_5	Duration (s)	Duration (µs)	Entries/t_Gate	Rate (Hz)
12.4	58470	1.74E-05	1.74E+04	4.72E+03	3.36E+09
24.8	96360	2.98E-05	2.98E+04	3.89E+03	3.23E+09
26	99944	3.10E-05	3.10E+04	3.84E+03	3.22E+09
28	105815	3.30E-05	3.30E+04	3.78E+03	3.21E+09
29	108726	3.40E-05	3.40E+04	3.75E+03	3.20E+09
30	111684	3.50E-05	3.50E+04	3.72E+03	3.19E+09
31	114665	3.60E-05	3.60E+04	3.70E+03	3.19E+09
32	117598	3.70E-05	3.70E+04	3.67E+03	3.18E+09
34	123232	3.90E-05	3.90E+04	3.62E+03	3.16E+09
35	126204	4.00E-05	4.00E+04	3.61E+03	3.16E+09
36	128944	4.10E-05	4.10E+04	3.58E+03	3.14E+09
38	134597	4.30E-05	4.30E+04	3.54E+03	3.13E+09
39	137503	4.40E-05	4.40E+04	3.53E+03	3.13E+09
40	140332	4.50E-05	4.50E+04	3.51E+03	3.12E+09
41	143035	4.60E-05	4.60E+04	3.49E+03	3.11E+09
42	145812	4.70E-05	4.70E+04	3.47E+03	3.10E+09
43	148626	4.80E-05	4.80E+04	3.46E+03	3.10E+09
44	151395	4.90E-05	4.90E+04	3.44E+03	3.09E+09
45	154118	5.00E-05	5.00E+04	3.42E+03	3.08E+09
46	156883	5.10E-05	5.10E+04	3.41E+03	3.08E+09
47	159625	5.20E-05	5.20E+04	3.40E+03	3.07E+09
48	162326	5.30E-05	5.30E+04	3.38E+03	3.06E+09
49	165048	5.40E-05	5.40E+04	3.37E+03	3.06E+09
50	167823	5.50E-05	5.50E+04	3.36E+03	3.05E+09
52	173226	5.70E-05	5.70E+04	3.33E+03	3.04E+09
54	178638	5.90E-05	5.90E+04	3.31E+03	3.03E+09
56	184156	6.10E-05	6.10E+04	3.29E+03	3.02E+09
58	189722	6.30E-05	6.30E+04	3.27E+03	3.01E+09
60	195126	6.50E-05	6.50E+04	3.25E+03	3.00E+09
62	200454	6.70E-05	6.70E+04	3.23E+03	2.99E+09

$\times 3$

$\times 4$

Target evolution

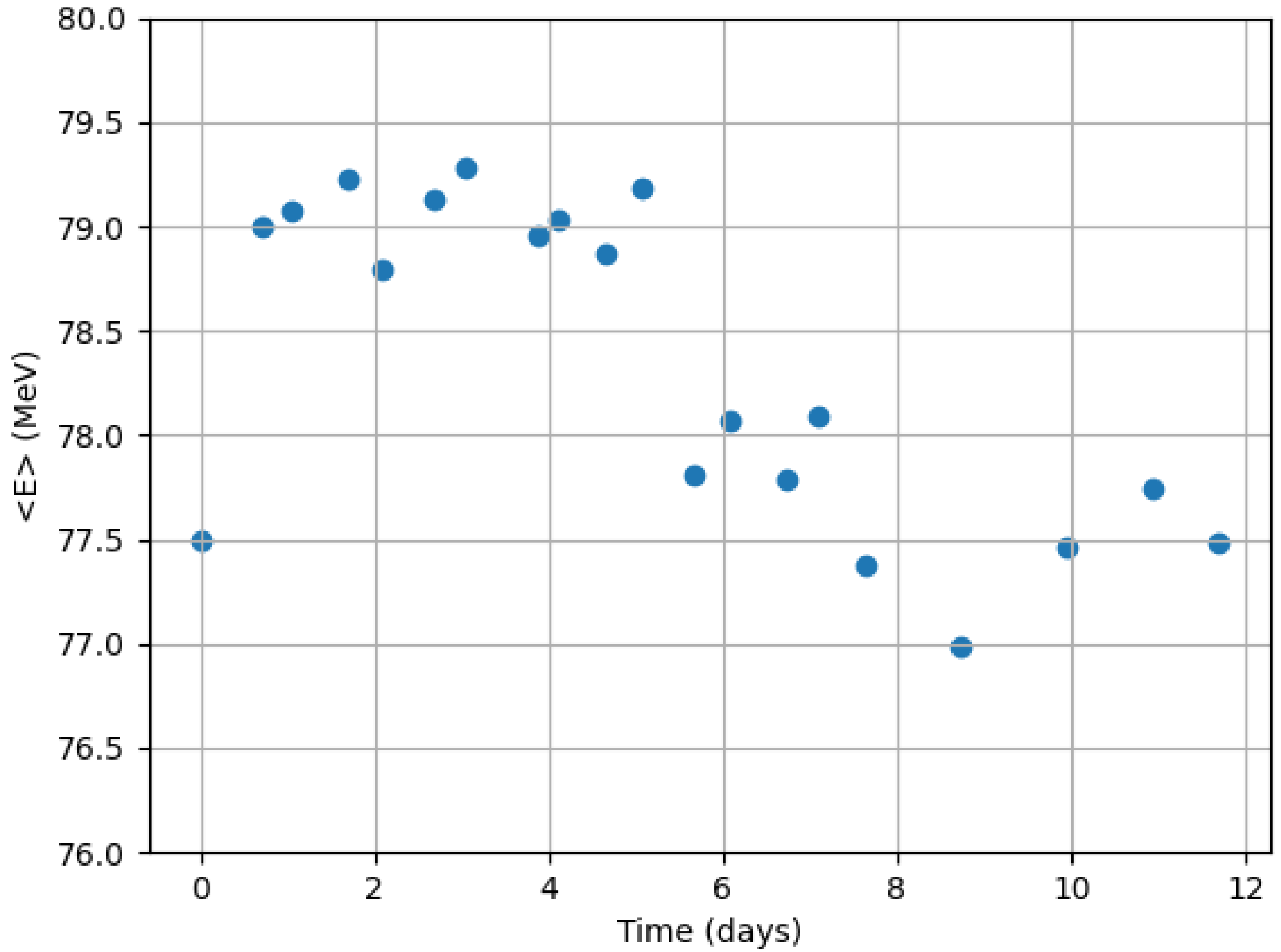

Analysis – Δt_{Gate} – ^{100}Nb

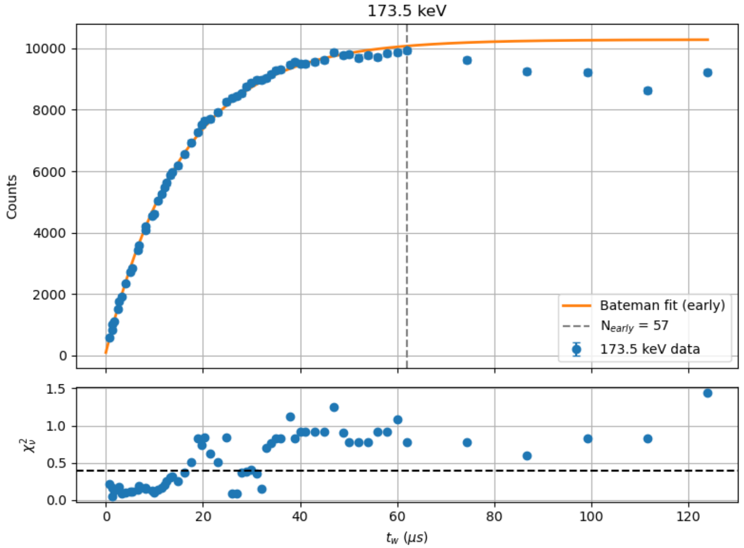

$t_{1/2}$ = 11.06 ± 0.10 μs
χ^2 / ndf = 2.14
p-value = 2.145e-06

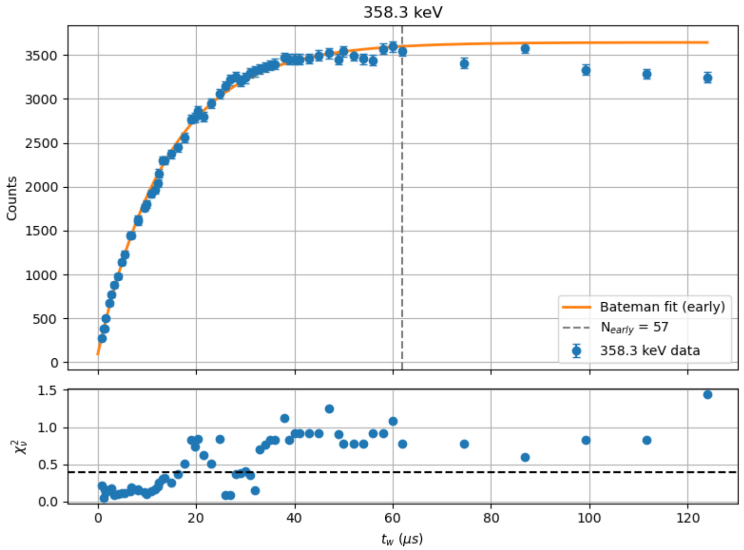

$t_{1/2}$ = 9.83 ± 0.15 μs
χ^2 / ndf = 1.31
p-value = 6.427e-02

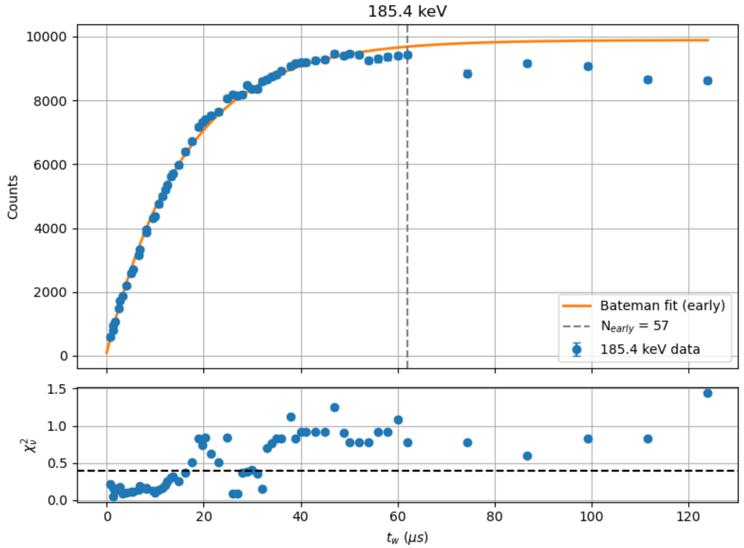

$t_{1/2}$= 11.15 ± 0.10 μs
χ^2 / ndf = 3.91
p-value = 2.987e-16

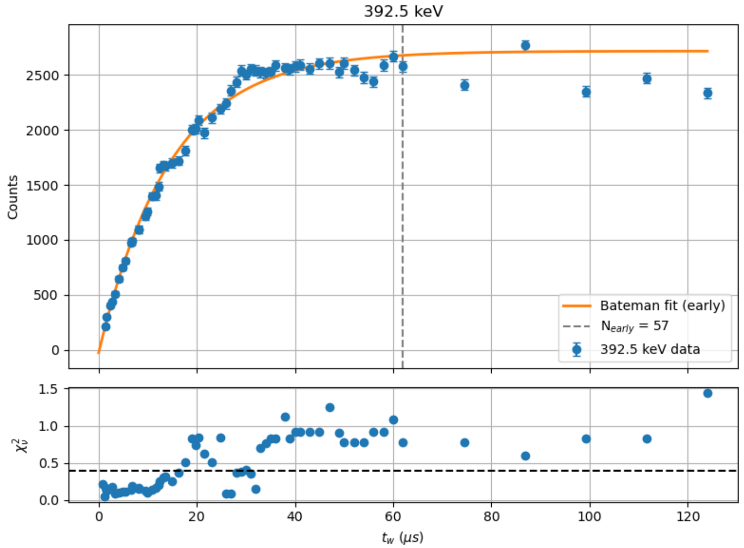

$t_{1/2}$= 10.09 ± 0.18 μs
χ^2 / ndf = 3.34
p-value = 4.996e-15

Analysis – Δt_{Gate} – ^{100}Nb

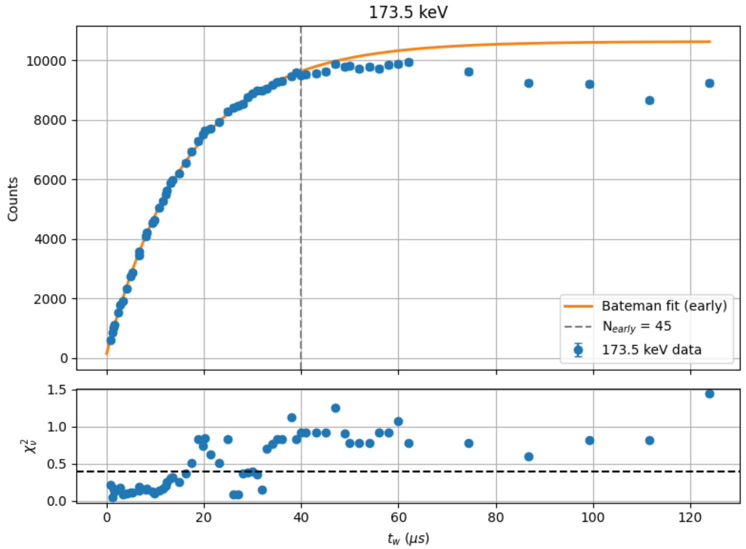

$t_1/_2$ = 11.79 ± 0.16 μs
χ^2 / ndf = 1.35
p-value = 6.427e-02

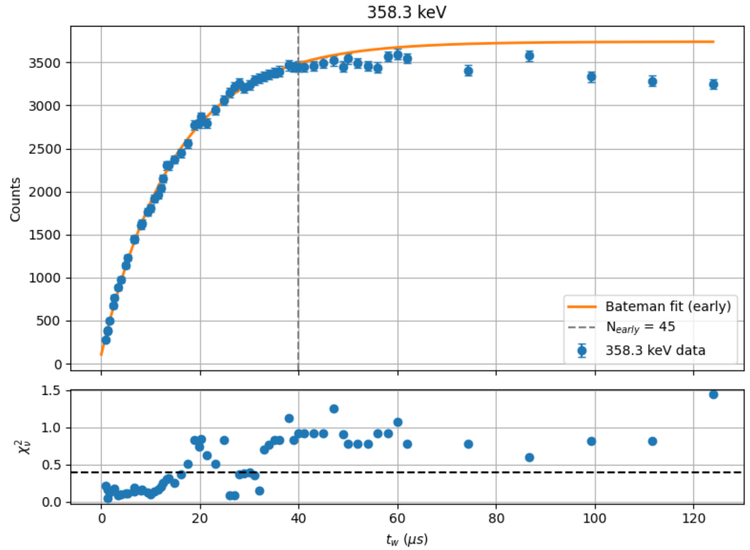

$t_1/_2$ = 10.39 ± 0.22 μs
χ^2 / ndf = 1. 16
p-value = 2.163e-01

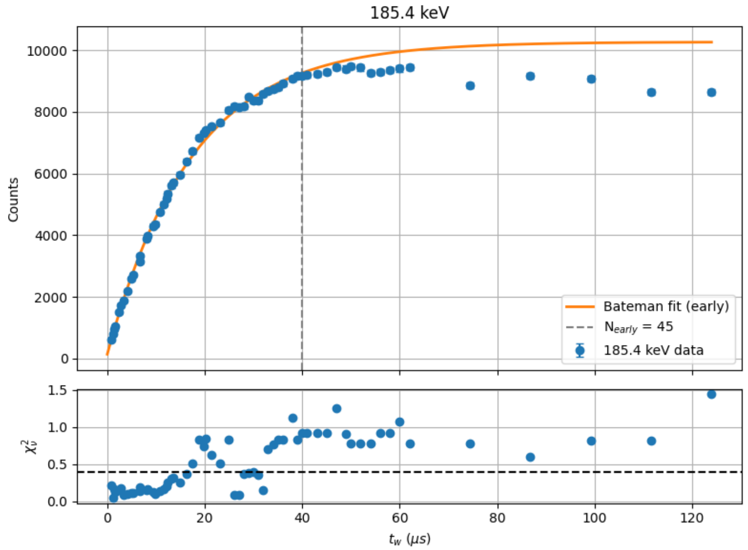

$t_1/_2$= 12.00 ± 0.16 μs
χ^2 / ndf = 3.06
p-value = 9.947e-11

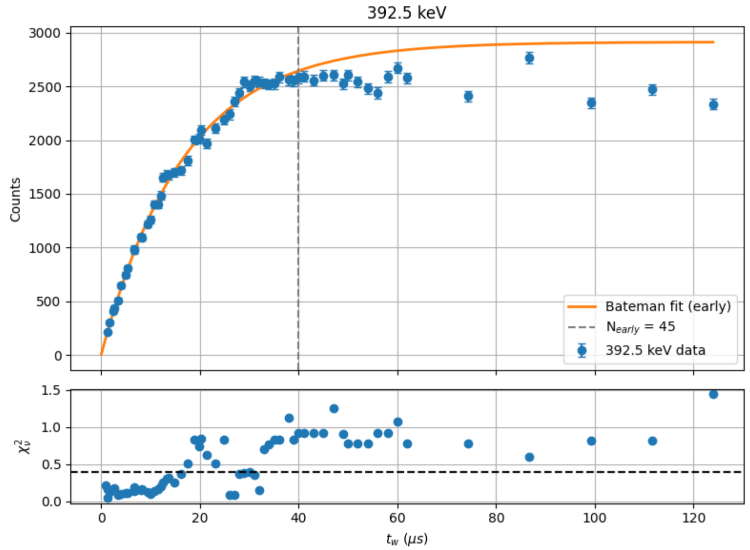

$t_1/_2$= 11.64 ± 0.31 μs
χ^2 / ndf = 2.11
p-value = 5.271e-5

^{88}Br

$t_{1/2}$= **5.3 ± 0.3 μs** (IAEA)

vs

Fit experimental data with function $f = A + B * (1 - e^{-\lambda t})$:

110.9 keV: λ = 1.2019e−01 ± 1.0444e−03 $t_{1/2}$ **= 5.77 ± 0.05**

Quality of the fit: χ² / ndf = 1.71, p-value = 1.5e−01

☺

159.2 keV: λ = 1.2877e−01 ± 1.0513e−03 $t_{1/2}$ **= 5.38 ± 0.04**

Quality of the fit: χ² / ndf = 1.81, p-value = 1.2e−01

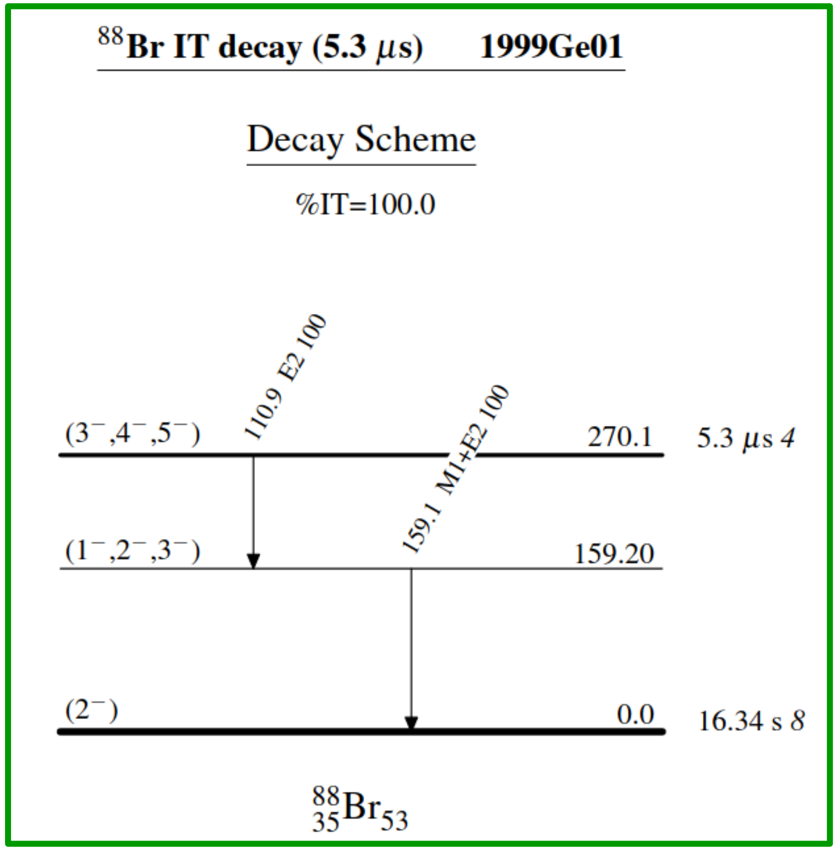

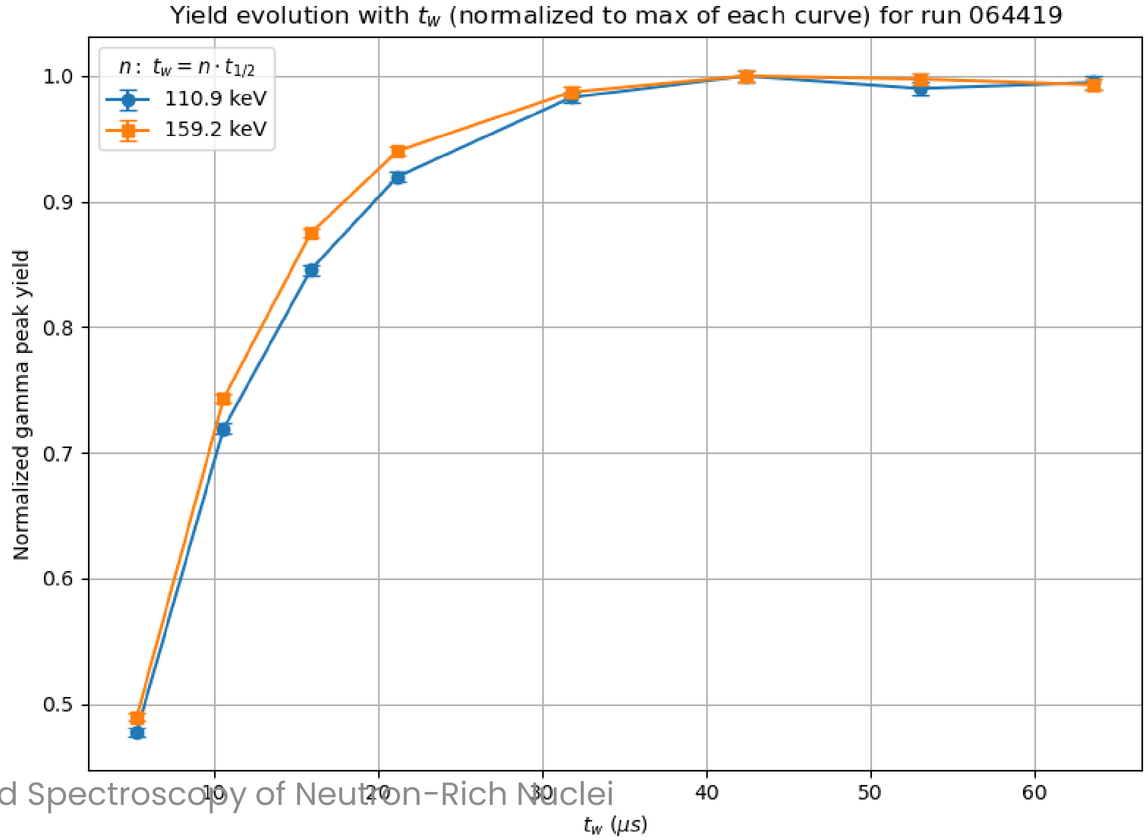

^{129}Sn

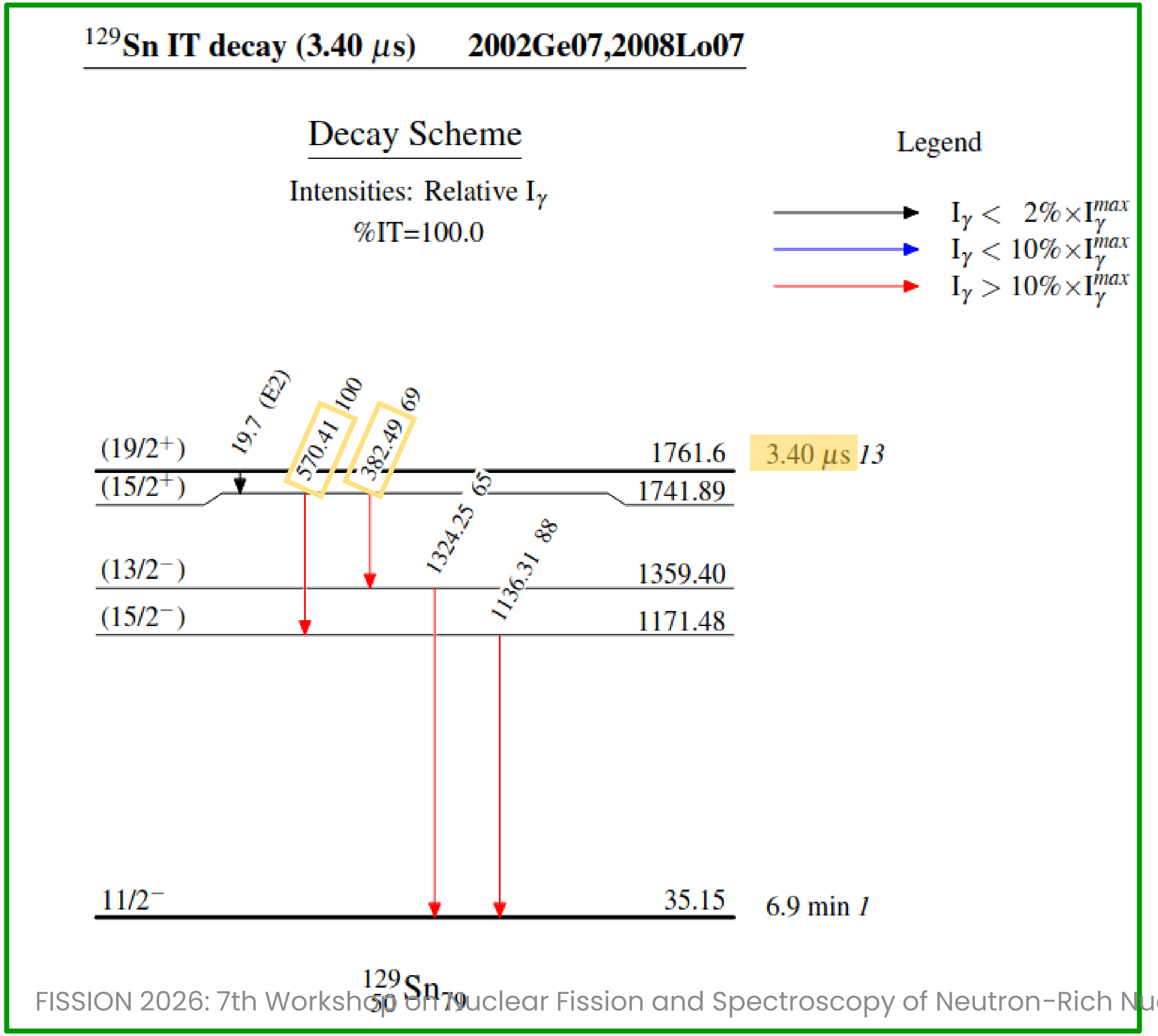

129Sn IT decay (3.40 μs) 2002Ge07,2008Lo07
Decay Scheme
Intensities: Relative Iγ
%IT=100.0
Legend
Iγ < 2%×Iγmax
Iγ < 10%×Iγmax
Iγ > 10%×Iγmax
19.7 (E2)
570.41 100
382.49 69
1324.25 65
1136.31 88
(19/2+) 1761.6 3.40 μs 13
(15/2+) 1741.89
(13/2−) 1359.40
(15/2−) 1171.48
11/2− 35.15 6.9 min 1
129 50 Sn79

^{129}Sn

$t_{1/2}$ = **3.4 ± 0.2 μs** (IAEA)

vs

Fit experimental data with function $\mathbf{f = A + B * (1 - e^{-\lambda t})}$:

382.5 keV: λ = 2.1553e-01 ± 3.5996e-03 $t_{1/2}$ **= 3.22 ± 0.05**
Quality of the fit: χ^2 / ndf = 1.34, p-value = 2.5e-01

570.4 keV: λ = 2.1413e-01 ± 8.4292e-03 $t_{1/2}$ **= 3.24 ± 0.13**
Quality of the fit: χ^2 / ndf = 4.45, p-value = 1.3e-03

382.5 keV: λ = 1.8592e-01 ± 8.2569e-03 $t_{1/2}$ **= 3.73 ± 0.17**
Quality of the fit: χ^2 / ndf = 16.75, p-value = 9.7e-14

570.4 keV: λ = 2.0176e-01 ± 1.0225e-02 $t_{1/2}$ **= 3.44 ± 0.17**
Quality of the fit: χ^2 / ndf = 14.14, p-value = 1.5e-11

KE = 62

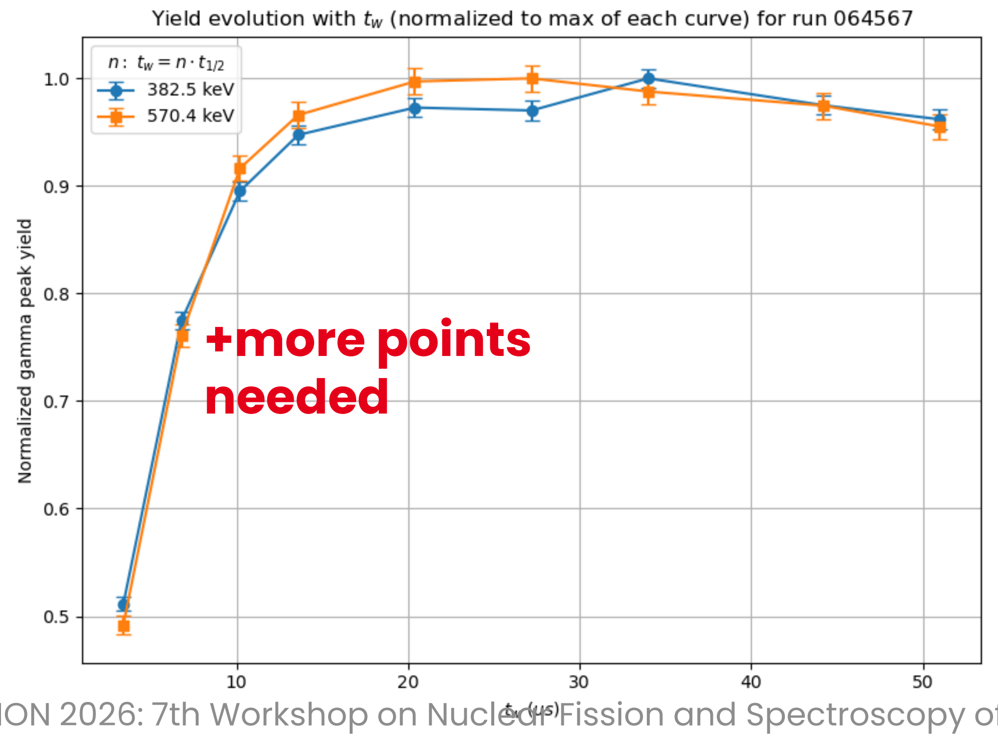

KE = 74

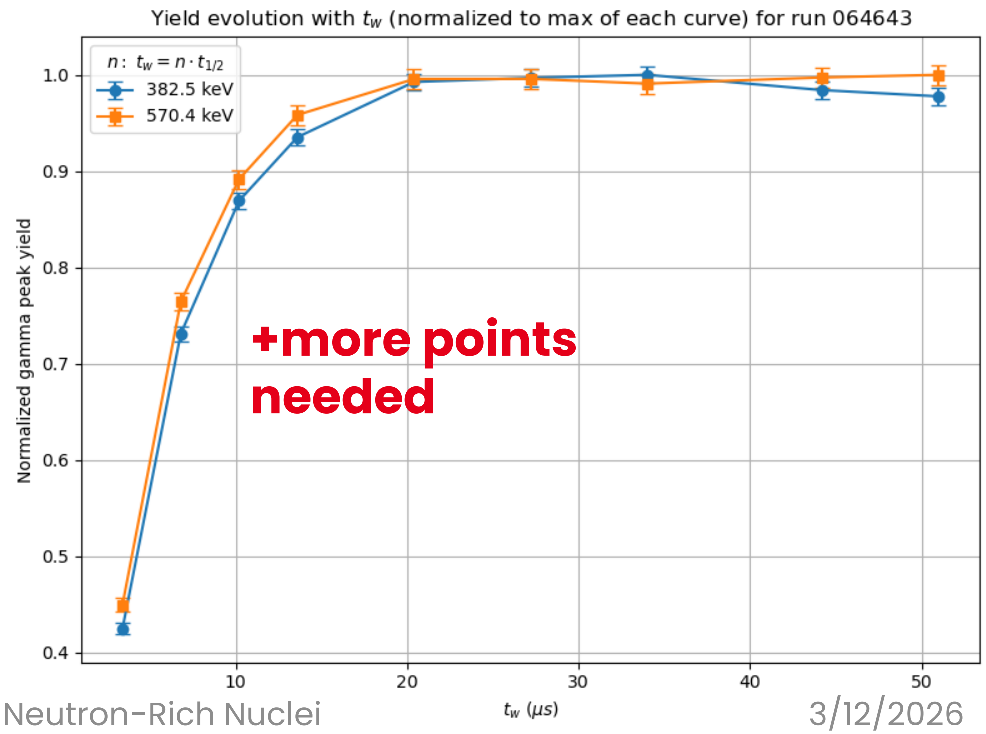

Correct central value but not always good fit

^{131}Sb – Study Case

IDENTIFICATION CARD

^{131}Sb

Ground State: $t_{1/2} = 23.03$ min

Metastable States: (IAEA, NNDS)

1. $E_{level} = 2165.6$ keV, $t_{1/2} = 1.1$ μs
2. $E_{level} = 1687.2$ keV, $t_{1/2} = 4.3$ μs
3. $E_{level} = 1676.1$ keV, $t_{1/2} = 91$ μs

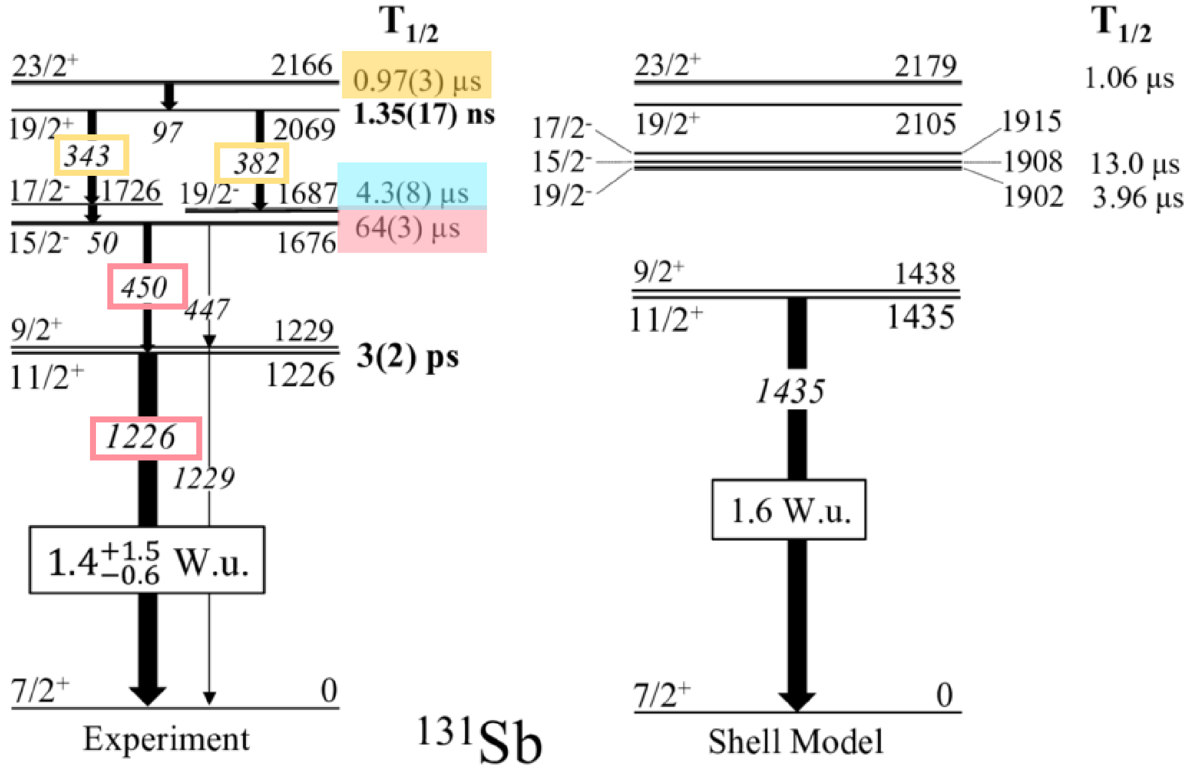

Lifetime measurements in 131131Sb at LOHENGRIN
S. Bottoni et al

^{131}Sb

Python Script Weighted Fit:
λ = 1.1524e+00 ± 2.7269 1/μs
$t_{1/2}$ = 0.60 ± 1.42 μs
<u>Quality of the fit:</u> χ^2 / ndf = 0.35, p-value = 9.1e-01

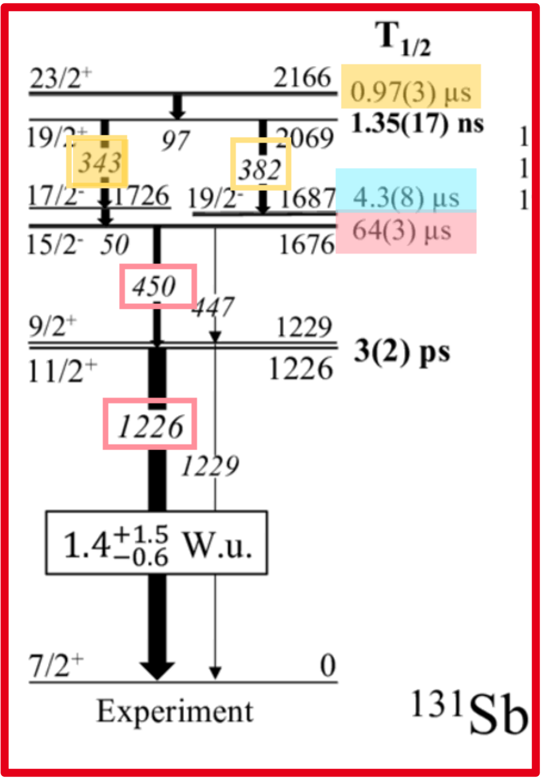

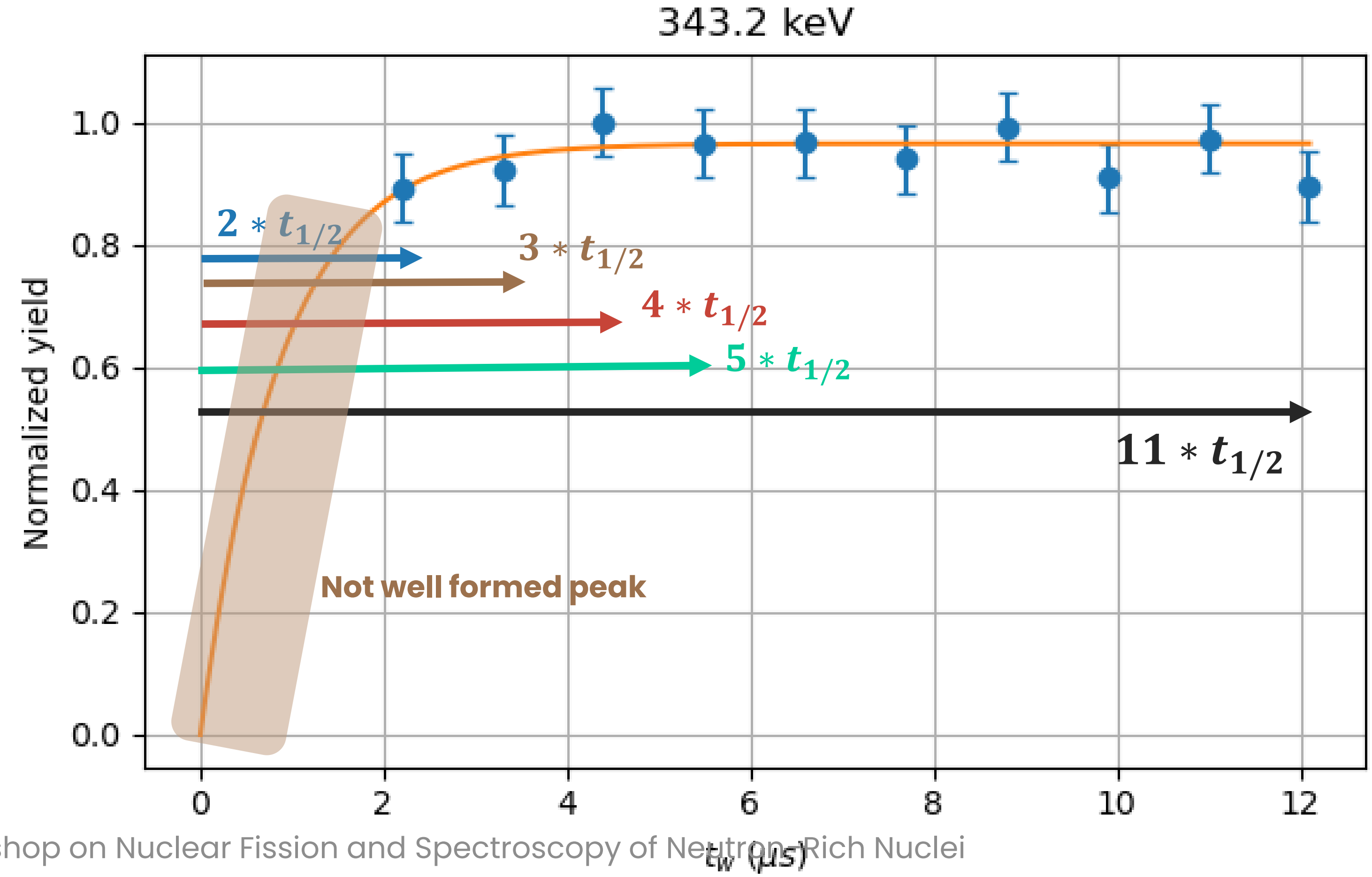

^{131}Sb

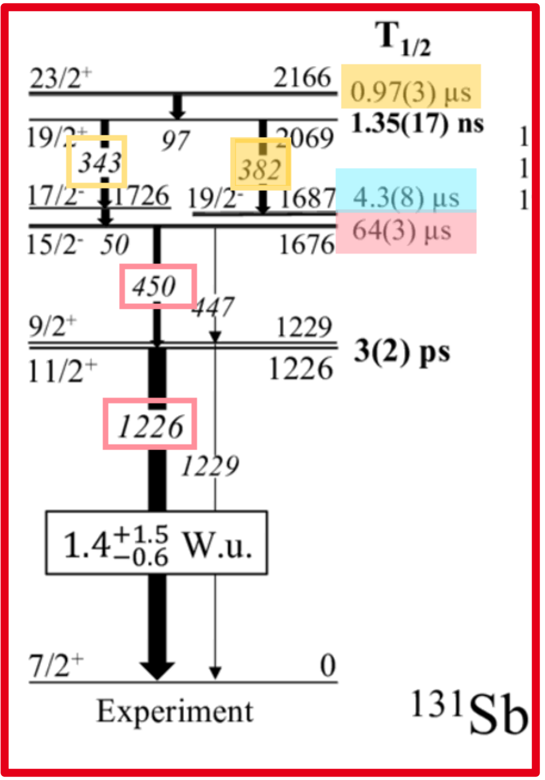

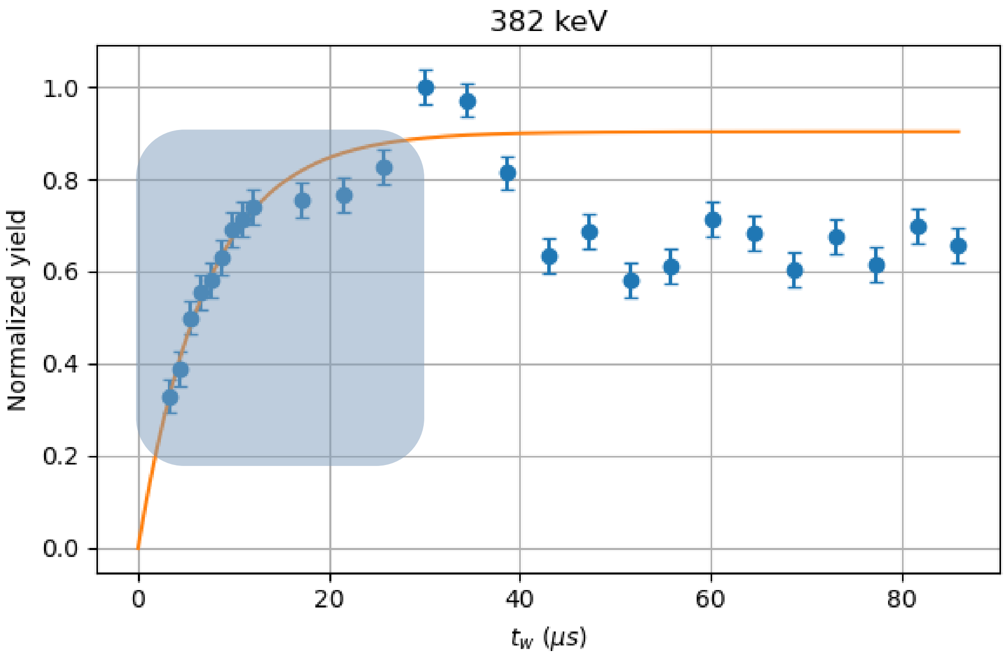

12 first points

Python Script Weighted Fit:

λ = 1.6562e-01 ± 3.2601e-02 1/µs

$t_{1/2}$ = 4.19 ± 0.82 µs

Quality of the fit:

χ² / ndf = 0.46, p-value = 9.1e-01

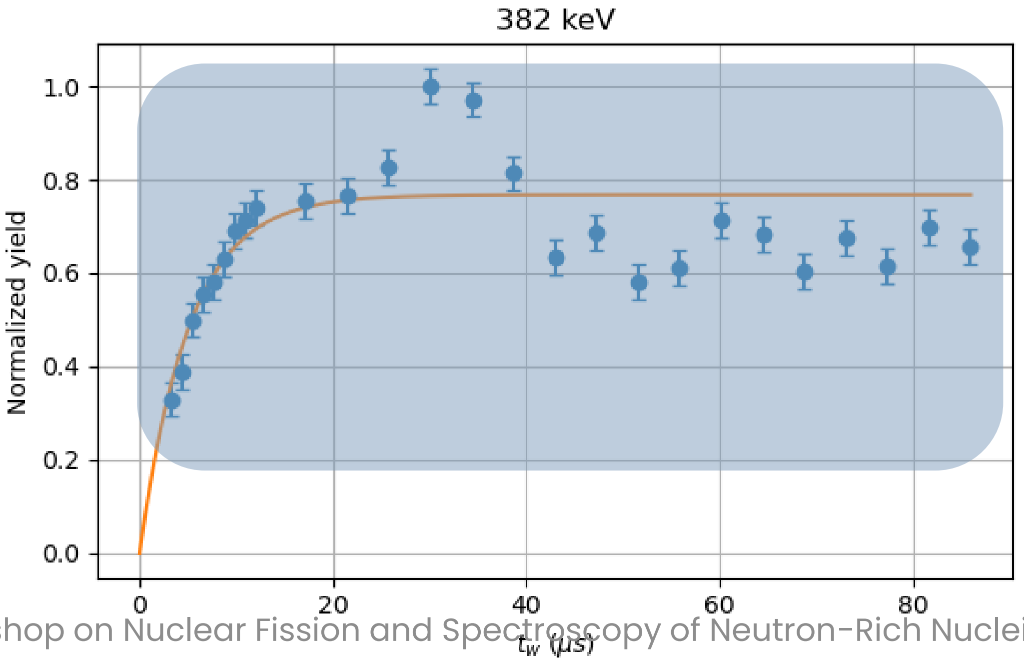

All points

Python Script Weighted Fit:

λ = 1.9555e-01 ± 2.9853e-02 1/µs

$t_{1/2}$ = 3.54 ± 0.54 µs

Quality of the fit:

χ² / ndf = 7.88, p-value = 1e-015

^{131}Sb

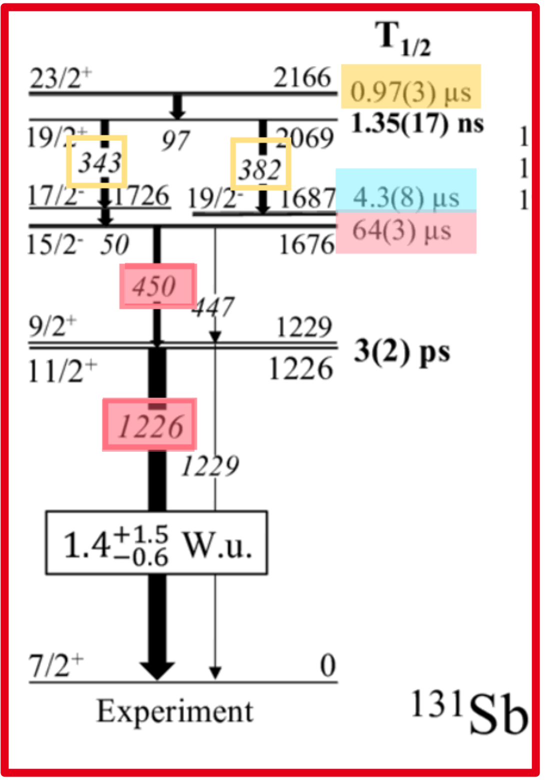

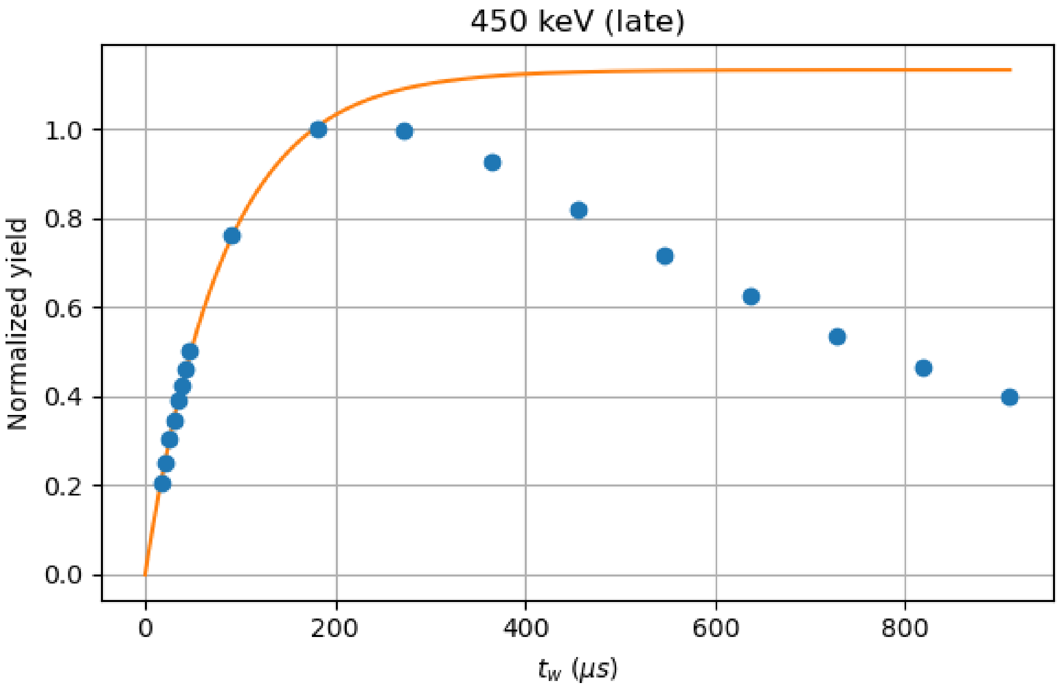

Python Script Weighted Fit:

λ = 1.2091e-02 ± 4.0769e-04 1/µs

$t_{1/2}$ = 57.33 ± 1.93 µs

<u>Quality of the fit:</u>

χ^2 / ndf = 1.60, p-value = 1.3e-01

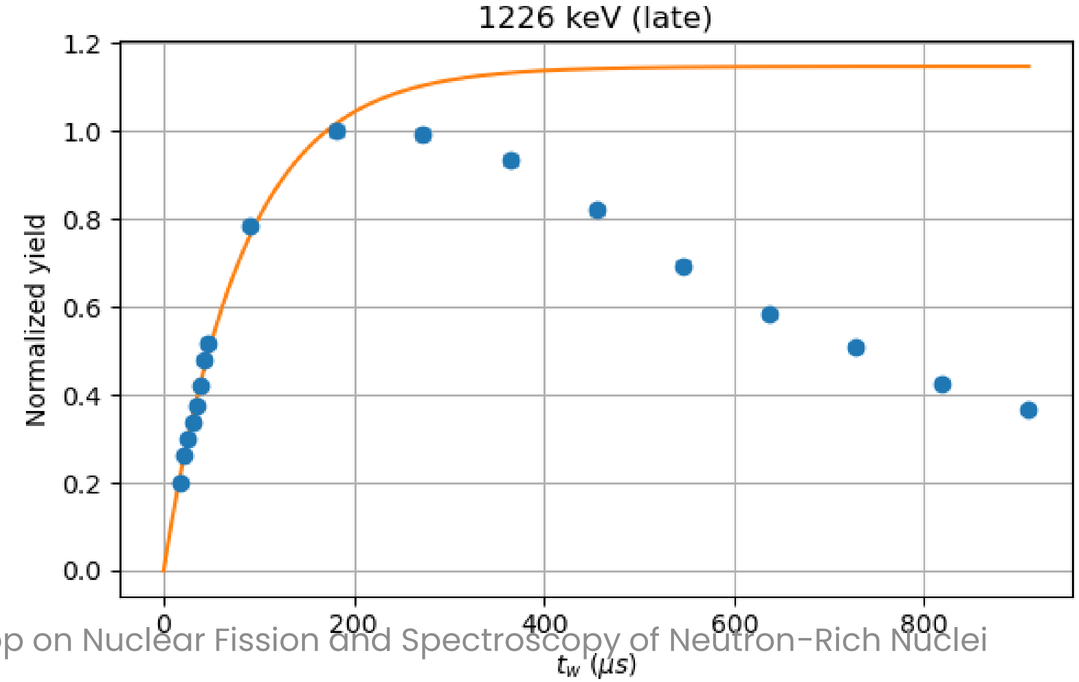

Python Script Weighted Fit:

λ = 1.2000e-02 ± 5.8706e-04 1/µs

$t_{1/2}$ = 57.76 ± 2.83 µs

<u>Quality of the fit:</u>

χ^2 / ndf = 4.1, p-value = 1.7e-04

^{131}Sb

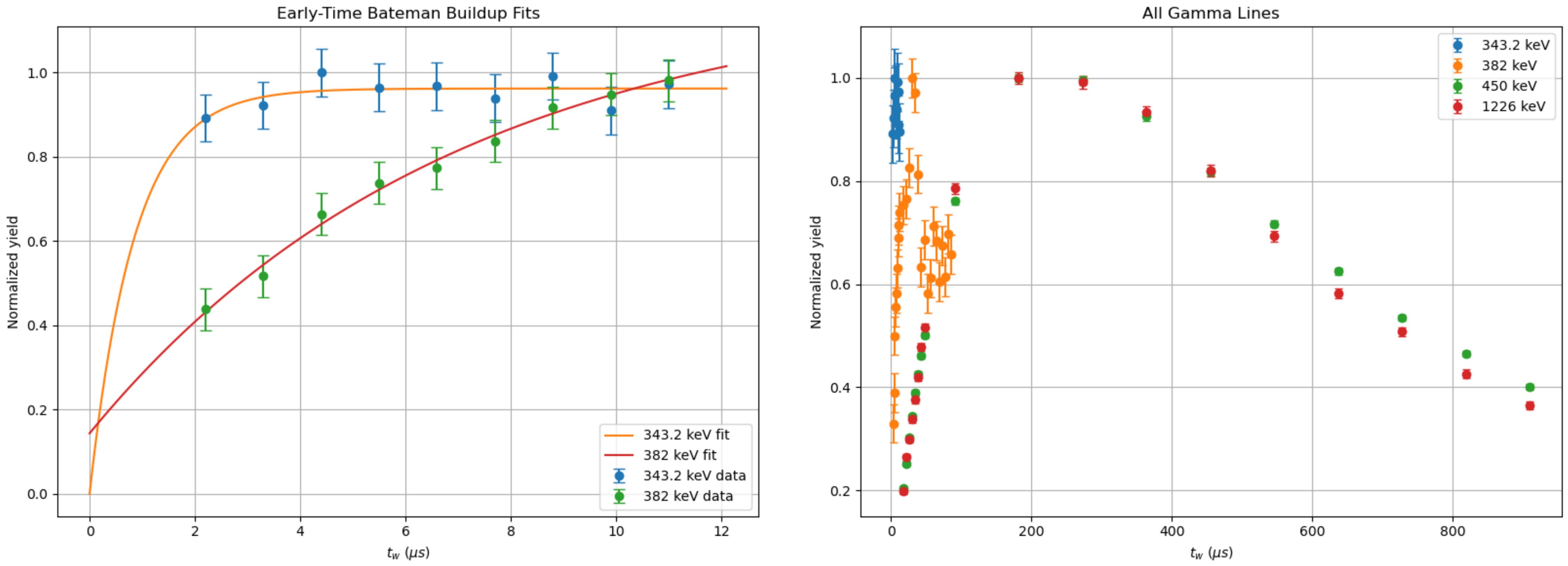

Early-Time Bateman Buildup Fits
Normalized yield
t_w (μs)
343.2 keV fit
382 keV fit
343.2 keV data
382 keV data
All Gamma Lines
343.2 keV
382 keV
450 keV
1226 keV

Analysis – ^{100}Nb from ^{241}Am(2n$_{th}$,f)

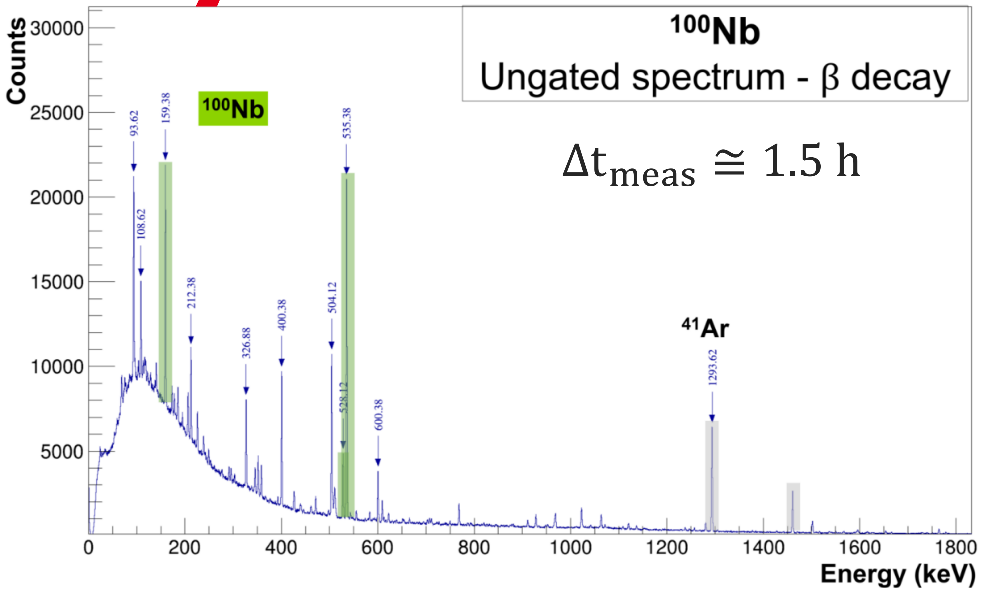

Ungated Spectrum

→ Ground state measurement → N_γ

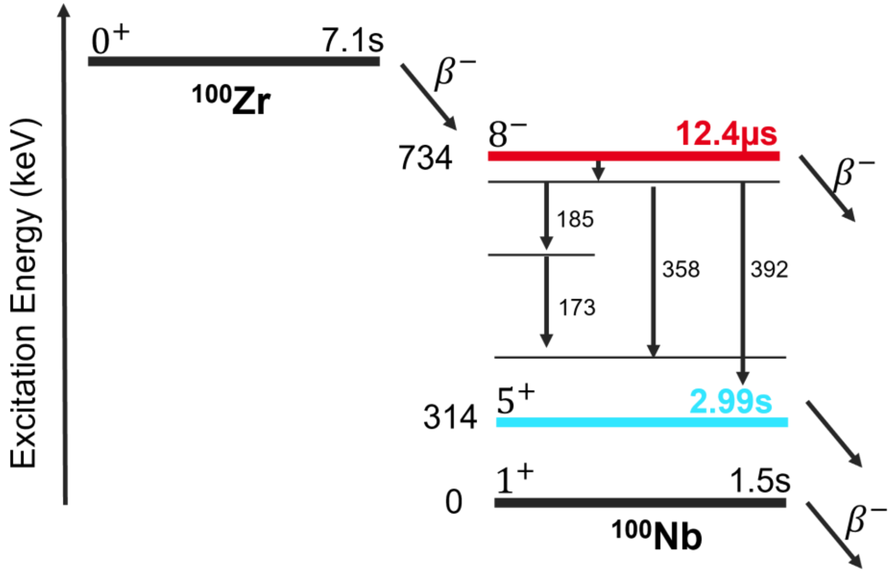

Analysis – ^{100}Nb from ^{241}Am(2n$_{th}$,f)

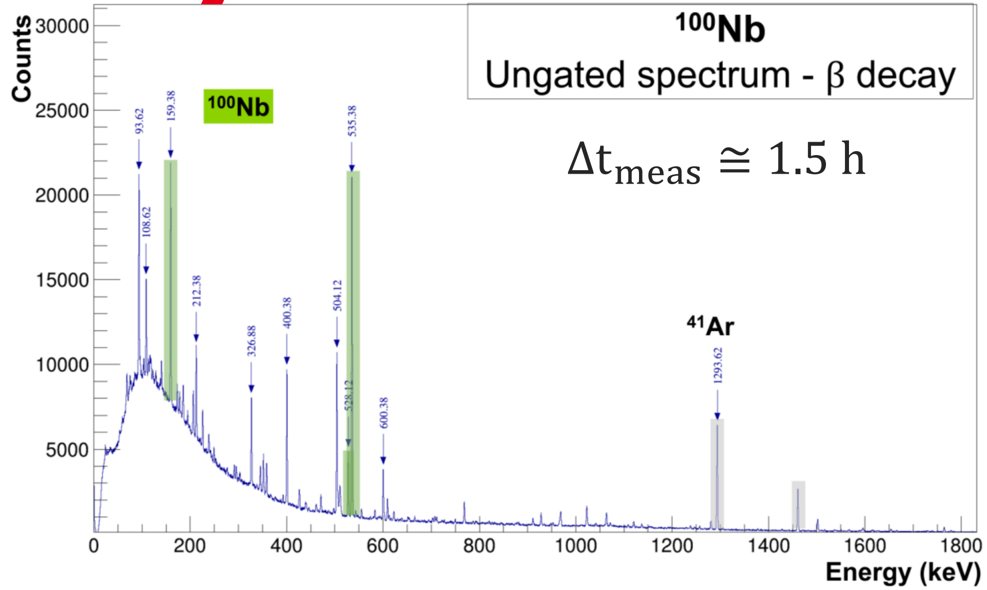

Ungated Spectrum

→ β-decay states measurement → N_γ, N_γ

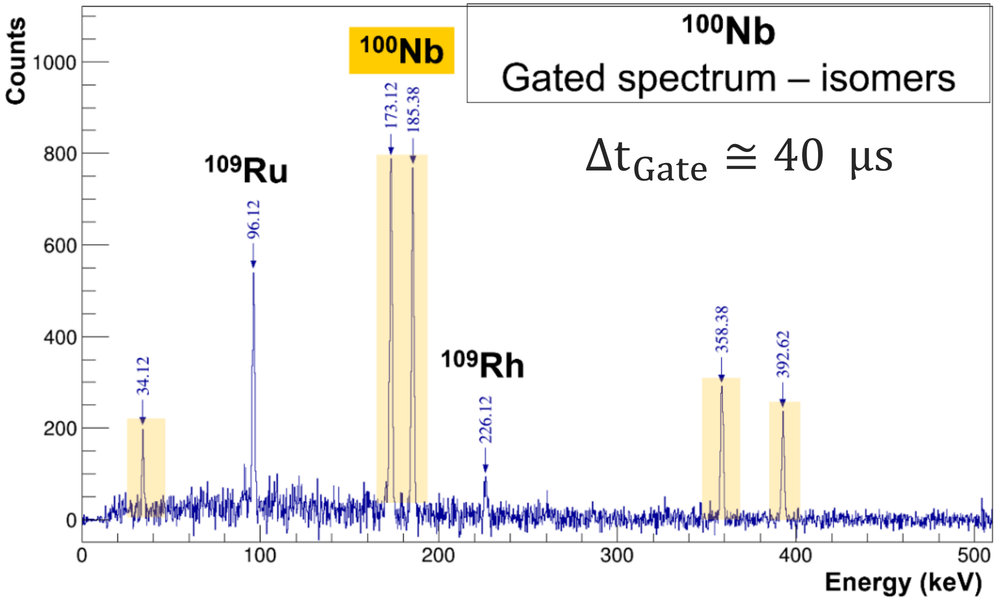

Gated Spectrum

Time coincidence between ionization chamber and HPGe detectors

→ μs Isomeric state measurement → N_γ

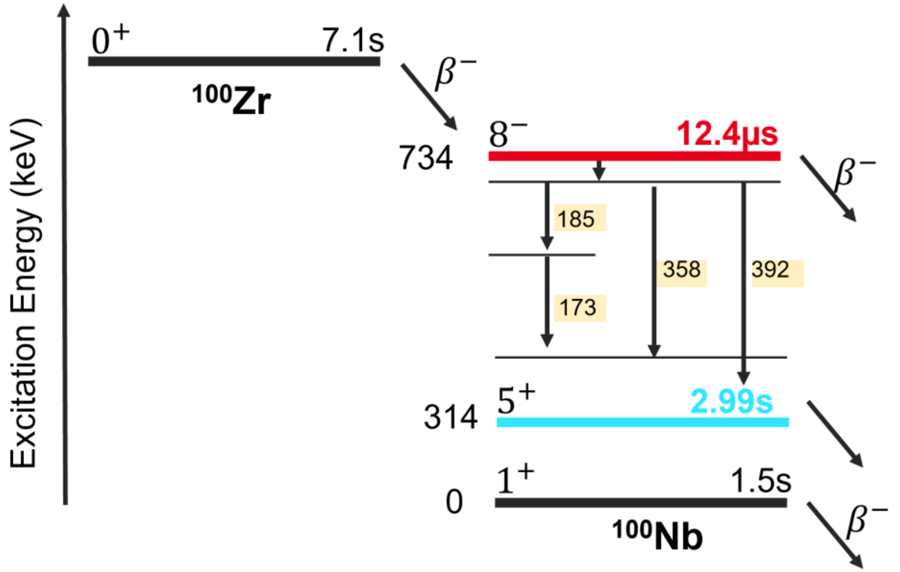

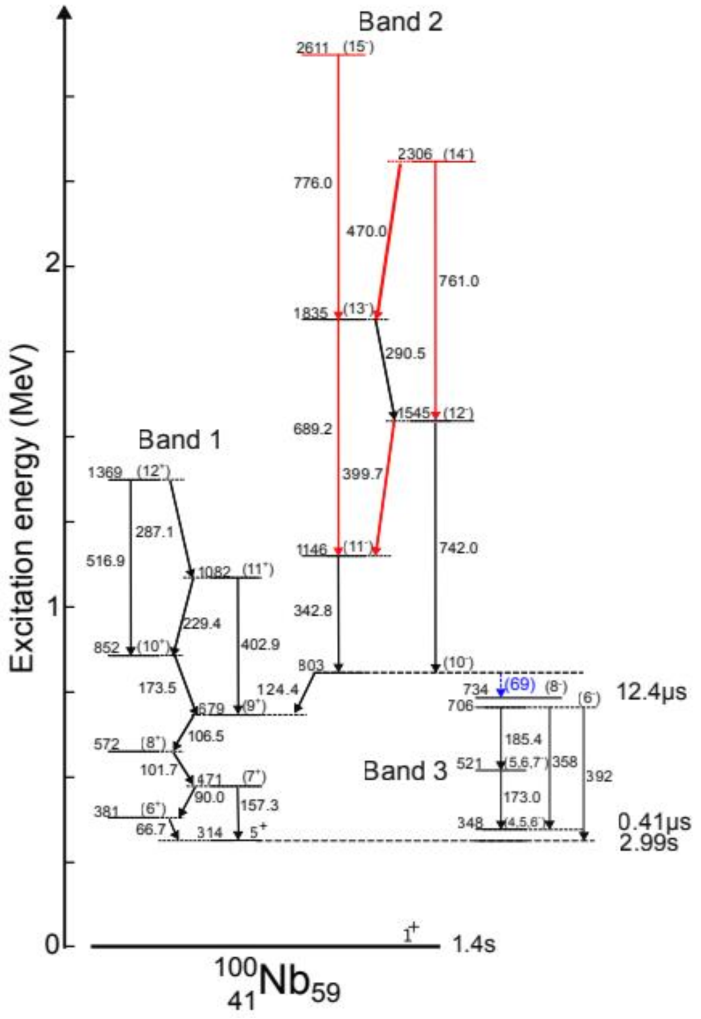

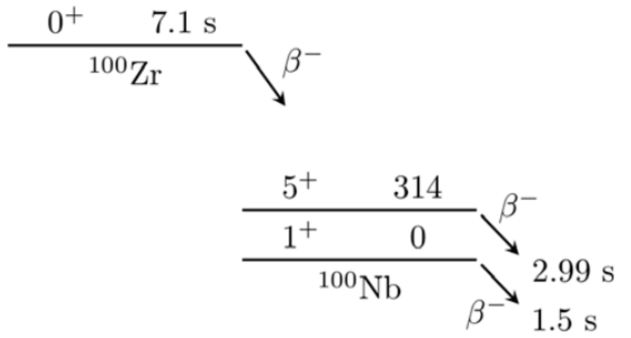

Figure 1. Scheme of the two isomers in ^{100}Nb. Spin-parity and energy (in keV) of both isomeric states, as well as the half-life of their β decay are presented. The decay of the ground state of the grandparent, ^{100}Zr, is also depicted.

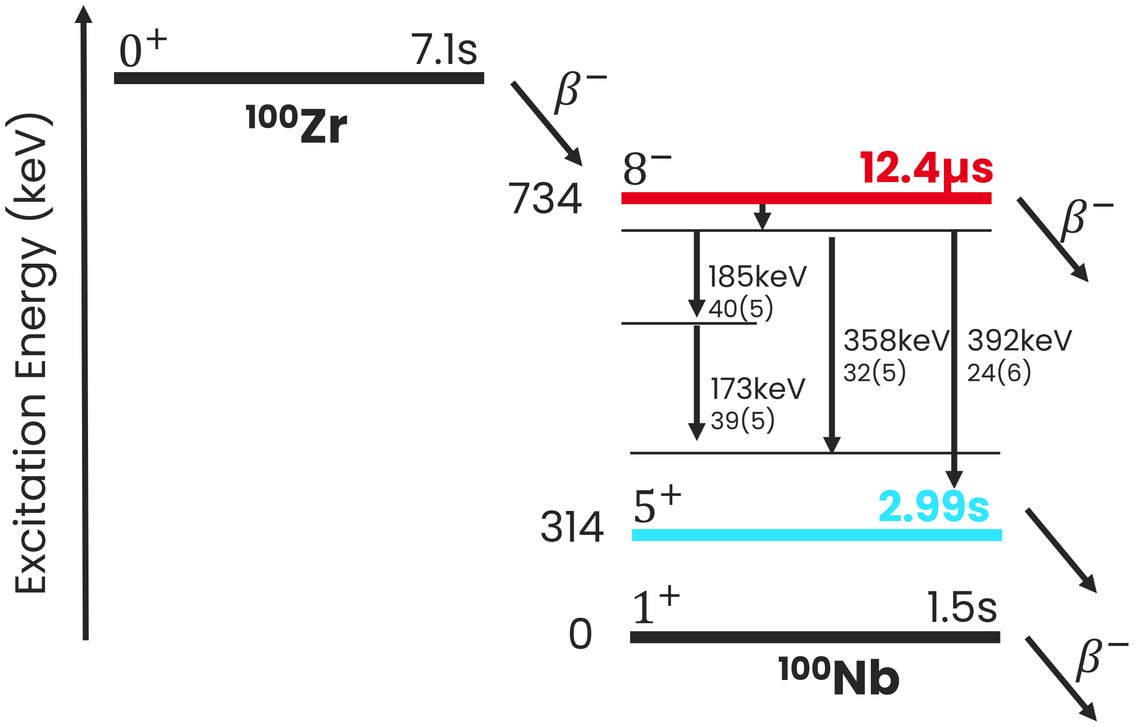

Experimental setup of LOHENGRIN spectrometer in ILL

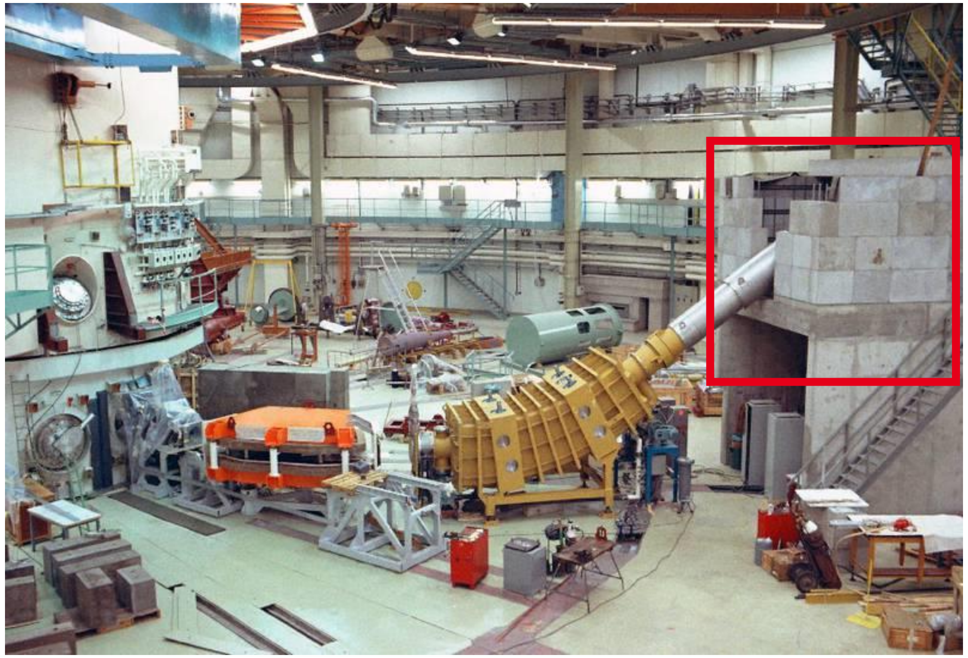

Choise of $\vec{B}$ and $\vec{E}$

Selection of $^{A}/_{q}$ and $^{E_K}/_{q}$ ratios

Only the isotopes of chosen $^{A}/_{q}$ are deflected into the exit slit

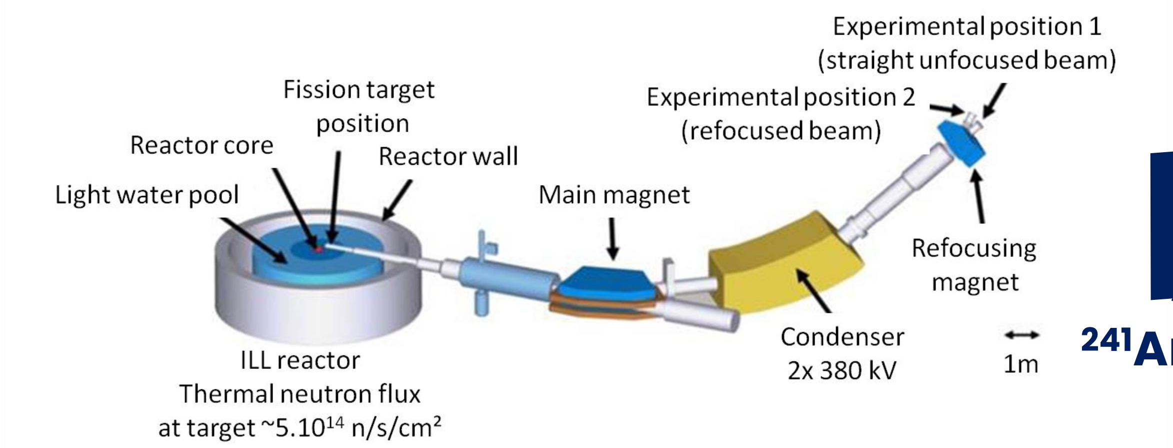

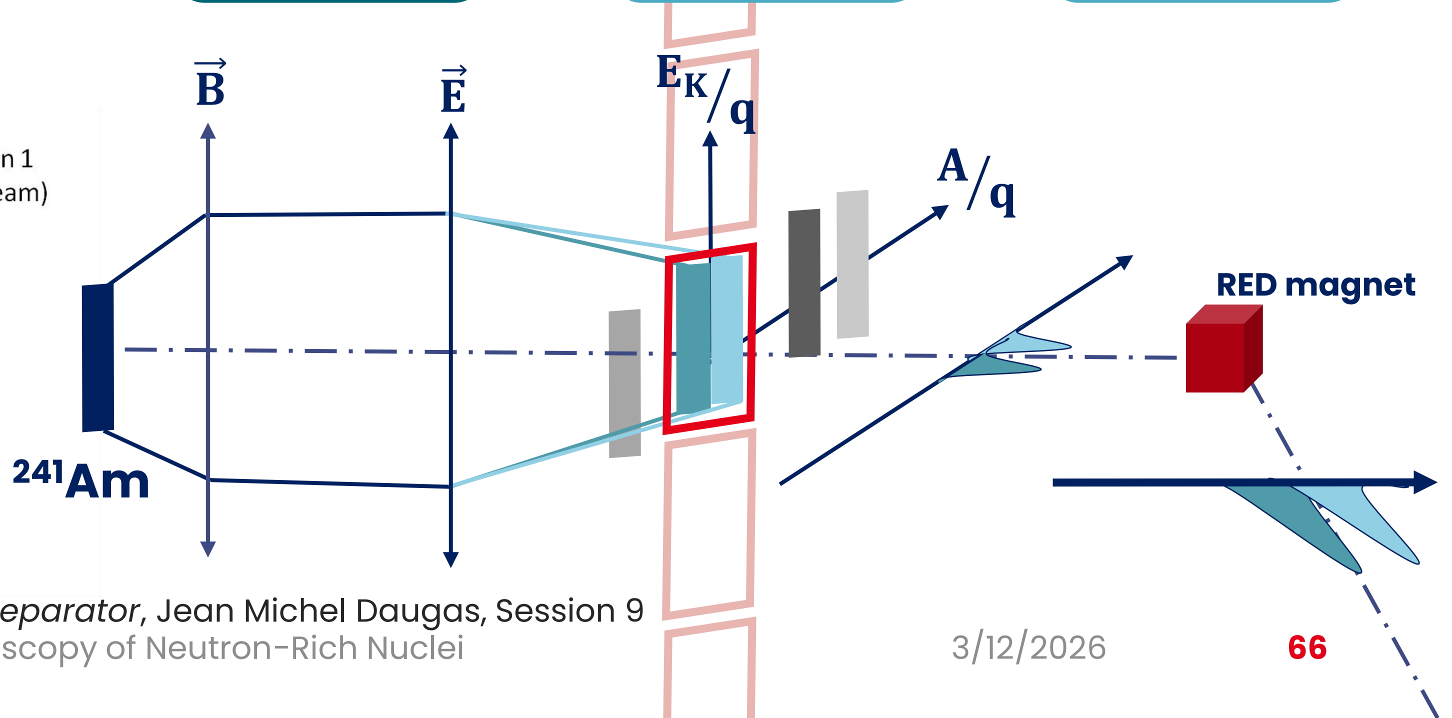

Motivation: Angular momentum generation mechanism of Fission Fragments

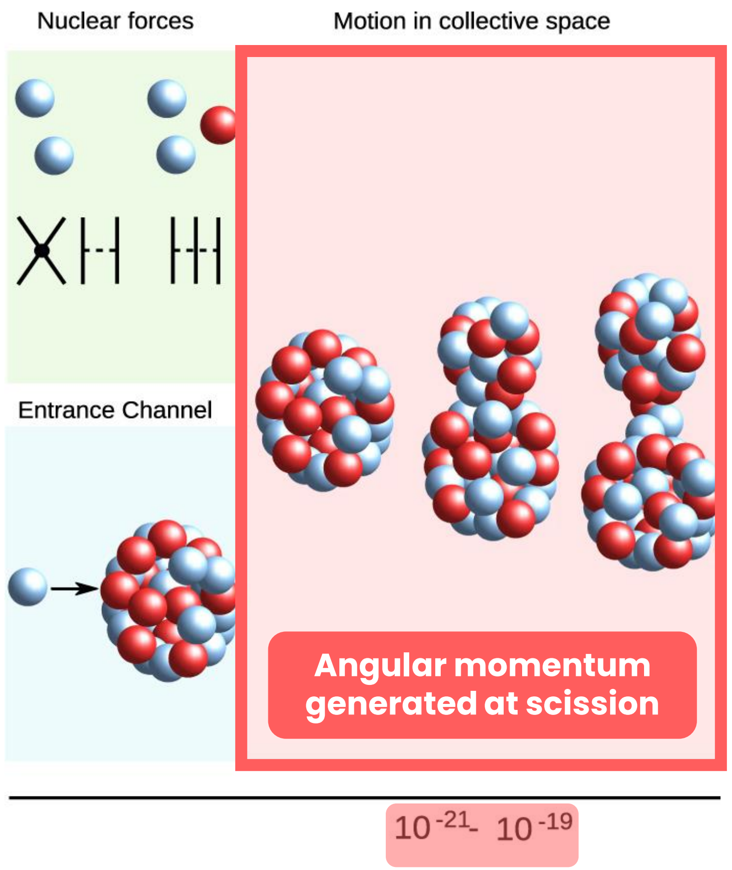

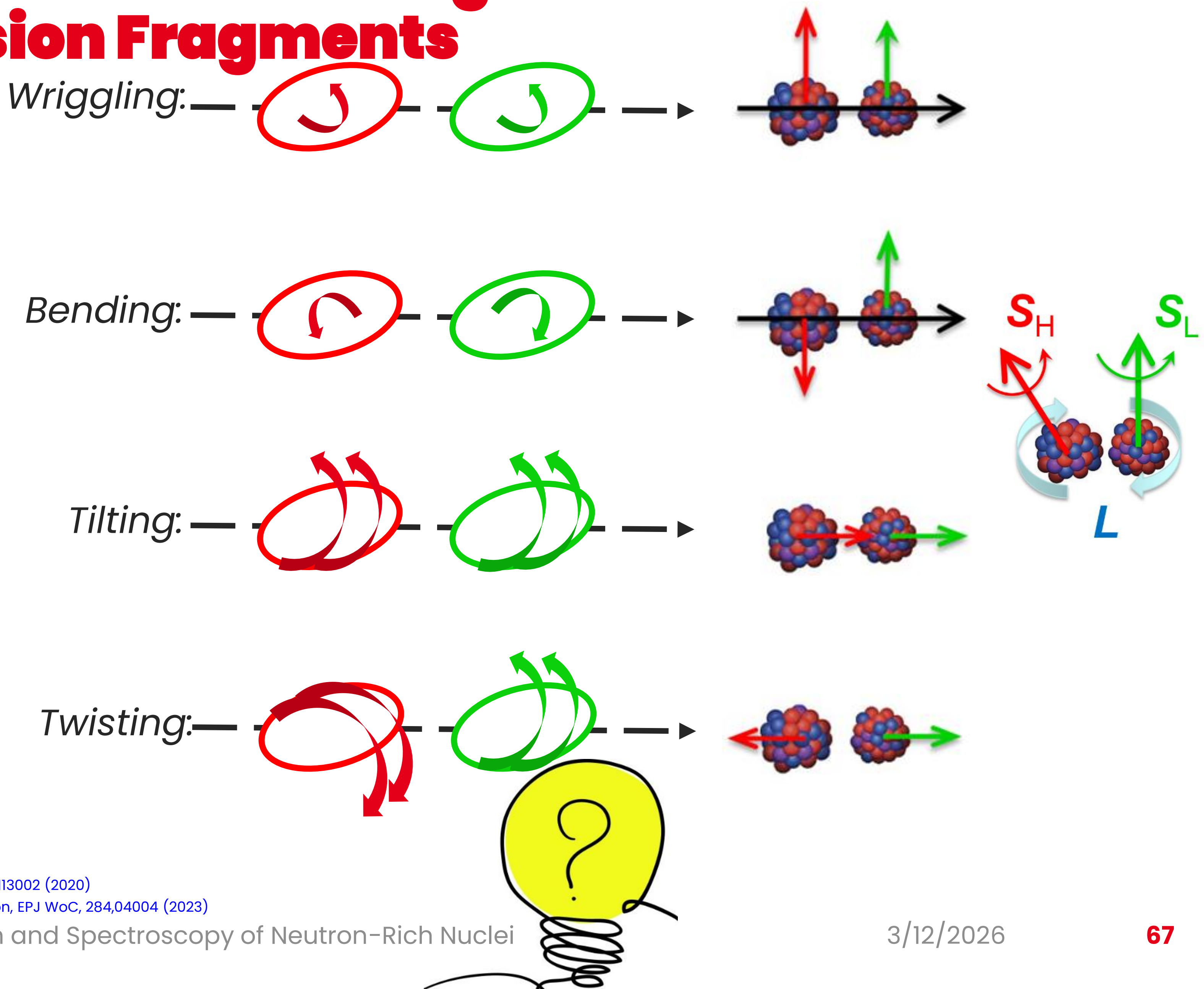

M. Bender *et al.*, *Future of nuclear fission theory*, J. Phys. G: Nucl. Part. Phys. 47 113002 (2020)

J. Randrup et al., Generation of Fragment Angular Momentum in Nuclear Fission, EPJ WoC, 284,04004 (2023)

Comparison with FIFRELIN

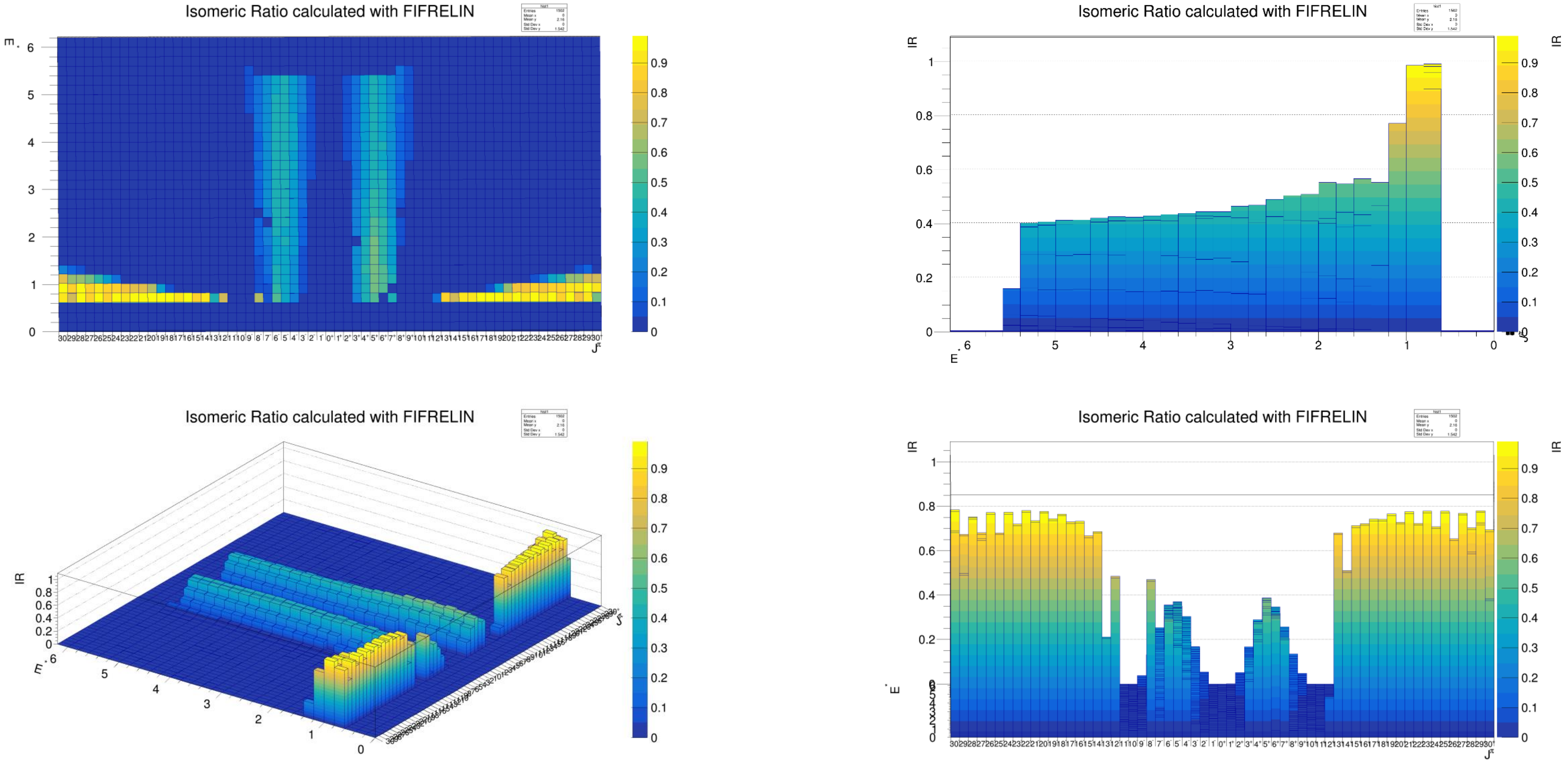

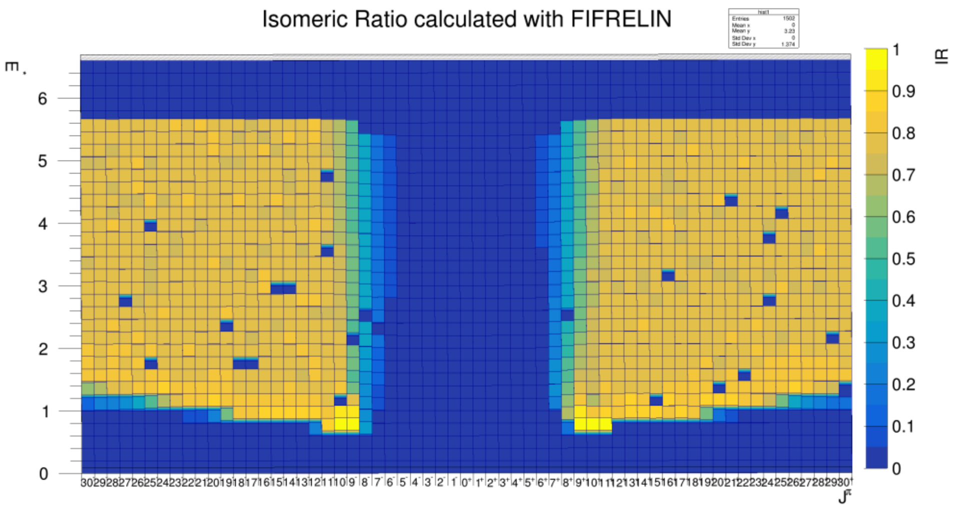

Isomeric Ratio calculated with FIFRELIN
E*
J^π
IR

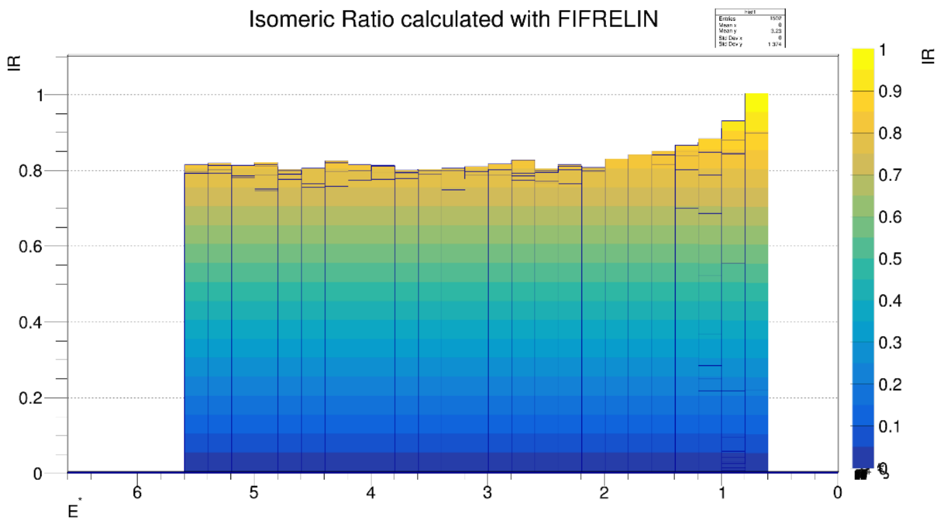

Isomeric Ratio calculated with FIFRELIN
IR
E*

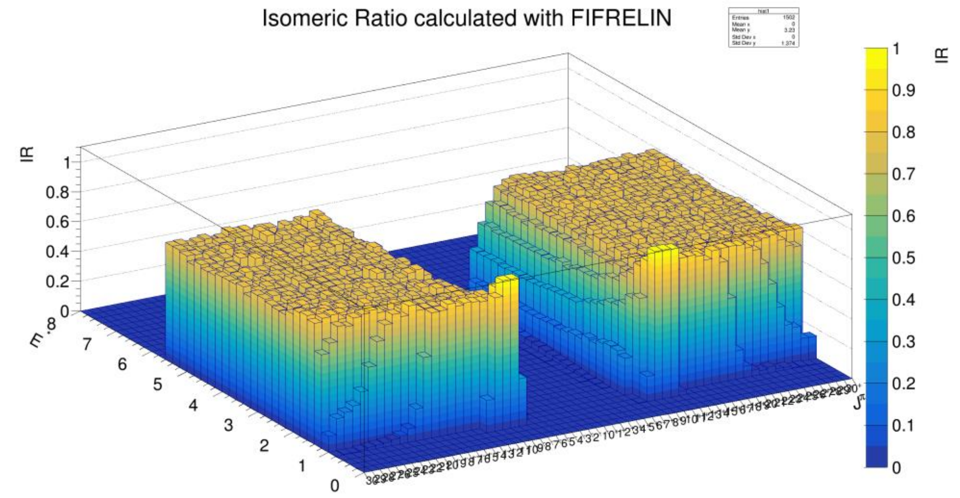

Isomeric Ratio calculated with FIFRELIN
IR
E*
J^π

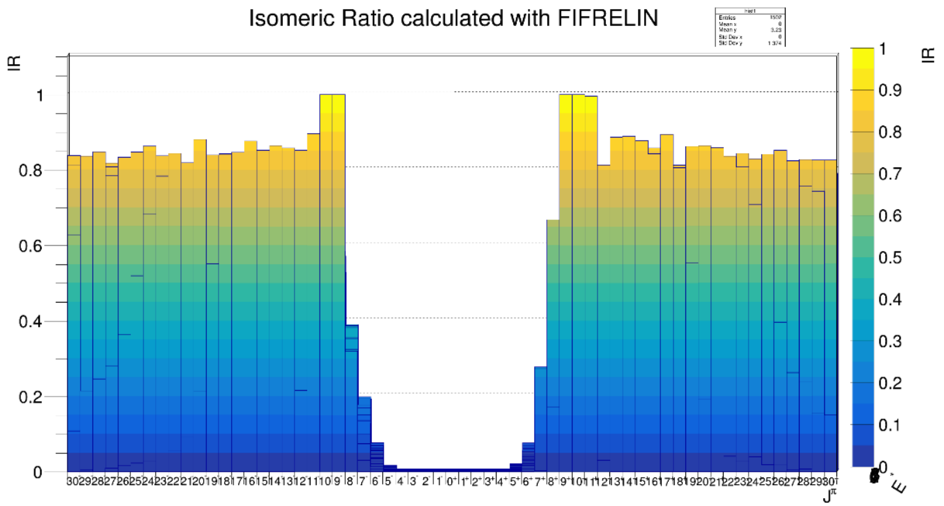

Isomeric Ratio calculated with FIFRELIN
IR
J^π

Comparison with FIFRELIN

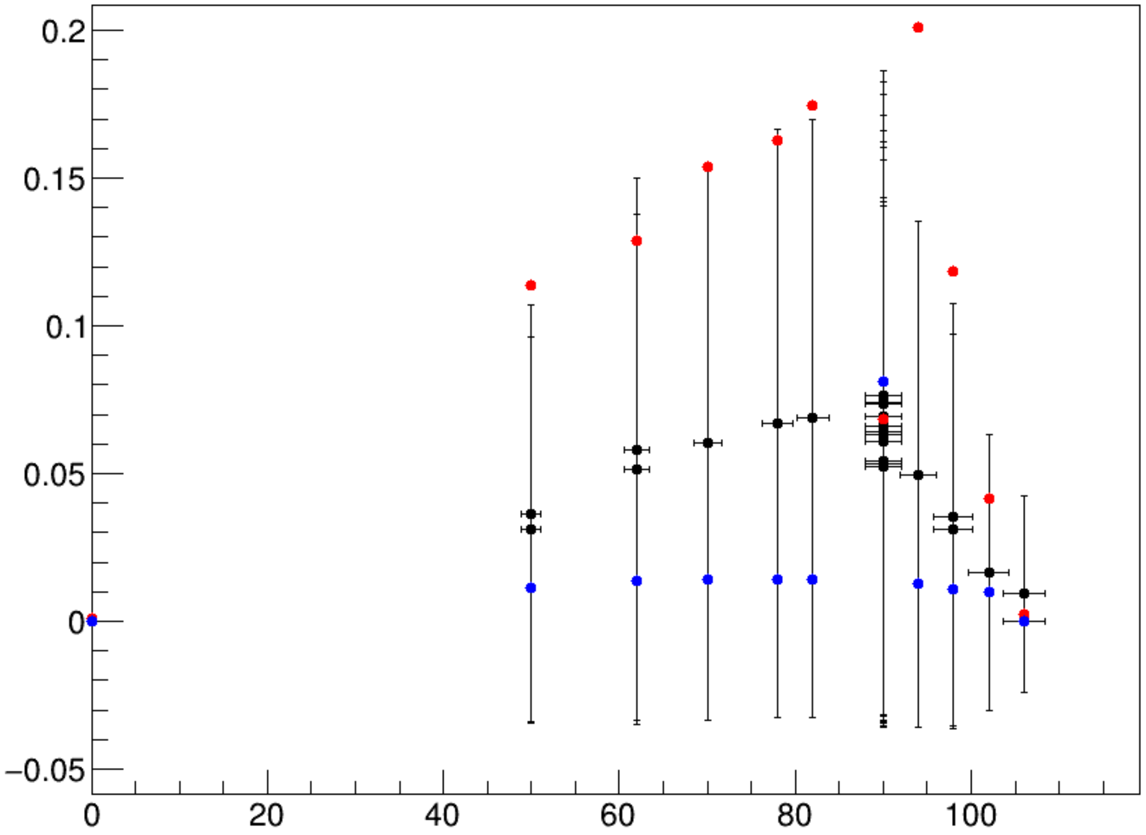

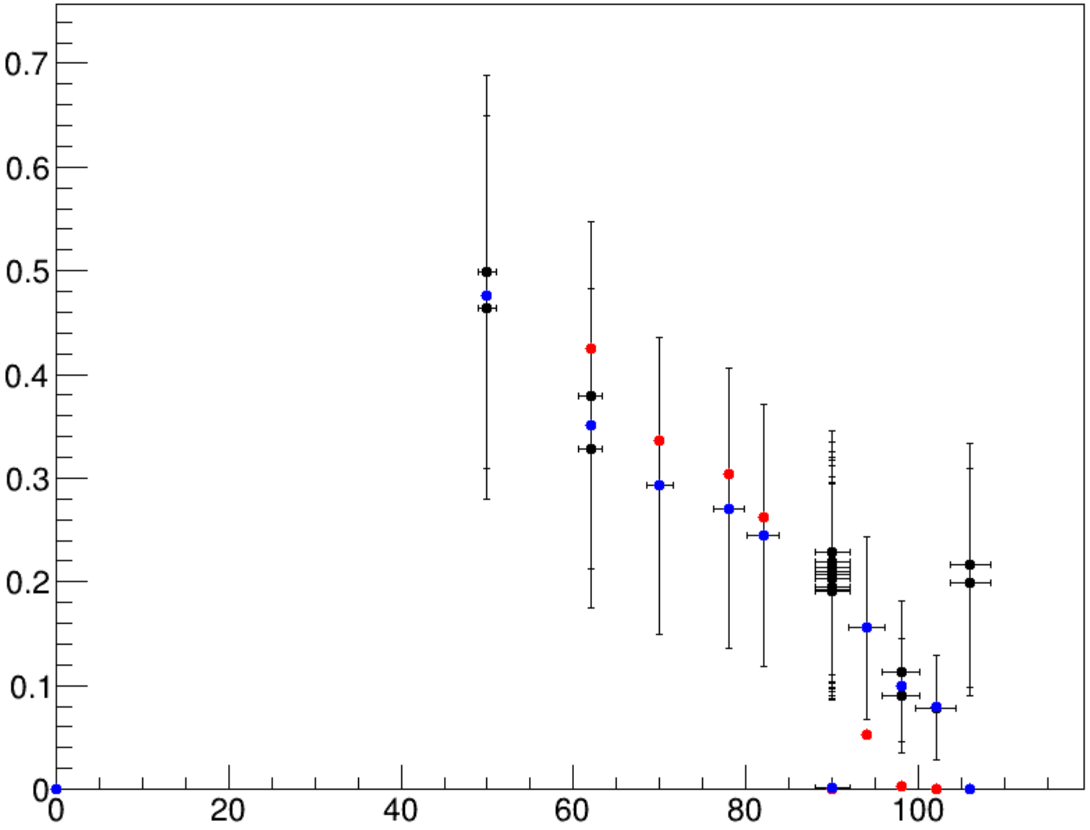

Comparison with FIFRELIN

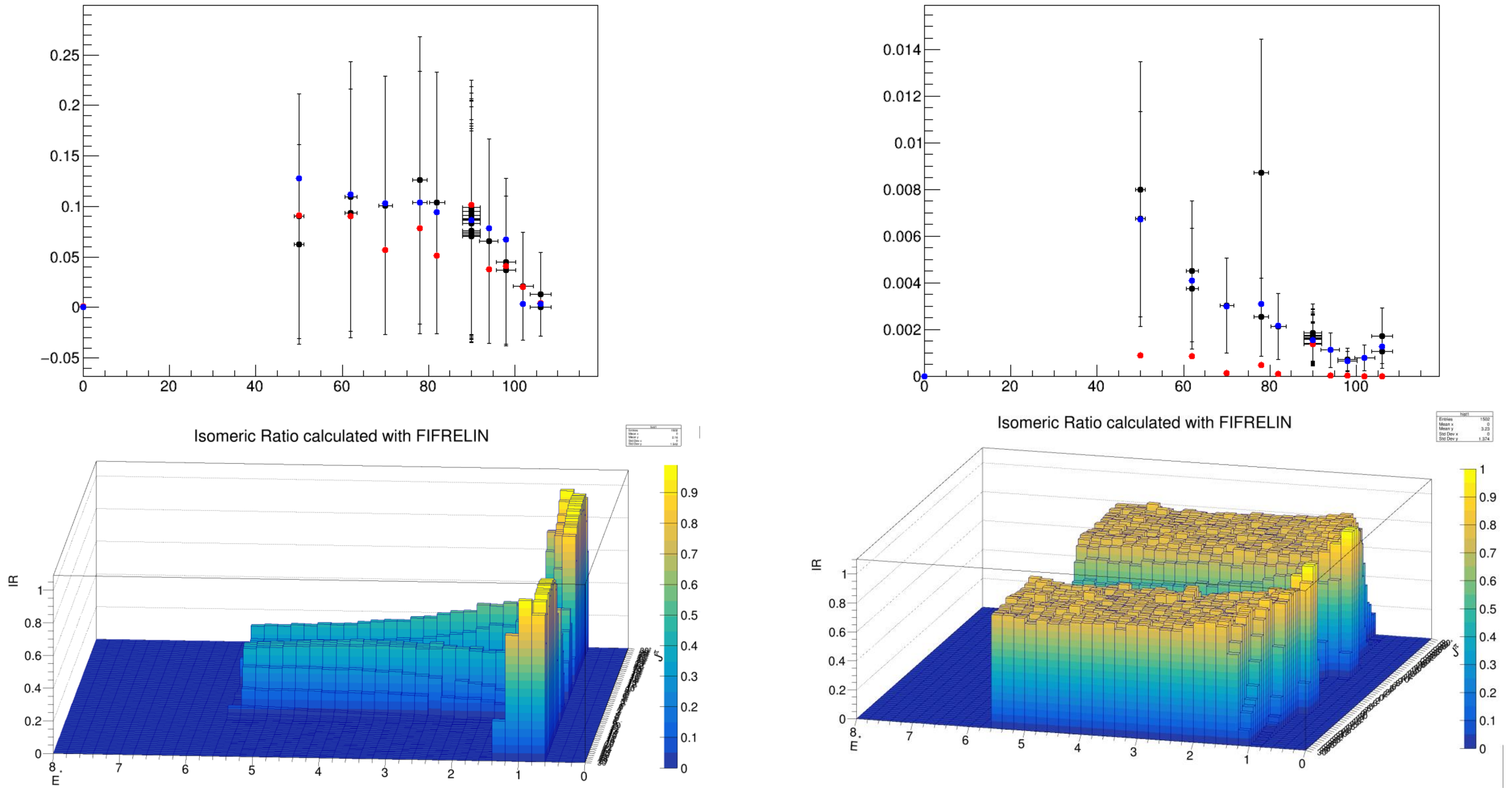

Bayesian J_{cutoff}